UNIVERSIDADE DE LISBOA

Faculdade de Farmácia da Universidade de Lisboa

Departamento de Química Farmacêutica e Fitoquímica

Triazene Prodrug Synthesis for MDEPT Strategy and their Hepatotoxic Evaluation

Fábio Miguel Figueiredo Santos

MESTRADO EM QUÍMICA FARMACÊUTICA E TERAPÊUTICA

Lisboa

2011

UNIVERSIDADE DE LISBOA

Faculdade de Farmácia da Universidade de Lisboa

Departamento de Química Farmacêutica e Fitoquímica

Triazene Prodrug Synthesis for MDEPT Strategy and their Hepatotoxic Evaluation

Fábio Miguel Figueiredo Santos

Dissertação orientada pela Professora Doutora Ana Paula Francisco e pela Professora Doutora Maria de Jesus Perry

Dissertação apresentada à Faculdade de Farmácia da Universidade de Lisboa para obtenção do grau de Mestre em Química Farmacêutica e Terapêutica

Lisboa

2011

Aos meus Pais

À minha namorada

Acknowledgments

A elaboração e realização da tese de mestrado que aqui vos apresento, só foi possível, graças a um conjunto admirável de pessoas, por quem tenho o maior respeito e admiração. Não querendo esquecer ninguém, a todos, o meu sincero agradecimento.

Dentro deste admirável grupo, existem pessoas a quem devo um especial agradecimento.

À Professora Doutora Ana Paula Francisco, orientadora desta tese de mestrado, por ter sido uma das pedras basilares ao longo desta dissertação devido à transmissão sábia dos seus conhecimentos científicos, à excelente dinâmica de trabalho que impôs, e também pela sua simpatia, apoio, dedicação e disponibilidade.

À Professora Doutora Maria de Jesus Perry, co-orientadora desta dissertação, pela sua dedicação a esta tese de mestrado, quer ao nível da transmissão de conhecimentos teóricos e práticos, quer ao nível das sábias sugestões e críticas elaboradas ao longo desta dissertação.

À Professora Doutora Maria Eduarda Mendes, docente na Faculdade de Farmácia da Universidade de Lisboa, pela dedicada e sensata cooperação demonstrada ao longo desta tese de mestrado.

Aos meus colegas de laboratório, quer na elaboração do trabalho científico propriamente dito, quer pelo fantástico ambiente no laboratório, e não só. Dentro deste grupo, um agradecimento especial para Ana Sofia Newton, Ana Neca, Cátia Vieira, Daniel Gonçalves, Daniela Miranda, Marisa Nogueira, Marta Magalhães, Ricardo Ferreira, Rita Capela, Teresa Almeida e Vanessa Cabral. Um reconhecimento meritório é necessário ao profissionalismo, dedicação e boa disposição do técnico de laboratório Sr. Francisco Manuel.

Aos meus pais, pela educação que me incutiram e pelo óptimo ambiente familiar por eles proporcionado.

À minha namorada, Ana Tavares, pelo constante apoio e motivação em todos os momentos cruciais ao longo desta dissertação.

A todos os meus amigos, em especial ao João Simões e ao Tiago Duarte, pela boa disposição e companheirismo por eles demonstrado.

Abstract

A new serie of anti-tumor triazene prodrugs was synthesized and evaluated concerning their potential application in melanocyte-directed enzyme prodrug therapy (MDEPT). MDEPT strategy emerged to overcome the selectivity and toxicity problems associated with melanoma chemotherapy and is based on the use of non-toxic prodrugs that will be selectively activated by tyrosinase overexpressed in malignant melanocytes, releasing a potent cytotoxic agent inside tumour cells. The synthesized prodrugs **21** are formed by an alkylating agent, the monomethyltriazene **23** (MMT), linked to a tyrosinase substrate, the hydroxyphenylpropionic acid **24**, by an amide linkage.

In the synthesis of prodrugs **21**, the amide-bond formation was tried with different methodologies, which involved carboxylic acid activation. The most efficient methods were O-(Benzotriazol-1-yl)-N,N,N′,N′-tetramethyluroniumtetrafluoroborate (TBTU) assisted by microwave irradiation (20% yield) and N,N'-Dicyclohexylcarbodiimide/4-dimethylaminopyridine (DCC/DMAP) (15% yield). Prodrug synthesis was achieved with yields that did not exceed 20 %.

All prodrugs **21** revealed to be chemically stable in isotonic phosphate buffer (PBS) at physiologic pH ($60 \leq t_{1/2}$ (h) ≤ 123), and most of them showed to be slowly hydrolyzed in human plasma ($3 \leq t_{1/2}$ (h) ≤ 49). Only prodrugs **21c-f** (3-(4-hydroxyphenyl)propionic acid derivatives) revealed to be excellent tyrosinase substrates ($1.5 \leq t_{1/2}$ (min) ≤ 5) with a fast release of MMT **23** after 250 seconds of tyrosinase activation.

The maximum percentage of glutathione depletion ($GSH_{depletion}$ (%)) induced by prodrugs **21**, when they were metabolized into cytotoxic quinones by rat liver microsomes, ranged from 34.6 ± 8.6 to 43.6 ± 2.0 for prodrugs **21c-f** and was 45.7 ± 5.0 and 63.5 ± 5.0 for prodrugs **21a,b** (3-(3-hydroxyphenyl)propionic acid derivatives), respectively. Prodrugs **21c-f** revealed to be less hepatotoxic than prodrugs **21a,b**.

Prodrugs **21c-f** are also less hepatotoxic than similar compounds described in the literature, which were evaluated by the same type of assay.

Triazene prodrugs **21c-f** are promising for application in MDEPT strategy, as they have a great stability, an excellent tyrosinase affinity, an efficient mechanism of MMT **23** release and a moderate hepatotoxicity.

Keywords: Melanoma; Tyrosinase; Prodrug; Triazene; MDEPT; Hepatotoxicity

Resumo

O cancro de pele pode-se manifestar de diversas formas, sendo o melanoma a forma mais agressiva deste tipo de cancro. Apesar do melanoma representar apenas 11% de todos os cancros de pele diagnosticados, é responsável por 90% das mortes associadas a este tipo de cancro. Segundo o *Institute of Cancer Research* a incidência do melanoma tem tendência a triplicar nos próximos 30 anos, sendo a mudança climática, a principal causa deste aumento. A taxa de mortalidade do melanoma é tão elevada, pelo facto de este ter a capacidade de metastizar e invadir diversas partes do corpo. Este processo de metástase dificulta muito o desenvolvimento de uma terapêutica eficaz para o melanoma.

O aparecimento do melanoma deve-se à transformação dos melanócitos normais em malignos. O risco de ocorrer esta transformação pode ser aumentado devido a factores genéticos (ex: mutação num gene supressor de tumores) ou ambientais (ex: exposição a radiação ultravioleta A e B). Nos melanócitos malignos, o processo de melanogénese encontra-se aumentado e os níveis da enzima tirosinase, que é essencial neste processo, estão muito acima dos níveis detectados nos melanócitos normais. Tendo em conta que a tirosinase só se encontra nos melanócitos, e que está sobre-expressa nos melanócitos malignos, esta tem sido considerada como um possível alvo para uma quimioterapia mais selectiva e menos tóxica.

A tirosinase tem como principais substratos os monofenóis e os *o*-difenóis, mas também tem a capacidade de oxidar outros tipos de compostos fenólicos e até não fenólicos. Alguns compostos aromáticos como por exemplo as *o*-diaminas, os *o*-aminofenóis e até as anilinas são referidos como substratos desta enzima.

Encontram-se descritas na literatura, duas abordagens para o tratamento de melanoma, onde a tirosinase é responsável pela libertação/formação de um agente citotóxico no tumor. Uma dessas abordagens é a *melanocyte-directed enzyme prodrug therapy* (MDEPT). A estratégia MDEPT envolve o uso de pró-fármacos não tóxicos,

formados pelo fármaco citotóxico ligado a um substrato da enzima tirosinase. Deste modo o pró-fármaco só é activado na presença da tirosinase, libertando-se assim o agente citotóxico em grande quantidade no tecido tumoral.

A dacarbazina **1** (DTIC) foi aprovada em 1975 pela *Food and Drug Administration* (FDA) para o tratamento do melanoma, e actualmente ainda é o composto mais efectivo em monoterapia para o tratamento deste cancro. A DTIC **1** pertence à classe dos triazenos, mais especificamente aos 1-aril-3,3-dialquiltriazenos, e o seu mecanismo de citotoxicidade envolve a formação de uma espécie alquilante, o ião metildiazónio, que vai alquilar as bases púricas e pirimídicas do ácido desoxirribonucleico (ADN) e assim induzir a morte celular.

Nesta tese de mestrado, uma nova serie de pró-fármacos de triazenos anti-tumorais foi sintetizada e avaliada em termos de potencial aplicação na estratégia MDEPT. Os pró-fármacos sintetizados **21** são constituídos pelo ácido hidroxifenilpropanóico **24** ligado através de uma função amida ao monometiltriazeno **23** (MMT). A escolha do ácido hidroxifenilpropanóico **24** deveu-se ao facto deste ácido ser um bom substrato da tirosinase. O MMT **23** foi escolhido, uma vez que o seu mecanismo de citotoxicidade envolve o ião metildiazónio, que é o mesmo agente alquilante responsável pela citotoxicidade da DTIC **1**. A função amida tem como objectivo dar estabilidade química aos pró-fármacos **21** de modo a manter a citotoxicidade do MMT **23** inactiva até a enzima tirosinase actuar nos pró-fármacos **21**.

A síntese dos pró-fármacos **21** envolveu a formação de uma ligação amida entre a amina secundária do MMT **23** e o grupo ácido carboxílico do ácido hidroxifenilpropanóico **24**. Em geral, as funções amida são sintetizadas a partir da junção de ácidos carboxílicos com aminas, no entanto esta união é muitas vezes um processo difícil e complexo. De modo a superar estas dificuldades, têm sido desenvolvidos vários métodos, nos quais a acilação da amida ocorre com ácidos carboxílicos previamente activados. Usualmente esta activação é realizada através do uso de agentes de acoplamento. Neste trabalho de investigação, a activação do ácido

carboxílico **24** foi efectuada com recurso a diversos agentes de acoplamento. Os agentes de acoplamento utilizados foram: N,N'-diciclohexilcarbodiimida/4-dimetilaminopiridina (DCC/DMAP), tetrafluoroborato de *O*-(benzotriazol-1-il)-*N,N,N',N'*-tetrametilurónio (TBTU), cloreto de 4-(4,6-dimetoxi-1,3,5-triazin-2-il)-4-metilmorfolina (DMTMM) e cloreto de tionilo. A formação da ligação amida foi também realizada recorrendo ao uso de irradiação por microondas. Os métodos mais eficientes foram DCC/DMAP e TBTU (irradiação por microondas) com rendimentos de 15% e 20% respectivamente. Os pró-fármacos **21** foram sintetizados com rendimentos que não excederam os 20%. Apesar dos baixos rendimentos, os pró-fármacos **21** foram obtidos com um elevado grau de pureza e em quantidades que possibilitaram a análise dos mesmos para aplicação na estratégia MDEPT.

Com o intuito de avaliar os compostos **21** como potenciais pró-fármacos para aplicação na estratégia MDEPT, foram realizados três tipos de ensaios de estabilidade a 37 ºC. O primeiro ensaio foi efectuado em tampão fosfato isotónico (PBS) pH 7,4, no qual se analisou a hidrólise química dos pró-fármacos **21** a pH fisiológico. Todos os pró-fármacos **21** revelaram ser quimicamente estáveis com semi-vidas que variaram entre as 60 e as 123 horas. O ensaio seguinte consistiu no estudo da hidrólise dos pró-fármacos **21** em plasma humano, visto que este contém um conjunto de enzimas que catalisam a hidrólise da função amida. Todos os pró-fármacos **21**, com a excepção do **21b** ($t_{1/2} \approx 3$ horas), revelaram ser hidrolisados lentamente com semi-vidas que variaram entre as 6 e as 49 horas. Com os resultados obtidos nestes dois ensaios é de esperar que a maioria dos pró-fármacos **21** alcance o tumor sem sofrer uma prematura decomposição. No último ensaio foi avaliada a afinidade dos pró-fármacos **21** para a enzima tirosinase de cogumelo, que serve de modelo para a tirosinase humana, e foi também analisada a eficácia dos compostos **21** no processo de libertação do agente citotóxico MMT **23** após activação pela tirosinase. Os resultados obtidos neste ensaio, revelaram que os pró-fármacos **21a,b** (derivados do ácido 3-(3-hidroxifenil)propanóico) têm uma fraca afinidade para a tirosinase com semi-vidas ($t_{1/2} \approx 20$ horas) demasiado longas para terem interesse como pró-fármacos para aplicação na estratégia MDEPT. Já

os pró-fármacos **21c-f** (derivados do ácido 3-(4-hidroxifenil)propanóico) demonstraram ser excelentes substratos da tirosinase com semi-vidas que variaram entre 1,5 e 5 minutos. A libertação do agente citotóxico MMT **23** foi confirmada, sendo bastante rápida para os pró-fármacos **21c-f**, nos quais foi detectada após 250 segundos de exposição destes compostos **21c-f** à enzima tirosinase.

Os pró-fármacos **21** contêm na sua estrutura uma função fenólica que pode ser oxidada nos hepatócitos por enzimas do citocromo P450, originando quinonas. As quinonas são espécies extremamente reactivas que se ligam facilmente a nucleófilos, tais como a glutationa (GSH), induzindo a sua depleção e promovendo fenómenos de hepatotoxicidade. A avaliação de hepatotoxicidade destes pró-fármacos **21** foi realizada através de um ensaio a 37ºC em que se calculou a percentagem de depleção da GSH ($GSH_{depleção}$ (%)). Os resultados obtidos revelaram que os pró-fármacos **21a,b** ($GSH_{depleção}$ (%) = 45,7 ± 5,0 e 63,5 ± 5,0, respectivamente) são mais hepatotóxicos que os pró-fármacos **21c-f** ($34,6 \pm 8,6 \leq GSH_{depleção}$ (%) $\leq 43,6 \pm 2,0$). Observou-se também que a hepatotoxicidade induzida pelos pró-fármacos **21c-f** é inferior à observada para a maioria dos compostos análogos que se encontram descritos na literatura, e que foram analisados pelo mesmo tipo de ensaio.

Os pró-fármacos **21c-f** possuem uma boa estabilidade química, uma excelente afinidade para a tirosinase, um mecanismo rápido para a libertação do MMT **23** e uma hepatotoxicidade moderada, para poderem ser considerados promissores para aplicação na estratégia MDEPT.

Palavras-Chave: Melanoma; Tirosinase; Pró-fármaco; Triazeno; MDEPT; Hepatotoxicidade.

General Index

List of Figures

List of Tables

List of Abbreviations, Acronyms and Symbols

- **3-HAP** 3-hydroxyacetophenone
- **3-HBA** 3-hydroxybenzoic acid
- **4-HA** 4-hydroxyanisole
- **4-HAP** 4-hydroxyacetophenone
- **4-HBA** 4-hydroxybenzoic acid
- **4-HPP** 3-(4-hydroxyphenyl)propionic acid
- **ACN** Acetonitrile
- **AIC** 5-aminoimidazol-4-carboxamide
- **Ar** Aromatic
- **BER** Base excision repair
- ***br*** Broad
- **B.P.** Boiling point
- **CYP450** Cytochrome P450
- ***d*** Doublet
- **DCC** N,N'-dicyclohexylcarbodiimide
- **DCM** Dichloromethane
- **DCU** N,N’-dicyclohexylurea
- ***dd*** Doublet of doublets
- **DETAPAC** Diethylenetriaminepentaacetic acid
- **DMAP** 4-Dimethylaminopyridine
- **DMF** N,N-Dimethylformamide
- **DMTMM** 4-(4,6-dimethoxy-1,3,5-triazin-2-yl)-4-methyl-morpholinium chloride
- **DNA** Deoxyribonucleic acid
- **DTIC** Dacarbazine
- **DTNB** 5,5'-dithiobis-2-nitrobenzoic acid
- **EC** Enzyme Commission

- **e.g:** For example (from the Latin expression exempli gratia)
- **ESI-MS** Electrospray ionization mass spectrometry
- **FDA** US Food and Drug Administration
- **FTIR** Fourier transform infrared spectroscopy
- **GC-MS** Gas chromatography-mass spectrometry
- **GSH** Glutathione
- **h** Hour(s)
- **HIS** Histidine
- **HMQC** Heteronuclear Multiple Quantum Correlation
- **HMT** Hydroxymethyltriazene
- **HMTIC** 5-(3-hydroxylmethyl-3-methyl-1-triazenyl)imidazole-4-carboxamide
- **HOAt** 1-hydroxy-7-azabenzotriazole
- **HOBt** 1-hydroxybenzotriazole hydrate
- **HPLC** High-performance liquid chromatography
- **Hz** Hertz
- **IR** Infrared
- ***J*** Coupling constant
- $\boldsymbol{k_{obs}}$ Observable rate constant
- **M** Molar concentration
- ***m*-** *Meta*
- **m.p** Melting point
- **MDEPT** Melanocyte-directed enzyme prodrug therapy
- **MGMT** Methyl-guanine methyl-transferase
- **min** Minute(s)
- **MMR** Mismatch repair system
- **MMT** Monomethyltriazene
- **MTIC** 5-(3-methyl-1-triazenyl)imidazole-4-carboxamide
- **MW** Molecular weight

- **n** Number of moles
- **nd** Not detected
- **nm** Nanometer
- **NMR** Nuclear magnetic resonance
- ***o-*** *Ortho*
- ***p-*** *Para*
- **PBS** Phosphate buffered saline
- **ppm** Parts-per-million
- ***s*** Singlet
- **Sat.** Saturated
- **Sol.** Solution
- ***t*** Triplet
- **TBTU** O-(benzotriazol-1-yl)-N,N,N′,N′-tetramethyluronium tetrafluoroborate
- **TEA** Triethylamine
- **THF** Tetrahydrofuran
- **TLC** Thin layer chromatography
- **TMZ** Temozolomide
- **Tris** Tris(hydroxymethyl)aminomethane
- $\mathbf{t_{1/2}}$ Half-live
- **UV** Ultraviolet

- **Ω** Ohm
- **δ** Chemical shift
- **ν** Frequency
- **λ** Wavelength

CHAPTER 1 – Introduction

1.1 – Melanoma disease

Skin cancer represents one third of all diagnosed cancers and its incidence is, at the moment, in expansion especially in young adults. This type of cancer can emerge in different types of skin cells (figure 1), being the most frequent the basal cell carcinoma, the squamous cell carcinoma and the malignant melanoma [1-3].

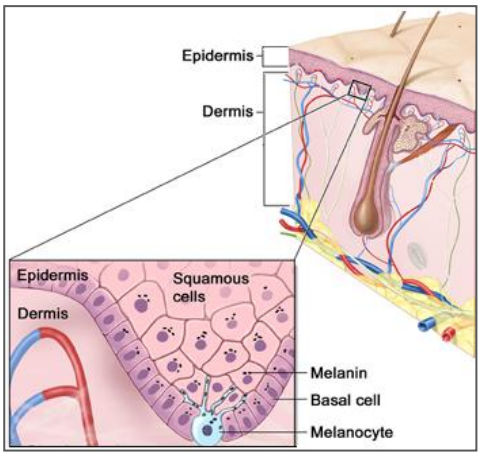

Figure 1 – Skin layers and some groups of skin cells. Adapted from [3].

The most aggressive form of skin cancer is the melanoma, which despite of only representing 11% of all skin cancer occurrences, is responsible for 90% of the deaths associated with skin cancer. According to the Institute of Cancer Research, the incidence of melanoma will triple in the next 30 years, due mainly, to climate change. In Portugal there are 700 new cases of malignant melanoma every year. Melanoma mortality rate is extremely high because this is the only form of skin cancer that has the ability to spread to secondary sites in the body via metastasis (figure 2). This metastasis ability is the major problem in the development of an efficient treatment for advanced metastatic melanoma [1,4,5].

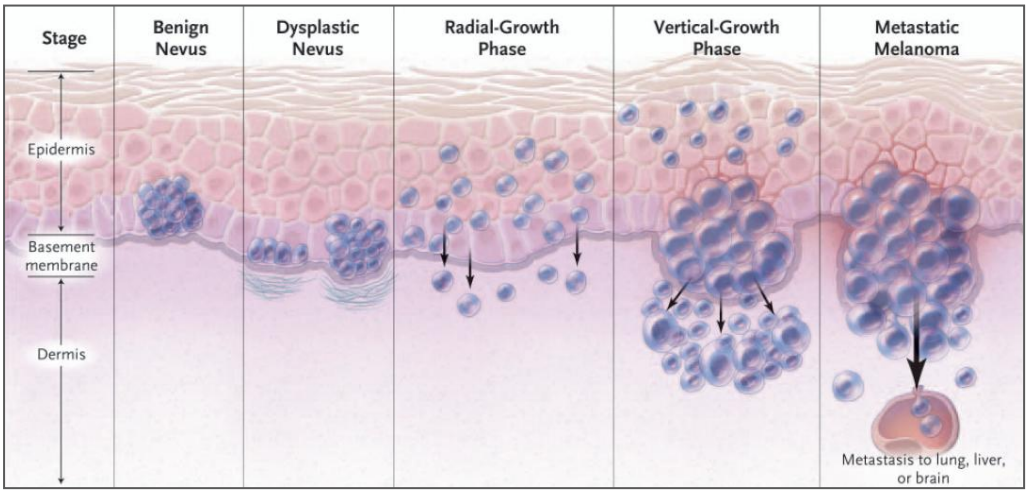

Figure 2 – Metastatic process in melanoma. Adapted from [6].

Malignant melanoma arises from malignant transformation of normal melanocytes [4]. The main risk factors for malignant transformation are:

- Genetic predisposition

Families with a history of melanoma, have mutations on certain genes (e.g: tumor suppressor genes), which increase the risk of malignant transformation.

- Environmental stressors

Exposure to ultraviolet radiation (UV_A and UV_B), which is responsible for genetic modifications in skin cells, increasing the production of growth factors and inducing the generation of reactive oxygen species that will damage the deoxyribonucleic acid (DNA) inside the melanocytes [6,7].

When malignant melanoma is diagnosed in early stages, it is highly curable, since it can be surgically removed. However in later stages, after metastasis and spreading to other locations, it is very difficult to treat and the options for medical treatment are restricted to biotherapy and chemotherapy. Standard chemotherapy agents are listed in table 1 [4,8].

Table 1 – Current chemotherapy agents for melanoma. Adapted from [4].

Chemotherapy Drug	Mode of Action	Advantages	Disadvantages
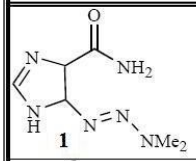 1 Dacarbazine	Alkylating agent	Only chemotherapy drug approved by the FDA for melanoma; produces 25% response for people with metastasis to surrounding skin and lymph nodes	Bone marrow depression; anaemia; anorexia; headache; seizures; given intravenously
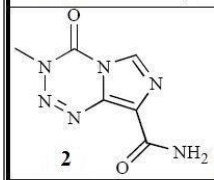 2 Temozolomide	Alkylating agent	Given orally but as effective as dacarbazine; it may offer better protection against development of brain metastasis	Nausea and vomiting; constipation; anorexia; headache; fatigue; risk of irreversible infertility in men; increased risk of catching pneumonia
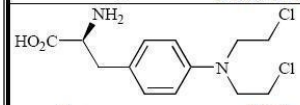 3 Melphalan	Bifunctional alkylating agent	Can be given orally	Bone marrow depression; nausea and vomiting; diarrhoea; alopecia; muscle atrophy
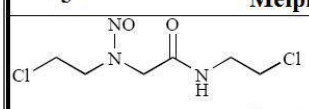 4 Lomustine	Alkylating agent and inhibits several steps in the synthesis of nucleic acids, also inhibits the repair of single strand breaks in the DNA chains	Can be given orally Does not cause indigestion like many other chemotherapy drugs	Marrow depression is sustained longer than for nitrogen mustards; can cause birth defects, risk of irreversible infertility in men; nausea; vomiting
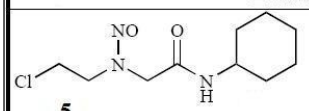 5 Carmustine	Alkylating agent and inhibition of several enzymes	Absence of significant cutaneous toxicity	Pulmonary toxicity, bone marrow toxicity; nausea and vomiting; kidney damage

In malignant melanocytes, the melanogenesis process is up-regulated and tyrosinase expression is noticed to increase during tumorigenesis. Due to this over-expression, tyrosinase has been considered as an exploitable target enzyme to search for selective and less toxic chemotherapeutic approaches for melanoma treatment [4,9,10].

1.2 – Tyrosinase

Tyrosinase (Monophenol monooxygenase, Enzyme Commission (EC) 1.14.18.1) is located within the melanosomes, which are organelles inside the melanocytes. This is a copper enzyme essential to the biosynthesis of melanins (figure 3). This oxidoreductase is able to bind dioxygen and is responsible for the catalysis of two different types of reactions [4,11,12]:

- Hydroxylation of monophenols to *o*-diphenols (monophenolase or cresolase activity, EC 1.14.18.1);
- Oxidation of *o*-diphenols to *o*-quinones (diphenolase or catechol oxidase activity, EC 1.10.3.1).

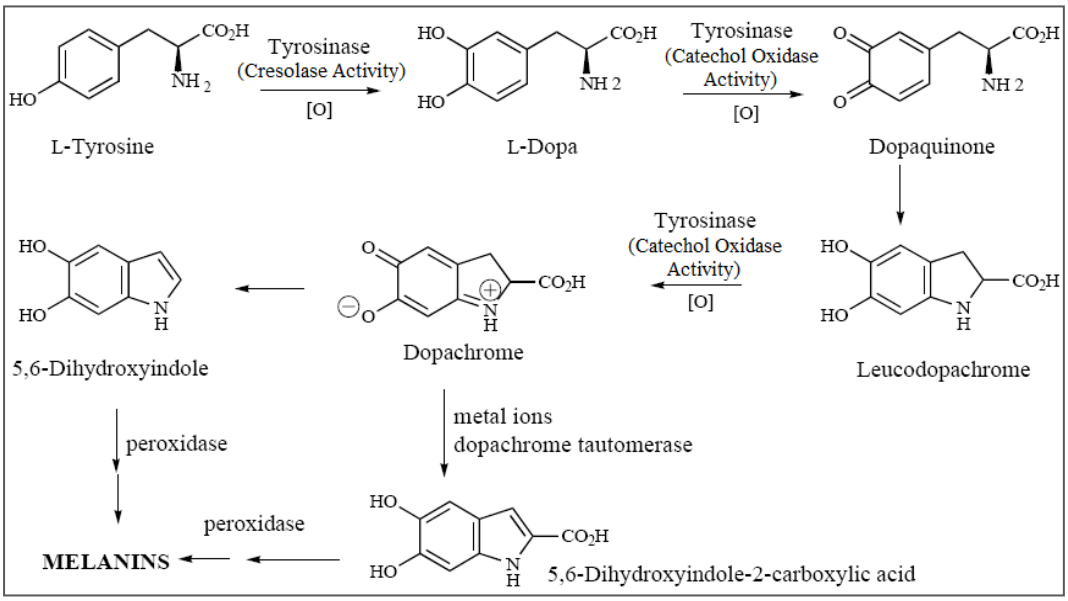

Figure 3 – Biosynthesis of melanins. Adapted from [4].

The active site of mammalian tyrosinase contains a binuclear copper cluster and is similar in mushroom tyrosinase (*Agaricus bisporus*). This fact explains why mushroom enzyme has been widely used as a model for mammalian enzyme [13].

An important feature of this active site is the coordination between the binuclear copper and the six histidine (HIS) residues (figure 4). This coordination is fundamental to enable the binding of molecular oxygen [4,14].

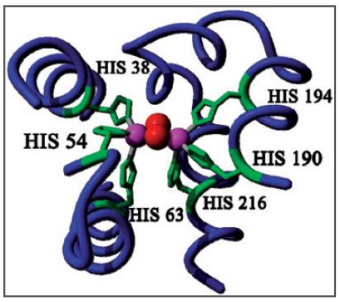

Figure 4 – Active site of *Streptomyces castaneoglobisporus* tyrosinase. Legend: Copper – magenta; Oxygen – red; HIS residues – green. Adapted from [14].

The enzymatic activity of tyrosinase can be described by two interpenetrating reactive cycles. In these cycles, tyrosinase active site can be in three different functional states, *met*-tyrosinase, *oxy*-tyrosinase and *deoxy*-tyrosinase (figure 5) [14].

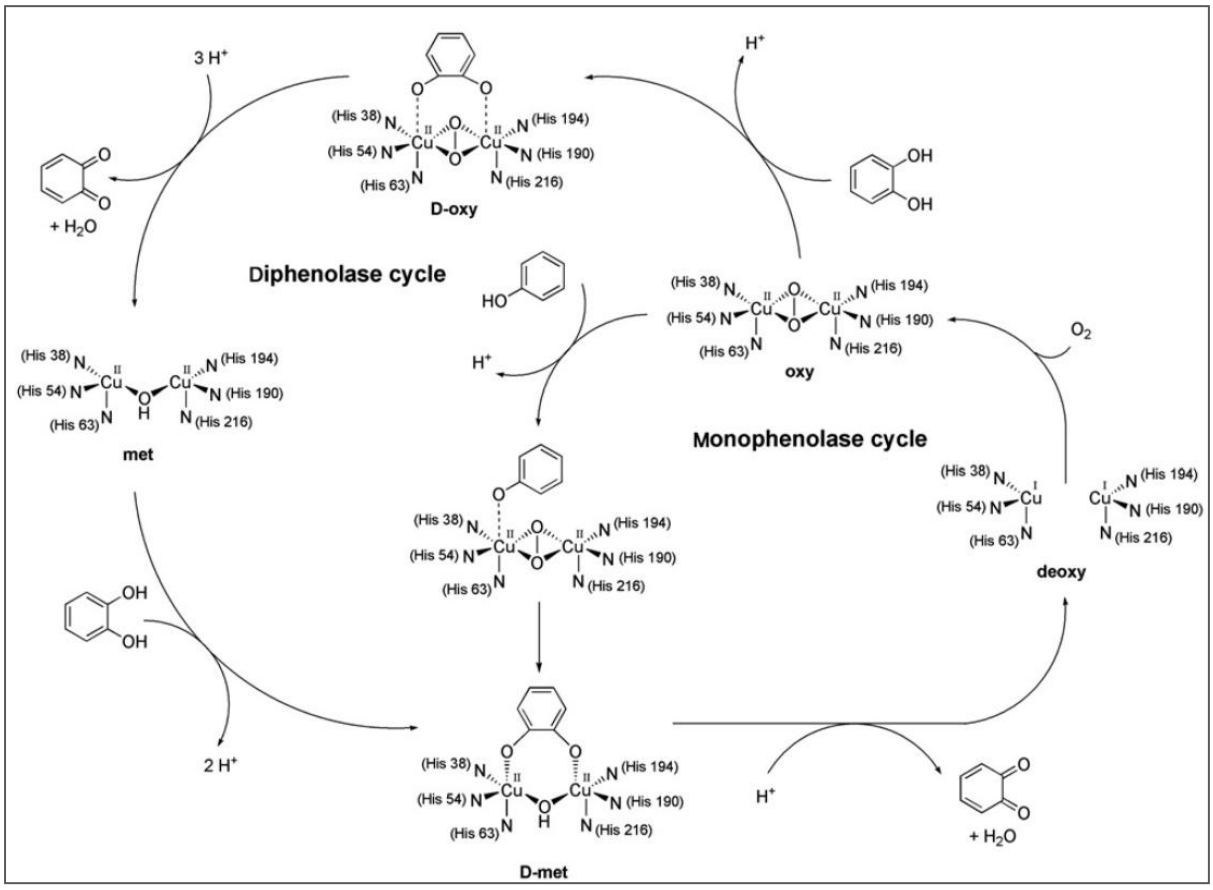

Figure 5 – The two different oxidation cycles and the different role in the oxidation process by the three different functional states of tyrosinase active site [14].

In general, there are two chemotherapeutic approaches for melanoma that involve tyrosinase for drug release. They have been referred as the "Achilles heel" and the "Trojan horse" approach [4,9].

"Achilles heel" approach is based on the selection of analogues of tyrosinase substrates, which are able to maximise the formation of reactive ortho-quinones by tyrosinase action. In this approach is very important to prevent the cyclization reaction (figure 6) of the ortho-quinones generated because this side reaction will deactivate their citotoxicity [4]. The major limitation of this approach is to achieve the necessary quinone levels for an efficient melanoma treatment. This limitation occurs due to the fact that the reaction rate of ortho-quinone reduction by endogenous thiols (e.g: glutathione (GSH)) is much higher than the reaction rate responsible for DNA and protein alkylation [9,15]. Quinones can also arrest DNA synthesis via thymidylate synthase inhibition [16].

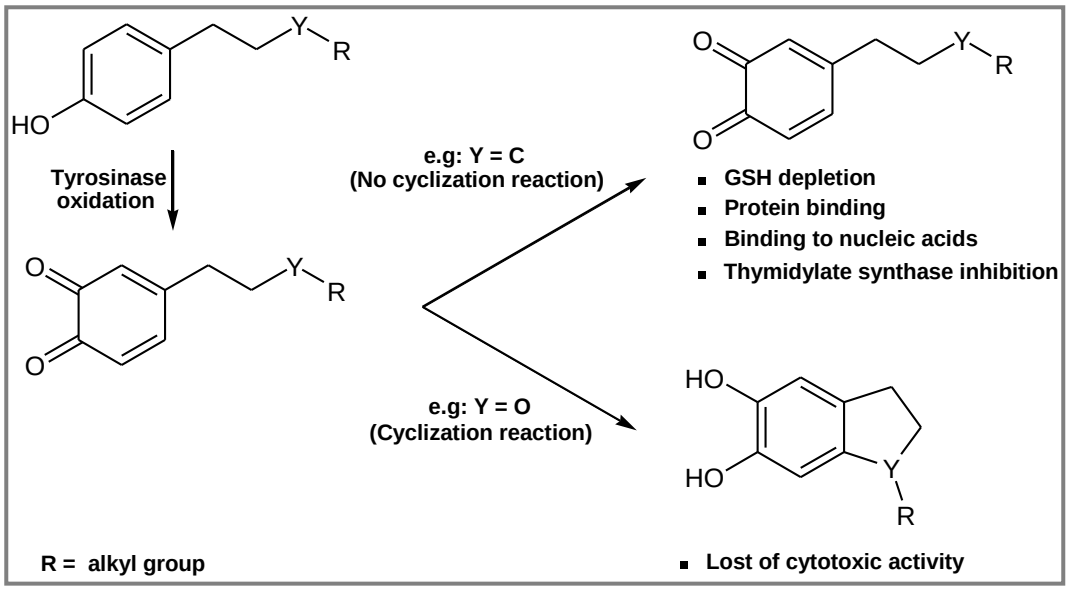

Figure 6 – Scheme of "Achilles heel" approach.

"Trojan horse" approach (figure 7) involves the use of non-toxic prodrugs, which will be activated in a tyrosinase dependent process. These prodrugs are structurally formed by a citotoxic moiety linked to a tyrosinase substrate. The citotoxic drug is released after tyrosinase oxidation. This approach is also known as melanocyte-directed enzyme prodrug therapy (MDEPT) [4].

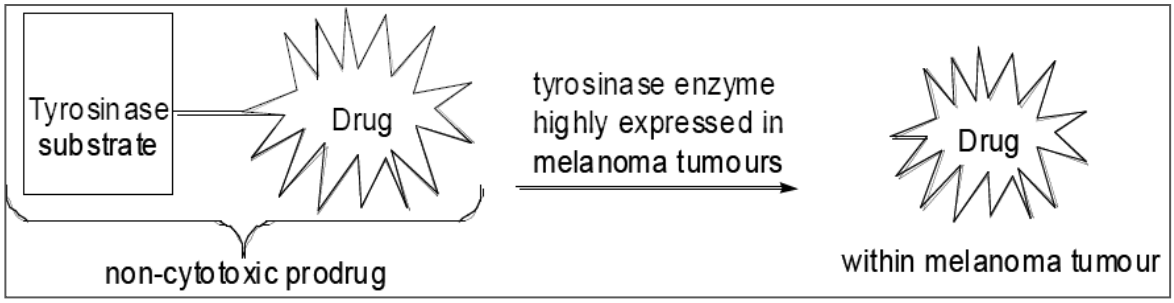

Figure 7 – Scheme of "Trojan horse" approach [4].

Apart from its natural substrates (monophenols and *o*-diphenols), tyrosinase has also the ability to oxidize a variety of other phenolic and non phenolic substrates. Many aromatic *o*-diamines and *o*-aminophenols have been reported to be quinonised by tyrosinase, and even aromatic monoamines (anilines) have been referred to be *o*-hydroxylated by this enzyme [17-19].

Riley and co-workers tested, by oximetry, twenty-six substituted phenols for their rate of oxidation by mushroom tyrosinase *in vitro*. Among the phenolic analogs studied it was found that 3-(4-hydroxyphenyl)propionic acid was a good tyrosinase substrate [20].

Tyrosinase can be considered a promising target enzyme for prodrug activation due to:

- It is only located in melanocytes and is over-expressed in melanoma cells;
- Turnover numbers are high for tyrosinase, resulting in a rapid prodrug activation;
- Total tyrosinase activity is correlated with the degree of malignancy:
    - 3667 to 46183 units of tyrosinase per mg of melanotic melanoma tissue;
    - 168 to 508 units of tyrosinase per mg of partially melanotic melanoma tissue;
    - 14 to 75 units of tyrosinase per mg of amelanotic melanoma tissue [21-23].

Despite of these good indicators, the prodrugs activated by tyrosinase have a phenolic or a catecholic moiety that can be oxidized in the corresponding cytotoxic quinones not only by tyrosinase but also by other undesired mechanisms (e.g: oxidation by liver cytochrome P450 isoenzymes (CYP450)).

1.3 – Prodrugs in anticancer chemotherapy

Prodrugs were initially defined in 1959 by Adrien Albert, as pharmacologically inactive compounds, which are converted into the active drug by a metabolic biotransformation [24]. Currently, the best definition of prodrugs establishes that they are chemical derivatives of an active drug pharmacologically inactive, which suffer a transformation process (spontaneous or enzymatic) within the body in order to release the active drug [25].

In terms of classification, prodrugs can be divided according with two major criteria, the chemical classification and its mechanism of activation [26]. According to chemical classification, prodrugs can be:

Carrier-linked prodrugs – Compounds that have the active drug linked to a carrier, which will be later released. The linker must be labile and the carrier must be biologically inactive and non-toxic [24,27]. Some types of carrier linked prodrugs:

- Macromolecular prodrugs – Compounds with the active drug linked to a polymer, which will increase the solubility, the stability and the drug distribution time [28];
- Drug-Antibody conjugates – Immunoconjugates, which have the active drug attached to an antibody specific for tumor-expressed antigens [29]:

- Mutual prodrug – Compounds that have two active drugs linked together and each drug acts as a promoiety for the other. This means that the carrier used, is another biologically active drug instead of some inert molecule [30];
- Drug-Enzyme Substrate conjugates: Compounds, which have the active drug linked to a specific or an analogue substrate of an enzyme. The substrate moiety will carry the drug directly to a specific enzyme, which will promote the release of the active drug [31].

Bioprecursors – Compounds that are metabolized into a new compound which is the active drug [26]. Some types of bioprecursors:

- Site-specific chemical delivery systems – Compounds which through sequential metabolic transformations, release the active drug in the desired target, thus overcoming the transport problems and diminishing the toxicity outer the targets [32];
- Bioreductive prodrugs – Compounds that have functional groups (e.g: quinones, nitroaromatics, N-oxides) that will be reduced/activated by the reducing environment or by bioreductive enzymes [31,33].

Based in the mechanism of activation, prodrugs can be:

Enzymatically activated – Prodrugs are activated by enzymes that are overexpressed and localised in the desired targets. This type of activation has as main benefits the fact of being a time- and tissue-controlled process and has as main challenges to overcome, inter- and intraspecies variability, genetic polymorphisms and the potential for drug-drug interactions [26].

Non-enzimatically activated – Prodrugs are activated by a chemical process (e.g: spontaneous chemical cleavage at physiological pH). The problems observed in enzymatic activation (e.g: inter- and intraspecies variability, genetic polymorphisms and drug-drug interactions) are solved by this mechanism, but in this type of activation,

there are chemical stability issues as insufficient half-live and the site of prodrug activation is undefined [26].

Prodrug strategy in drug discovery allows the overcoming of pharmaceutical, pharmacokinetic and pharmacodynamic problems. One of the most important areas of development that stimulates prodrug progress is the rationale design of them (e.g: prodrugs for anticancer therapy) in order to increase their selectivity for desired targets [26].

Almost all drugs used in the treatment of cancer are systemic antiproliferative agents (cytotoxins), which preferably eliminate cells during the division process, by attacking their DNA at some level (synthesis, replication, or processing). Despite of the advantages of using these cytotoxins as anticancer agents, due to their ability to eliminate a large number of tumor cells, their disadvantages have always been a main factor of concern. One of these disadvantages is the fact that these antiproliferative agents can affect normal cells (e.g: bone marrow cells). The other main disadvantage is that not all cancer cells have an exacerbated proliferation. These disadvantages make the therapeutic effectiveness of these antiproliferative agents very narrow [34,35].

In order to overcome these disadvantages, it is necessary to implement a strategy that makes these drugs more selective for tumor cells. To achieve this goal, it is required to seek out for tumor-specific mechanisms that will only transform the non-toxic prodrug into the citotoxic drug in the tumor region [34]. It is important to report that, cytotoxin prodrugs have been produced and used for a long time, but their activation was not specific for tumor cells, their use had only the goal of improving the bioavailability of the cytotoxins [35].

Tumor-activated prodrugs have been developed not only with the aim of improving the bioavailability of drugs but also to be activated by tumor-specific mechanisms, exploiting the differences at physiological, metabolic or genetic level between tumor and normal cells. The structure of these prodrugs (figure 8) can be subdivided in three parts: trigger, linker and effector. One of the major advantages of

this structural model is the possibility to optimize each different structural unit for their specific role [35,36].

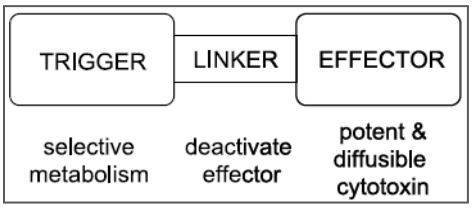

Figure 8 – Structure model of tumor-activated prodrugs [35].

The trigger role is prodrug transport to a specific location. The trigger is variable according to the tumor-specific mechanism present [35].

The linker is like a switch, at the beginning it maintains the prodrug inactive, but when the prodrug reaches the tumor-specific mechanism, the linker allows a rapid and a substantial release of the effector [35].

The role of the effector should be the elimination of the largest number of tumor cells in any conditions of pH and in any phase of cell cycle. The effector needs to have a significant bystander effect (figure 9), in order to diffuse into the neighbouring malignant cells around the tumor cells that are able to activate the prodrug. This is very important because tumor cells have a large diversification, so in all tumor cells population, probably only a few of them have the tumor-specific mechanism for prodrug activation. This diffusion must be limited in order to ensure that the effector does not reach normal cells in the neighbourhood. To get an effective bystander effect, the effectors must have an adequate stability and an appropriate diffusion, which can be obtained by building effectors that bind strongly to macromolecules such as DNA [25,35,36].

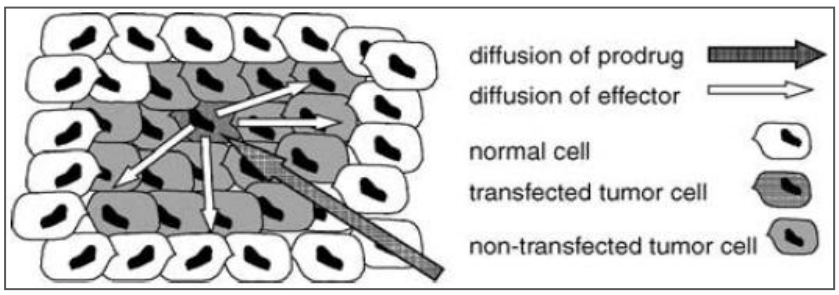

Figure 9 – Bystander effect [35].

1.4 – Triazenes in anticancer chemotherapy

Initially, anticancer chemotherapies were extremely cytotoxic, consisting of antitumor antibiotics, antimetabolites and alkylating agents. Considered as the oldest class of anticancer drugs, alkylating agents are a major cornerstone in the treatment of lymphomas, leukaemia and solid tumours. One important feature is the fact that these agents could be administered repeatedly with less induced resistance than other classes of anticancer drugs. Alkylating agents act as DNA alkylators, since they are able to form covalent bonds with purine bases. This alkylation process leads to crosslinking of DNA strands and induction of apoptosis. Presently, there are five major types of alkylating agents used in the chemotherapy of neoplastic diseases: nitrogen mustards, ethylenimines, alkyl sulfonates, nitrosoureas and triazenes [24,37-39].

Triazene compounds have in their structure (figure 10) three consecutive nitrogen atoms (triazenyl group). This group represents the active moiety of triazenes and is responsible for their chemical, physical and antitumour properties. Triazenes can be tri-, di-, mono- or non-substituted depending on the number of hydrogen substitutions by other groups in $R_{1,}$ R_2 and R_3 positions [40,41].

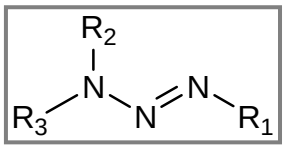

Figure 10 – Triazene general structure.

The first triazene compound **6** was synthesized in 1862 by Griess in the reaction between diazonium salts and nucleophilic nitrogen compounds [42].

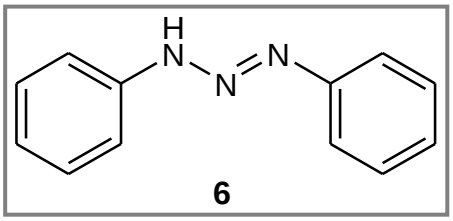

Currently, triazene compounds can be easily synthesized from anilines or alkyl azides (figure 11). In the aniline synthetic route, anilines are usually treated with nitrite ion under acidic conditions to form a diazonium salt, which reacts with a primary or secondary amine to provide the desired triazene with a high yield. To obtain triazenes from alkyl azides, a reaction between Grignard or alkyl lithium reactants and alkyl azides must occur [43].

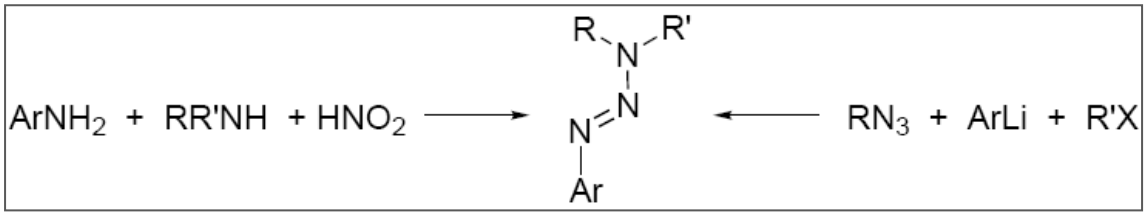

Figure 11 – General synthetic routes for triazenes [43].

In 1955, Clarke and co-workers reported for the first time the biologic activity of triazenes as antitumor agents. It was shown that 1-phenyl-3,3-dimethyltriazene **7** inhibited the growth of sarcoma 180 in mouse [44].

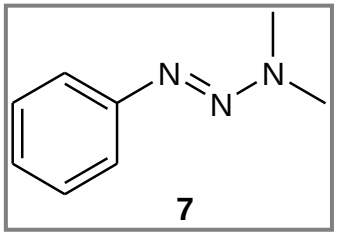

Anticancer activity of triazenes can be explained by the generation of methyldiazonium ion, the alkylating specie from triazenes. This alkylating agent is generated after several transformations of triazene compounds (figure 12) [45].

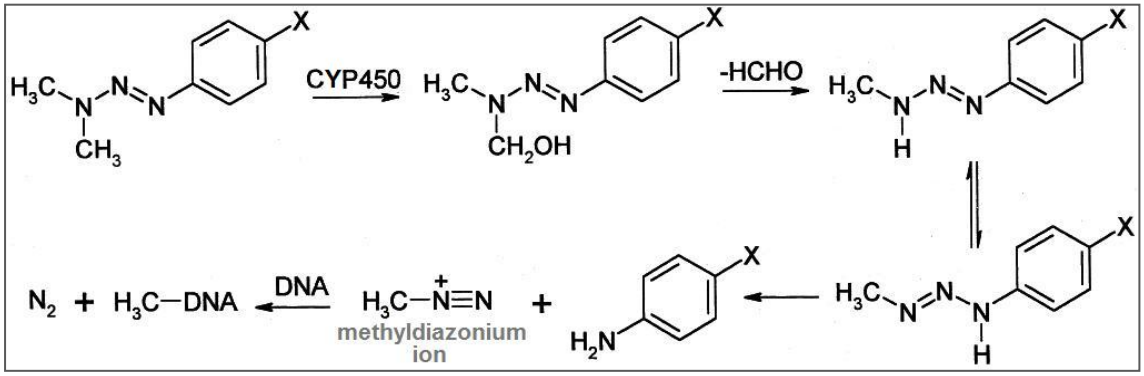

Figure 12 – Formation of methyldiazonium ion and its DNA alkylation reaction. Adapted from [45].

Among all the current chemotherapy agents used to treat melanoma (table 1), Dacarbazine (**1**, DTIC) and Temozolomide (**2**, TMZ) are triazene compounds of clinical interest [4,40].

More than three decades after its initial approval by US Food and Drug Administration (FDA) in 1975, DTIC **1** remains the most effective single-agent for the metastatic melanoma therapy, with a response rate between 15% and 25% [38,46,47].

DTIC **1**, i.e. 5-(3,3-dimethyl-1-triazenyl)imidazole-4-carboxamide belongs to triazene class of 1-aryl-3,3-dialkyltriazenes and is structurally related to purines. This compound emerged as the result of a rational attempt to produce interfering agents in the purine biosynthesis. Despite of DTIC **1** structurally resembles 5-aminoimidazol-4-carboxamide (AIC), which is an intermediate metabolite of purine biosynthesis, DTIC **1** is not classified as an antimetabolite because this is not its principal mechanism of action [38,40].

DTIC **1** is a prodrug and needs to be metabolized (figure 13), by liver microsomes (CYP450 isoenzymes), to give 5-(3-hydroxylmethyl-3-methyl-1-triazenyl)imidazole-4-carboxamide (HMTIC). Then HMTIC, by loss of formaldehyde, is converted to 5-(3-methyl-1-triazenyl)imidazole-4-carboxamide (MTIC), which is the cytotoxic agent. MTIC decomposes spontaneously into the major metabolite AIC and methyldiazonium ion, which is the alkylating specie. This alkylating agent is responsible for producing methyl adducts in DNA. Methylation on the O^6 position in guanine is largely responsible for the antineoplastic (and also mutagenic) effect of DTIC **1**, as it can promote an incorrect base pairing with thymine (figure 14). These adducts lead to apoptosis or if the cell survives, induce somatic point mutations in DNA helix [38,40,48].

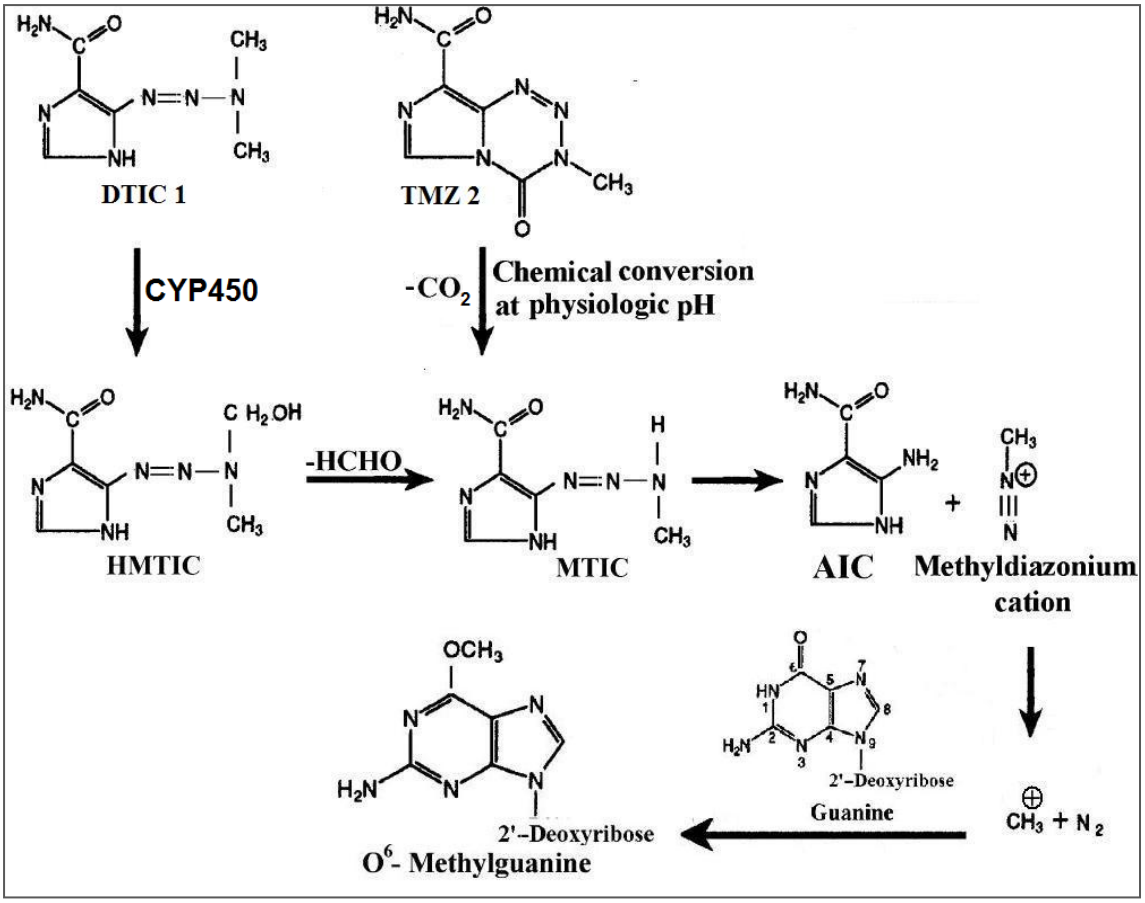

Figure 13 – DTIC 1 and TMZ 2 activation and mechanism of DNA alkylation. Adapted from [40].

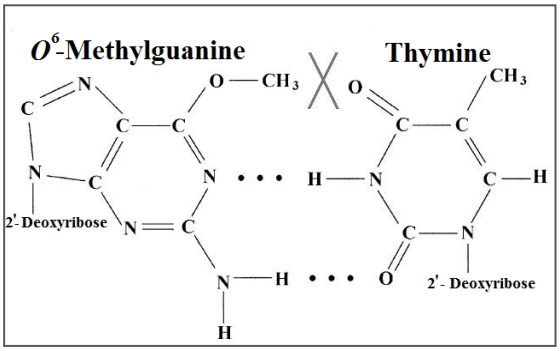

Figure 14 – Incorrect base pairing between *O*^{6}-methylguanine and thymine. Adapted from [40].

TMZ **2** received FDA approval for the treatment of anaplastic astrocytome and glioblastoma multiforme. Studies have also been done to show its activity in the treatment of malignant melanoma [37,49].

TMZ **2**, i.e. 8-carbamoyl-3-methylimidazo[5,1-d]-1,2,3,5-tetrazin-4(3*H*)-one belongs to a triazene class named acyl-substituted triazenes. It was first synthesized in 1984 and is a 3-methyl analogue of the mitozolomide **8**, which has demonstrated antineoplastic activity against malignant melanoma but with severe side effects. In terms of function and structure TMZ **2** is similar to DTIC **1** [40,43].

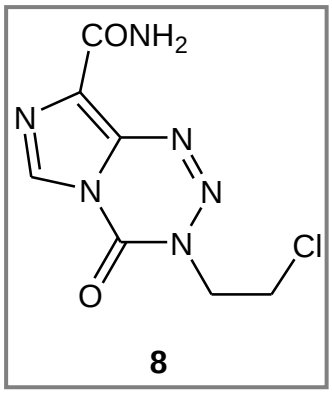

8

Considered as a MTIC prodrug, TMZ **2** is directly activated to MTIC (active metabolite of DTIC **1**) by a spontaneous chemical decomposition at physiological pH (figure 13). After generation of MTIC, the process of DNA alkylation is the same as for DTIC **1** [38,40,45].

Human cells have developed defensive mechanisms that lead to drug resistance. This is a major problem because it can narrow the efficiency of alkylating drugs. Cytotoxic effects of triazene compounds and cell resistance to them depend on at least three DNA repair systems, methyl-guanine methyl-transferase (MGMT), mismatch repair (MMR) and base excision repair (BER). MGMT removes alkyl adducts from the O^6 position of DNA guanine. High levels of MGMT are responsible for normal and tumor cell resistance to triazenes. This resistance problem is overcome by the use of triazenes in the presence of MGMT inhibitors, which increases triazene citotoxicity against target cells expressing high MGMT levels. MMR repairs biosynthetic errors generated during DNA replication. This system is not able to repair the DNA damage caused by triazenes, and promotes their cytotoxic effects with activation of cell cycle arrest and apoptosis. BER is able to repair other types of DNA methylation caused by

triazenes. Therefore, triazene citotoxicity can be enhanced with the use of BER inhibitors [37,40,48].

1.5 – MDEPT strategy

As described before, tyrosinase expression in melanoma becomes up-regulated leading to a marked raise in tyrosinase levels inside the cancerous cells. The basis for MDEPT strategy (figure 15) is to "hijack" this enzyme, from its biological pathway, to convert non-toxic prodrugs into citotoxic drugs that will promote the death of cancerous cells. The three components of these prodrugs must have the following characteristics:

- Trigger – This entity must be a good tyrosinase substrate, as an analogue or a derivative of natural substrates of tyrosinase. This entity will confer selectivity in the MDEPT strategy;
- Linker – Structure with the function of maintaining the non-toxic prodrug stable until it reaches the enzyme. This structure will be responsible for reducing the toxicity in other parts of the body;
- Effector - This unit has to possess a known citotoxic mechanism and an effective bystander effect. This unit is responsible for the efficiency of MDEPT strategy, by eliminating a considerable number of cancerous cells [1,4,50-52].

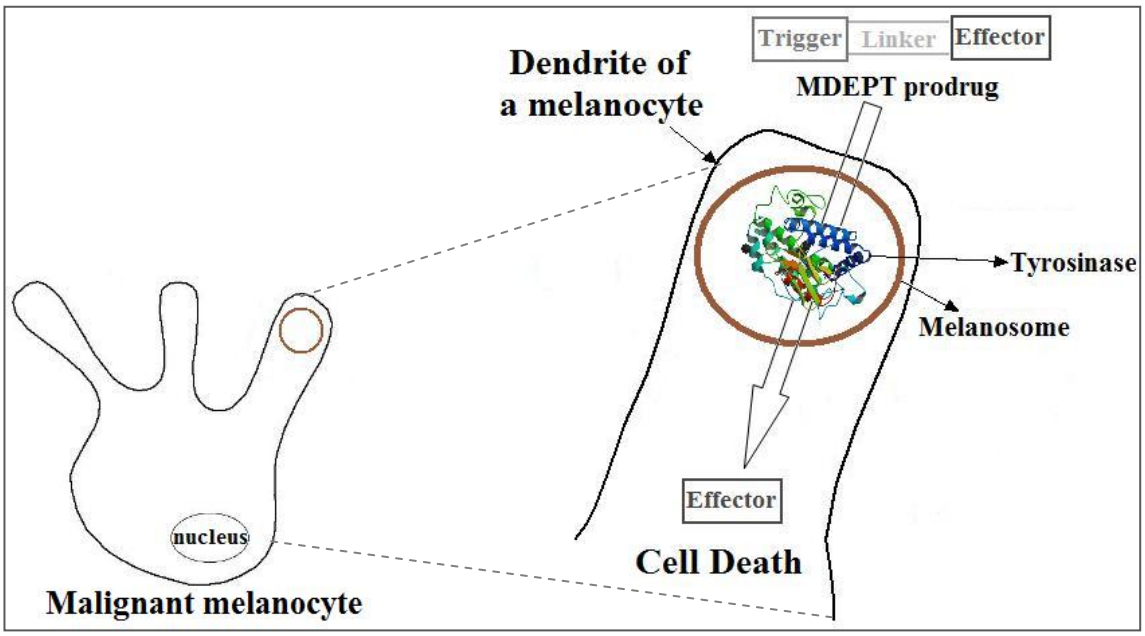

Figure 15 – MDEPT strategy. Tyrosinase structure (PDB 1WX2)

MDEPT strategy has as major advantages:

- It offers a highly selective triggering mechanism for drug delivery;
- It relies on tyrosinase, which is a good enzyme for prodrug activation [22,50].

The major disadvantage of MDEPT strategy is due to the use of prodrugs with phenolic and catecholic moieties that can lead to toxicity in undesired parts of the body, namely in the liver [22,53].

The first reference to MDEPT strategy was done by Jordan and co-workers in 1999 [51]. Since then, there have been several reports in literature about this strategy with different triggers, linkers, effectors and mechanisms for drug release.

In 1999, Jordan and co-workers synthesized a phenyl mustard prodrug **9**, which has a dopamine moiety linked to phenyl mustard by a carbamate unit [51].

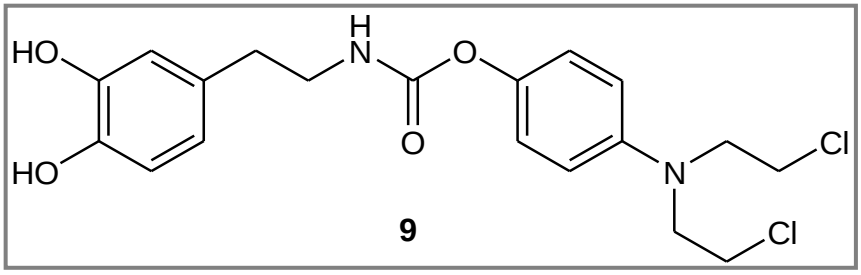

9

After the synthesis of prodrug **9**, Jordan and co-workers ascertained its efficacy to act in MDEPT strategy, using scanning oximetry, gas chromatography-mass spectrometry (GC-MS) and cytotoxic assays. Results from citotoxicity assays revealed an increase in the cytotoxic activity of prodrug **9** against tyrosinase-upregulated cell lines when compared with cell lines displaying little or absent tyrosinase activity. The nitrogen mustard release was verified by GC-MS evaluation, suggesting that prodrug **9** was indeed a substrate for tyrosinase. Analysis of these results led the authors to propose a tyrosinase-dependent mechanism for drug release, in which the ortho-quinone generation is followed by a cyclization pathway (figure 16) [51].

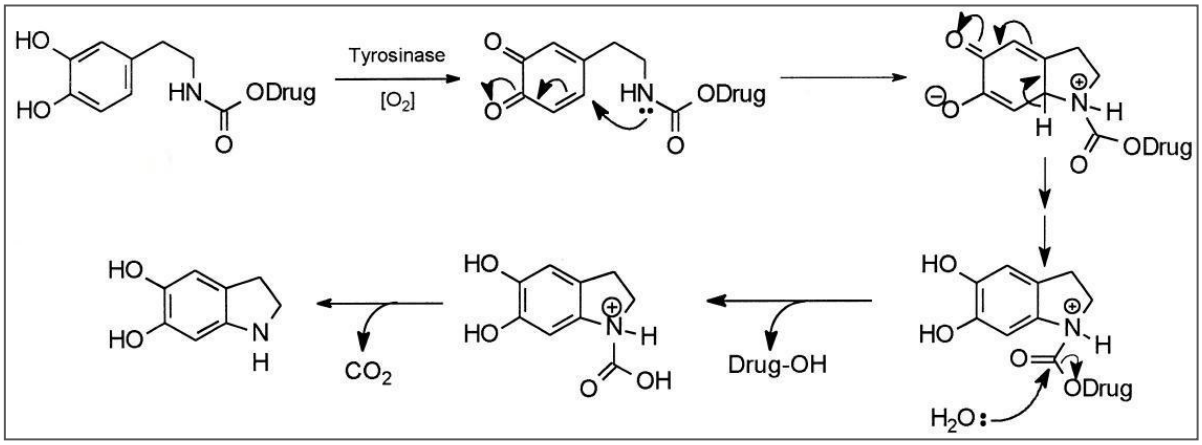

Figure 16 – Mechanism of drug release proposed by Jordan and co-workers [51].

In 2001, the same research group synthesized a more extensive range of prodrugs **10**-**16** and examined their ability to be oxidised by tyrosinase. Three different types of prodrugs were synthesized: phenyl mustard prodrugs **10**-**14**, bis-chloroethyl amine mustard prodrugs **15a**-**c** and daunomycin prodrug **16**. The cytotoxic entities used were previously applied as anticancer drugs in clinic trials. The activation of prodrugs **10-16** by tyrosinase was proposed to undergo by the same mechanism referred in 1999 (figure 16) [52].

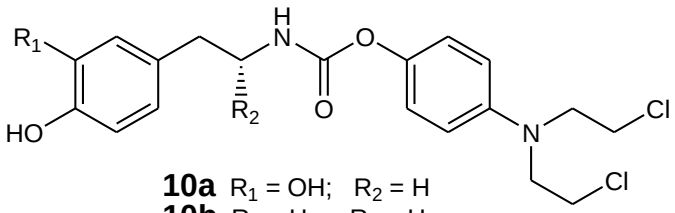

10a R_1 = OH; R_2 = H
10b R_1 = H; R_2 = H
10c R_1 = H; R_2 = CO_2Me

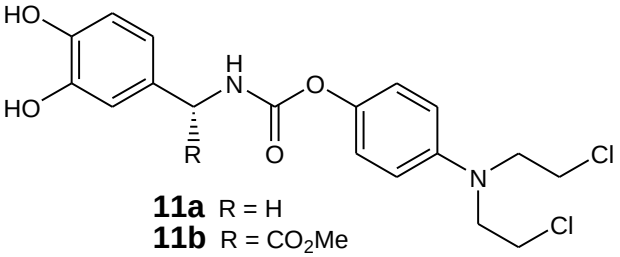

11a R = H
11b R = CO_2Me

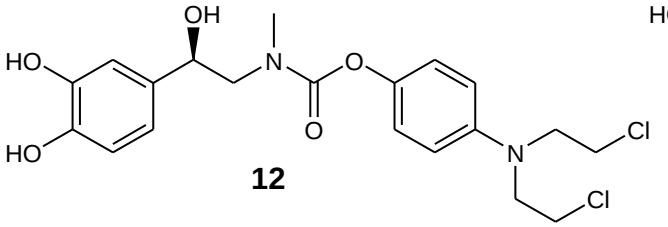

12

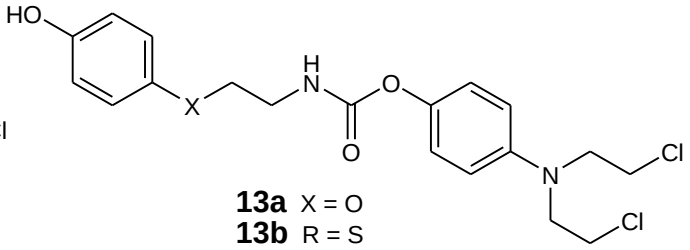

13a X = O
13b R = S

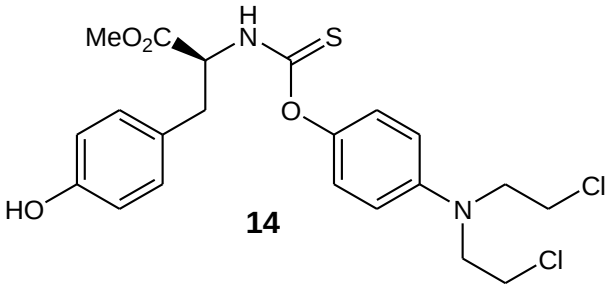

14

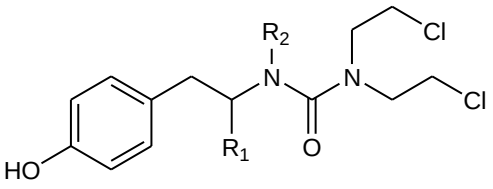

15a R_1 = H; R_2 = H
15b R_1 = H; R_2 = Me
15c R_1 = CO_2Me; R_2 = H

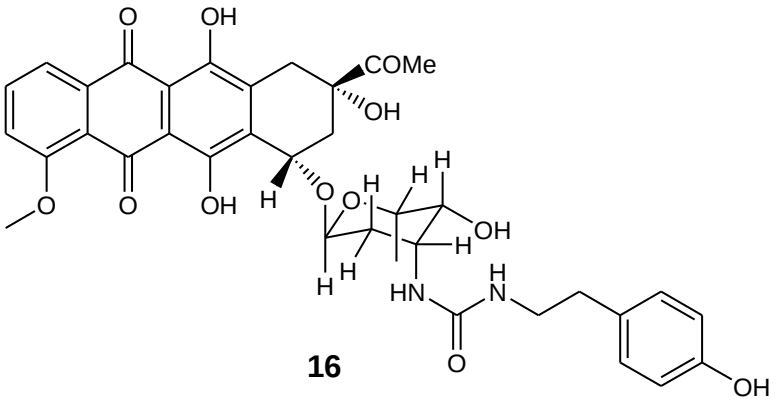

16

Additionally Jordan and co-workers found that:

- Prodrug **15a** was an excellent substrate for tyrosinase;
- Prodrugs **10a,b** and **15c** were as good tyrosinase substrates as tyrosine methyl ester;
- Prodrugs **13a,b** showed a slower oxidation rate due to heteroatom incorporation in the trigger part of the prodrug;
- Nitrogen methylation in prodrug **15b** reduced its rate of oxidation nearly 10 times in comparison with prodrug **15a**;
- Transformation of carbamate linker (prodrug **10c**) into a thiocarbamate linker (prodrug **14**) led to a decrease of tyrosinase oxidation;
- Prodrug **16**, not surprisingly, was a poor tyrosinase substrate due to the steric hindrance caused by daunomycin;
- The worst tyrosinase substrate was prodrug **11b**, which was not oxidised by tyrosinase [52].

Jordan and co-workers also monitored the drug release in the presence of tyrosinase. The study showed the release of phenol mustard drug from prodrugs **10a,b**. However in the case of prodrug **15a**, the drug release was not detected, probably due to the instability of this compound in aqueous media [52].

In 2002, Jordan and co-workers synthesized a new prodrug **17**, which was a derivative of prodrug **10b**. The change carried out, was the introduction of a urea linker (prodrug **17**) instead of a carbamate linker (prodrug **10b**) [54].

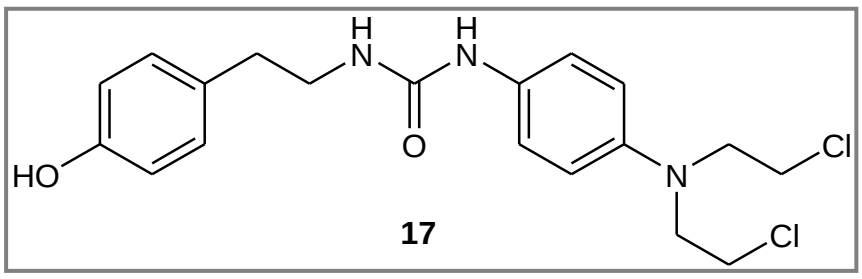

17

The results obtained showed that prodrug **17** was as good substrate for tyrosinase as prodrug **10b**. Jordan and co-workers also proved the release of the cytotoxic drug from prodrug **17**, when exposed to tyrosinase. They assumed that prodrug **17** released the cytotoxic drug after tyrosinase activation by the same mechanism proposed in 1999 (figure 16) [54].

In 2005, Knaggs and co-workers synthesized two novel series of MDEPT prodrugs **18** and **19**. The trigger units of prodrugs **18** were found to be substrates of tyrosinase with 70% of the oxidation rate when compared with L-tyrosine. In prodrugs **19**, the trigger unit was also reported as being a good substrate for tyrosinase [39].

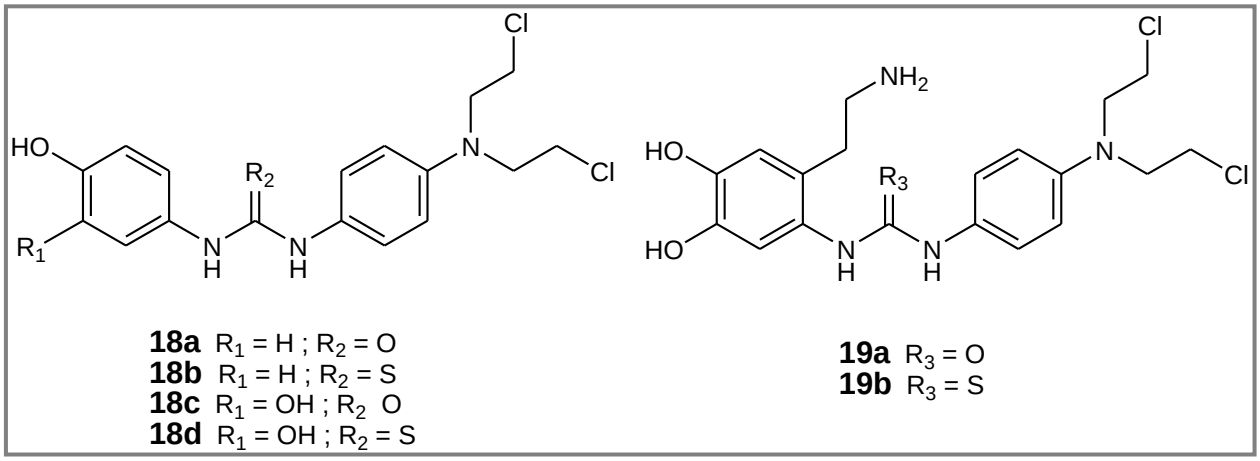

For each serie, they hypothesised a different mechanism of drug release after tyrosinase activation. For prodrugs **18**, they proposed a drug release mechanism based on the generation of the orthoquinone, followed by the release of the drug from a reactive intermediate instable in aqueous conditions (figure 17) [39,55].

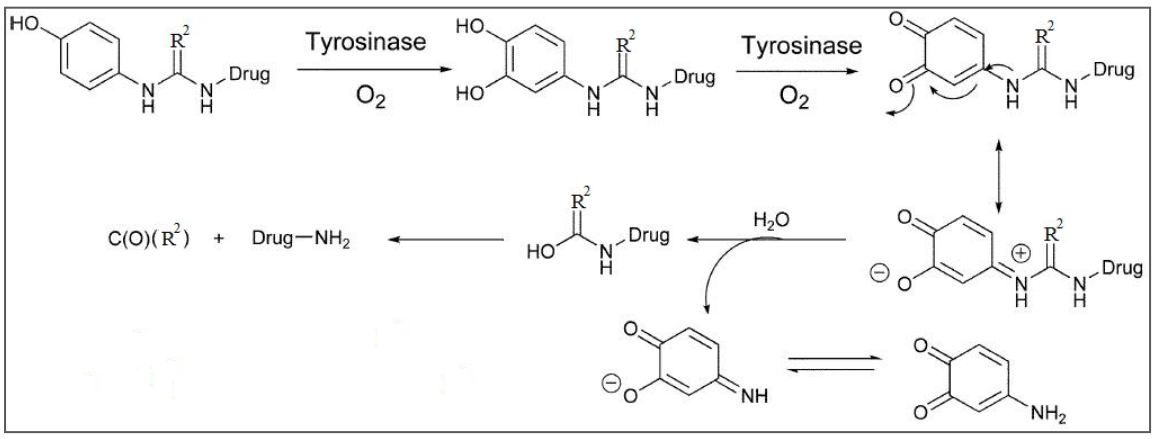

Figure 17 – Mechanism of drug release for prodrugs 18 [39].

The drug release pathway from prodrugs **19** (figure 18) was proposed as result of 6-aminodopamine oxidation by tyrosinase in the corresponding orthoquinone. This orthoquinone can initiate a rapid intramolecular cyclisation mechanism and the drug is released from a reactive intermediate instable in aqueous conditions [39,56].

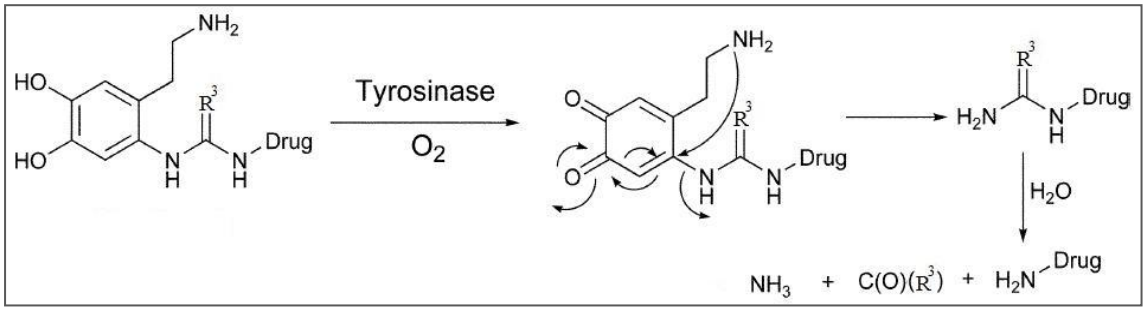

Figure 18 – Mechanism of drug release for prodrugs 19 [39].

The results obtained by oximetry studies were:

- Prodrugs **18a-d** were oxidised at rates compared to L-tyrosine;
- Prodrugs **19a**,**b** were oxidised at slower rates [39].

In addition to oximetry studies, this research group performed high-performance liquid chromatography (HPLC) studies in order to evaluate if prodrugs **18** and **19** can release the cytotoxic drug after tyrosinase oxidation. Results from these study showed that drug release was only successful in the urea linked prodrugs and was more effective in prodrugs **18a**,**c** than in prodrug **19a** [39].

Knaggs and co-workers also evaluated the citotoxicity of urea prodrugs **18a,c** and **19a** in a tyrosinase rich and tyrosinase absent cell line. The results showed that prodrug citotoxicity was greater in tyrosinase rich line, so prodrug citotoxicity was enhanced by tyrosinase activation [39].

More recently, in 2009, Perry and co-workers synthesized a new class of MDEPT prodrugs **20**, which were dopamine- and tyramine- derivatives of triazenes. Prodrugs **20** had in their structure [50]:

- Tyramine trigger (prodrugs **20a-d**) and dopamine trigger (prodrugs **20e-g**), which are known good substrates for tyrosinase;
- Urea linkage, which was previously proved to be a useful linker as it maintains the prodrug intact until it reaches tyrosinase;
- Triazene effector, more specifically, the monomethyltriazene (MMT). MMTs are known cytotoxic entities that are able to alkylate nucleic acids [40].

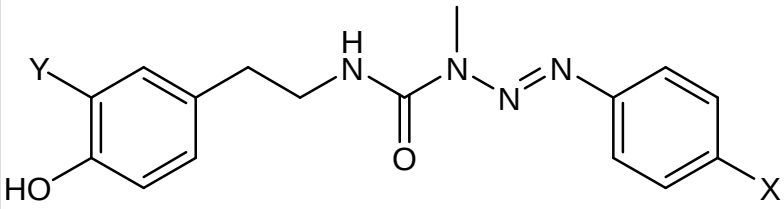

20a X = CH_3CO; Y = H
20b X = CO_2Et; Y = H
20c X = CN; Y = H
20d X = Me; Y = H
20e X = CH_3CO; Y = OH
20f X = CO_2Et; Y = OH
20g X = Me; Y = OH

Studies to evaluate the ability of prodrugs **20** to act as tyrosinase substrates showed that they were rapidly oxidized in the presence of tyrosinase with half-lives between 6 and 18 minutes, thus revealing that they are excellent tyrosinase substrates [50].

Studies from the reaction mixtures between tyrosinase and prodrugs **20** showed that they were rapidly converted by tyrosinase into a metabolite that did not correspond either to the cytotoxic agent MMT or its aniline decomposition product. This metabolite was further identified as the *o*-quinone. However, the release of the cytotoxic MMT did not occur under the reaction conditions used (figure 19) [50,57].

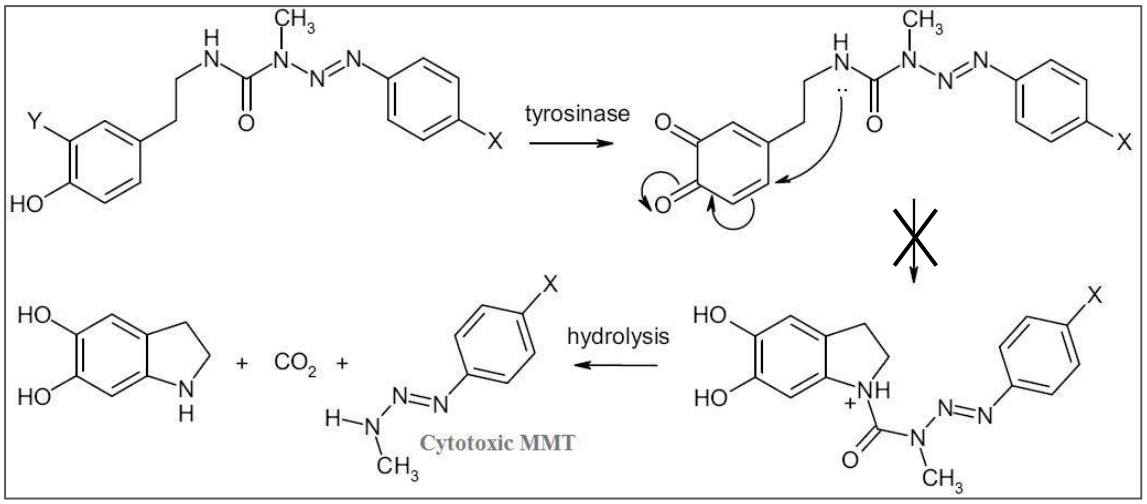

Figure 19 – Drug release pathway hypothesized by Perry and co-workers. Adapted from [50].

1.6 – Quinone-induced hepatotoxicity

CYP450 family is composed by monooxygenase enzymes, which are largely located inside the hepatocytes. These enzymes play a crucial role on the mono-oxygenation of xenobiotics and some endogenous substrates. Aromatic compounds such as MDEPT prodrugs, which have in their structure phenol or catechol moieties can easily suffer a metabolization process by liver CYP450, giving rise to toxic quinones [58,59].

Quinone toxicity results from the fact that quinones are Michael acceptors and in addition to that, they are also highly redox active molecules. In the literature there are two accepted mechanisms for quinone hepatotoxicity (figure 20):

- **Arylation/alkylation reactions** of important biological constituents. Since quinones are Michael acceptors, they can react covalently with thiols, such as GSH or with cysteine residues of proteins, to produce adducts that ultimately will cause cellular damage;

- **Oxidative stress**, by superoxide anion generation via quinone and semiquinone interconversion. In these processes, large quantities of superoxide anion radicals are produced, leading to severe oxidative stress. These radicals can promote a variety of damage effects in healthy cells such as oxidation of proteins, lipids and DNA as well as activation of several signalling pathways involved in some human pathologies [58-60].

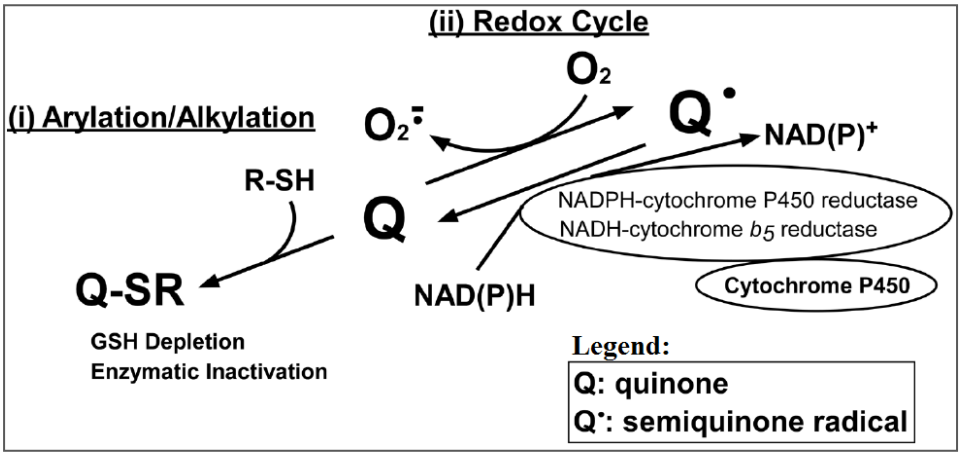

Figure 20 – Mechanisms of quinone-induced hepatotoxicity [58].

4-hydroxyanisole (4-HA), which has a phenolic moiety in its structure revealed to be very efficient in melanoma treatment in clinical trials, however these clinical trials were discontinued because this compound caused serious liver toxicity. Its hepatotoxicity is explained by the fact that this compound is metabolized into a toxic quinone specie by liver CYP450 via arene epoxidation (figure 21) [61-64].

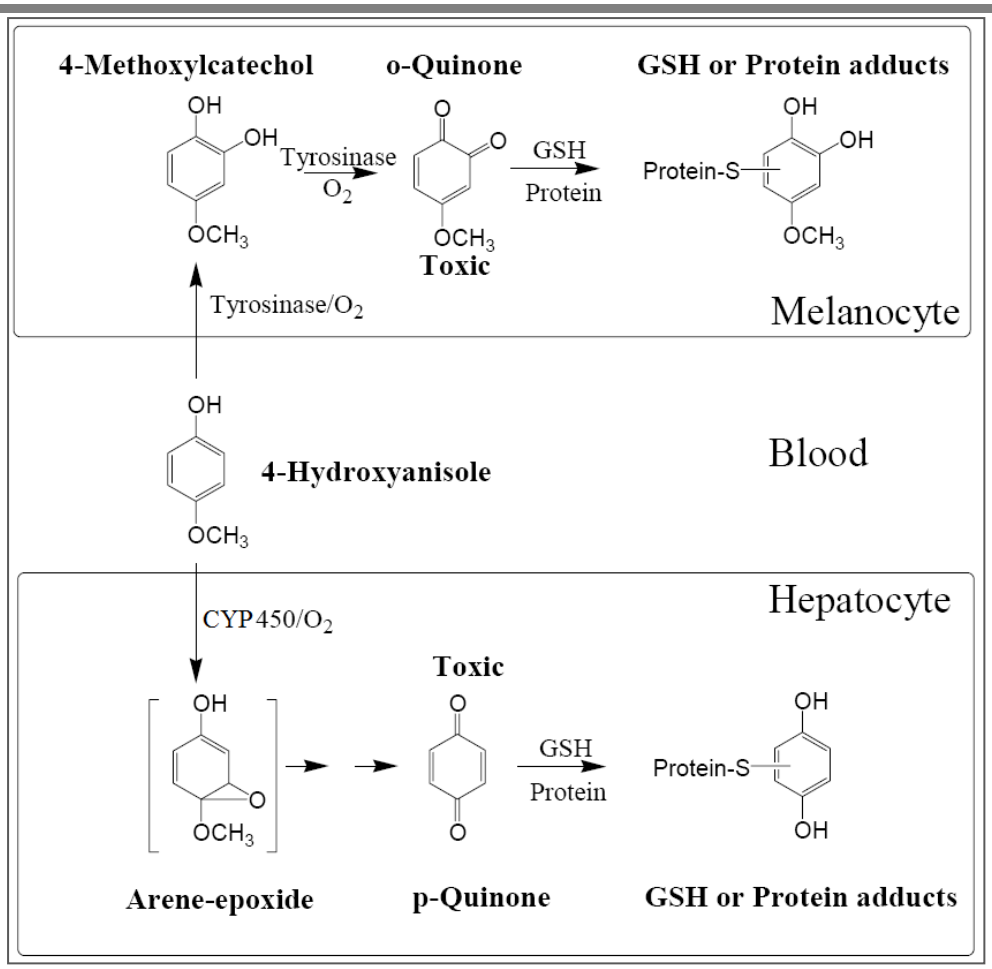

Figure 21 – Metabolism pathway for 4-HA in melanocyte (melanoma treatment) and in hepatocyte (hepatotoxicity). Adapted from [61].

1.7 – Goal of master thesis

The main goal of this research work is to develop a new serie of triazene prodrugs with potential application in a MDEPT strategy. This research work was divided in three parts:

- **Triazene-prodrug synthesis –** It was synthesized a new serie of triazene-based prodrugs **21**, in which the triggers and the effectors were linked by an amide function. The triggers used were hydroxyphenylpropionic acid derivatives, since 3-(4-hydroxyphenyl)propionic acid is a good tyrosinase substrate. The effectors

used were a serie of MMTs, which are cytotoxic entities with a known and efficient cytotoxic mechanism. The linker used was an amide linkage due to the fact that our research group experimented an urea linkage in prodrugs **20** without success and because amide functions are stable in physiological conditions (37 ºC, pH 7.4) and in the presence of plasma enzymes.

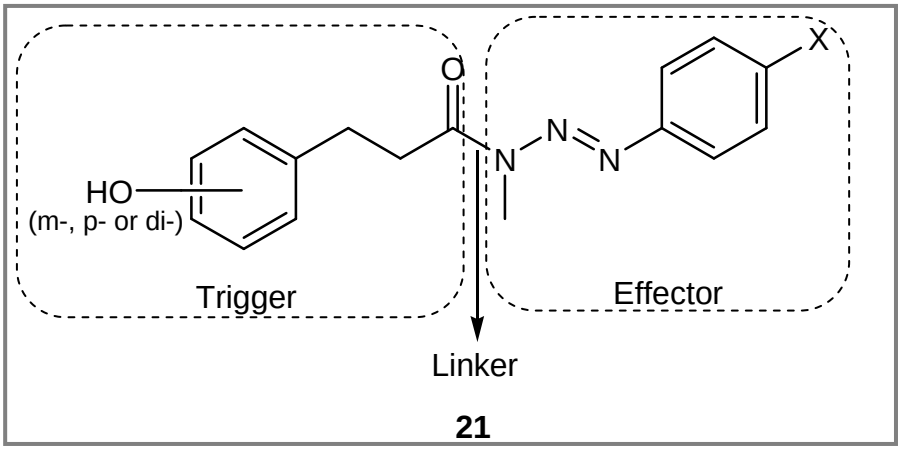

21

- **Evaluation of prodrugs stability in isotonic phosphate buffer (PBS), human plasma and in the presence of tyrosinase** – Stability studies, in aqueous media and human plasma aimed to assess if prodrugs **21** are stable before they reach tyrosinase, inside the melanocytes. Mushroom tyrosinase assay was important to evaluate if prodrugs **21** are good tyrosinase substrates and if they release the citotoxic agent, the MMT, after tyrosinase oxidation.

- **Hepatotoxicity assessment of prodrugs** – Hepatotoxicity evaluation was necessary to verify if prodrugs **21** are hepatotoxic, because they have in their structure, phenolic or catecholic moieties that can be possibly metabolized by CYP450 enzymes into cytotoxic quinones.

CHAPTER 2 – Synthesis of Triazene Prodrugs

2.1 – Introduction

Amide bonds are very important in the composition of biological systems and are present in many natural products such as proteins. Amides also have a key role for medicinal chemists. In fact carboxamide group appears in more than 25% of known drugs [65]. In general, prodrugs with an amide linkage have a suitable stability *in vivo*, due to the fact that amide bonds are very stable to aqueous hydrolysis at physiological pH, and to enzymatic hydrolysis by plasma enzymes [66,67].

Amide bonds are typically synthesized from the union of carboxylic acids and amines. However, amide formation between a carboxylic acid and an amine is a difficult condensation process. When the amine is directly mixed with the carboxylic acid, an acid-base reaction occurs, to give a stable salt (figure 22). The equilibrium process shown in figure 22 also reveals that the amide bond formation is not as favourable as its hydrolysis process. The equilibrium between salt and amide bond can be reversed with the use of high temperatures, however the integrity of the substrates could be affected [65,68].

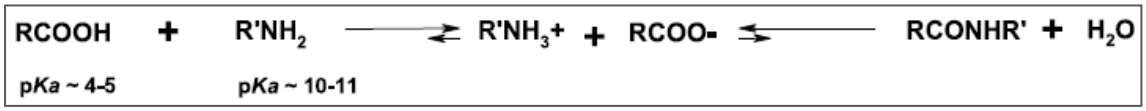

Figure 22 – Condensation reaction between a carboxylic acid and an amine. Adapted from [65].

To face the challenges associated with amide bond formation such as low yields, decomposition and difficult purification procedures, numerous methods have been developed in order to form this linkage in mild conditions. Acylation of amines usually involves a previous conversion of the carboxylic acid to a more reactive functional group. Carboxy moieties can be activated as acyl halides, mixed anhydrides, acyl azides or activated esters. Preparation of these more reactive derivatives is usually carried out using coupling agents [65,68].

Carboxylic acid activation could be attempted with different types of coupling agents such as N,N'-dicyclohexylcarbodiimide/4-dimethylaminopyridine (DCC/DMAP), O-(benzotriazol-1-yl)-N,N,N′,N′-tetramethyluroniumtetrafluoroborate (TBTU), 4-(4,6-dimethoxy-1,3,5-triazin-2-yl)-4-methyl-morpholinium chloride (DMTMM) and thionyl chloride. Amide coupling could also be attempted with the use of a zirconium catalyst.

- Activation with DCC/DMAP

DCC, which is a carbodiimide, has been frequently used for amide bond formation since 1955 [68,69]. In this one-pot procedure (figure 23), DCC and the carboxylic acid react together to form the *O*-acylurea. This specie is slowly converted into an unreactive N-acylurea. To prevent and diminish this side reaction, is necessary to use an additive, as DMAP, which reacts faster with *O*-acylurea to form an intermediate specie that stills active enough to couple with the amine in order to synthesize the final amide product. In this process, triethylamine (TEA) is used to regenerate the DMAP catalyst and an urea by-product, the N,N'-dicyclohexylurea (DCU) is formed. DCU is usually insoluble in the reaction medium and can be removed by filtration [65,68,70].

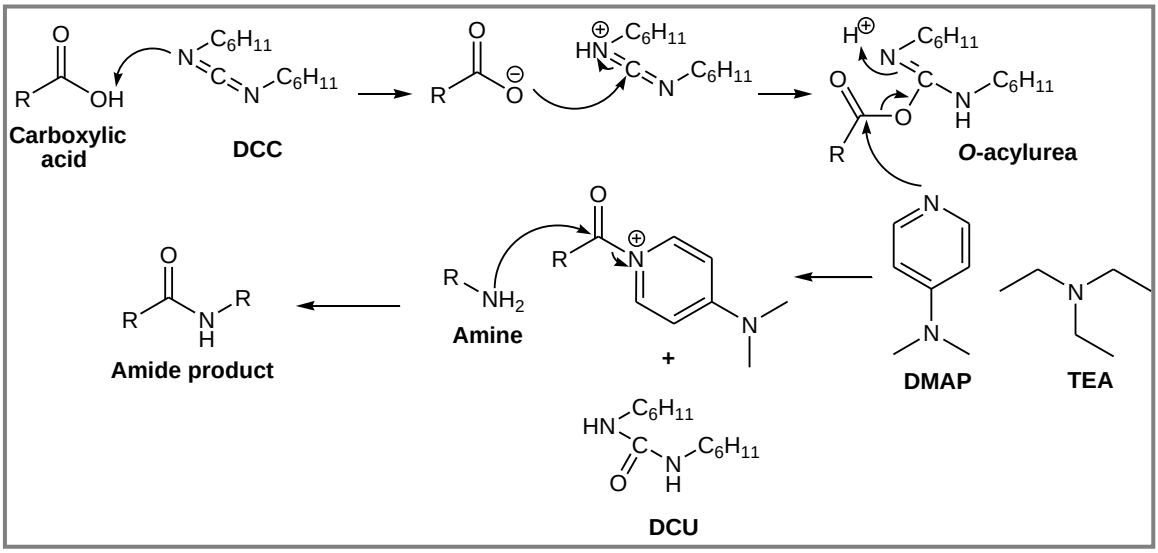

Figure 23 – Amide coupling activation with DCC/ DMAP.

- Activation with TBTU

Numerous coupling agents are based on the 1-hydroxybenzotriazole/1-hydroxy-7-azabenzotriazole (HOBt/HOAt) system and uronium/aminium salts. TBTU is an uronium salt that has been used in highly efficient amide coupling reactions, especially in peptide synthesis [65,71]. This one-pot coupling synthesis (figure 24) is executed by mixing the carboxylic acid and the amine in the presence of TBTU and TEA. TEA is used to deprotonate the carboxylic acid and the carboxylate ion formed reacts with TBTU to form the activated acid and $^{(-)}$OBt. A side reaction can also occur with the amine reacting with TBTU to form a guanidinium by-product. This side reaction can be diminished by adding HOBt to the reaction. $^{(-)}$OBt readily reacts with the activated acid to generate an OBt active ester that suffers a nucleophilic attack by the amine in order to form the final amide linkage. In the formation of the OBt active ester, an urea by-product is generated [65,68]. The by-products formed can be removed by aqueous extraction.

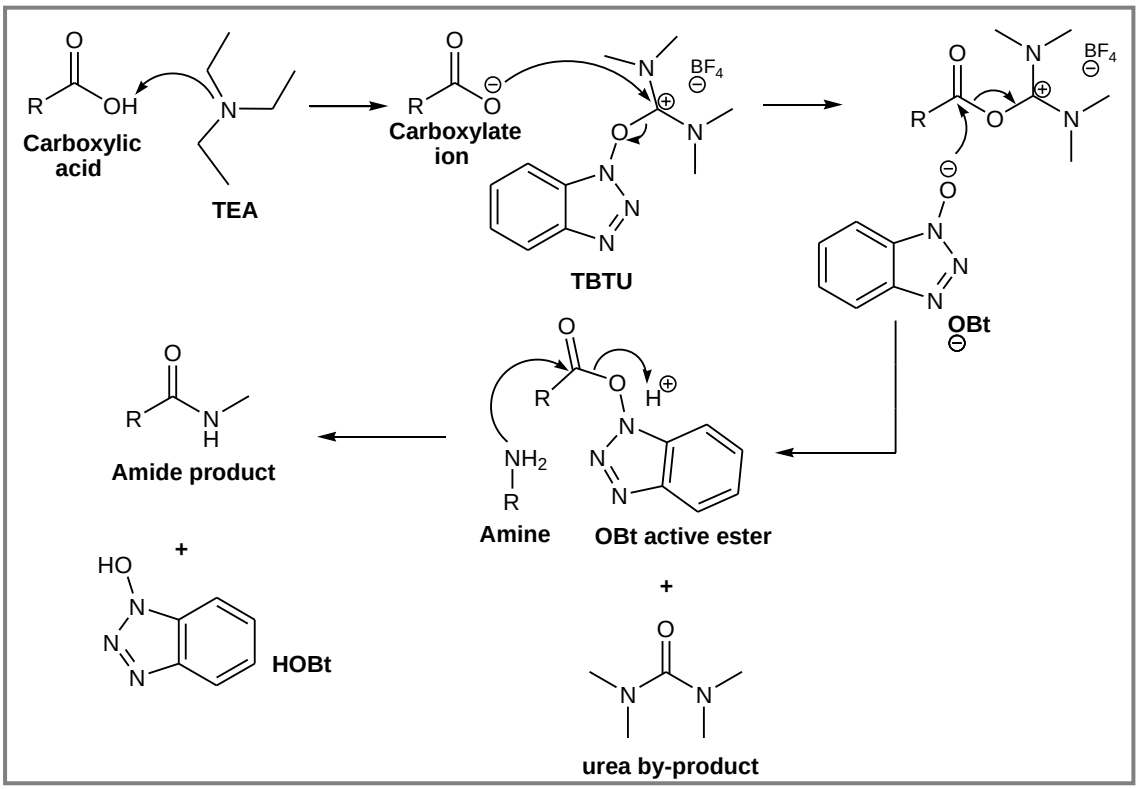

Figure 24 – Amide coupling activation with TBTU.

- Activation with DMTMM

DMTMM, which is a triazine derivative, has been described to be an effective activating coupling agent, not only for ester bond formation, but also for amide coupling and peptide synthesis [68,72]. In this synthesis (figure 25), the first step is a nucleophilic aromatic substitution, in which N-methylmorpholine reacts with 2-chloro-4,6-dimethoxy-1,3,5-triazine to form DMTMM. An advantage of this process is the fact that N-methylmorpholine can be used in excess, so no additional base is required, as N-methylmorpholine is able to deprotonate the carboxylic acid and generate the carboxylate ion. The carboxylate ion formed reacts with DMTMM to form an activated ester that suffers a nucleophilic attack by the amine to form the final amide product. In this process a triazinone by-product is formed but it is easily removed by aqueous extraction [65].

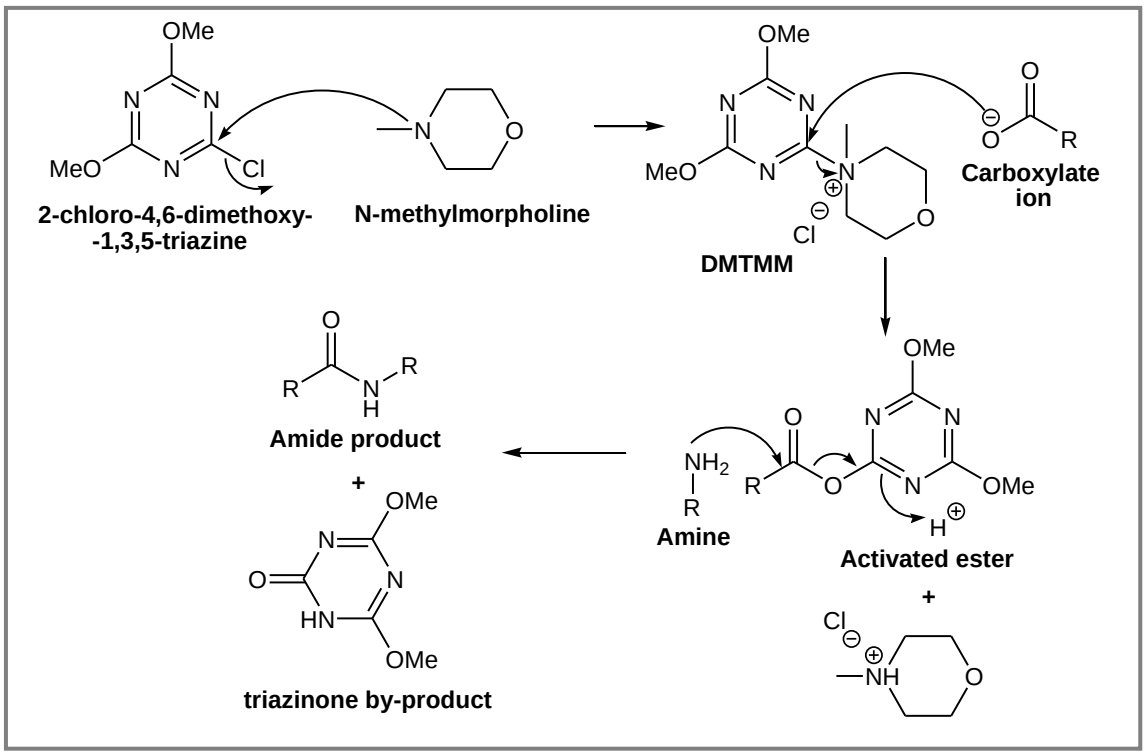

Figure 25 – Amide coupling activation with DMTMM.

- Activation with thionyl chloride

Acyl chlorides are one of the easiest methods for activation of carboxylic acids. This is usually a two-step activation process (figure 26), involving first the conversion of the carboxylic acid into the acyl chloride and then the amide coupling between this specie and the amine to form the amide linker. The presence of a base (e.g: NEt_3, iPr_2NEt or N-methylmorpholine) is usually required, in order to trap the formed HCl and to avoid the conversion of the amine into its unreactive HCl salt [65]. Amide coupling can also be enhanced with catalytic amounts of DMAP, by generation of the acylpyridinum salt, which is a reactive intermediate [73].

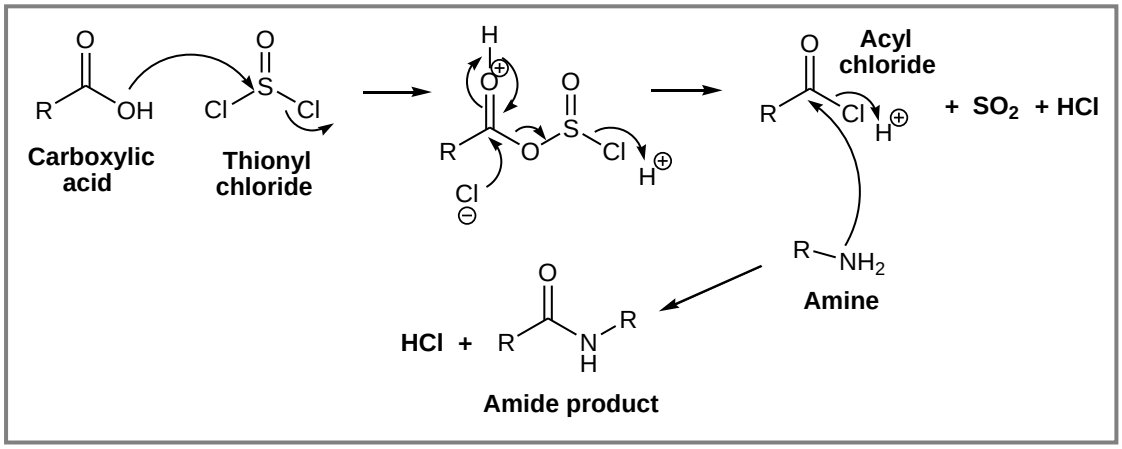

Figure 26 – Amide coupling activation with thionyl chloride.

- Activation with zirconium

Organometallics have become a major tool in modern organic synthesis with successful reports in the literature for amide coupling. These compounds have coordination bonds between metal and heteroatoms such as oxygen or nitrogen in the organic ligands. This coordination is very useful in stoichiometric and catalytic processes. In the amide coupling between esters and amines, catalytic amounts of metal mediators are usually required [74-76].

Zr(Ot-Bu)$_4$/HOBt system was described by Yang and co-workers to be efficient in ester-amide exchange [76]. In this one-pot method (figure 27), Zr(Ot-Bu)$_4$ and HOBt react together to form a Zr-OBt specie, which is responsible for the coordination between ester and amine. This coordination enhances the generation of the final amide product [74].

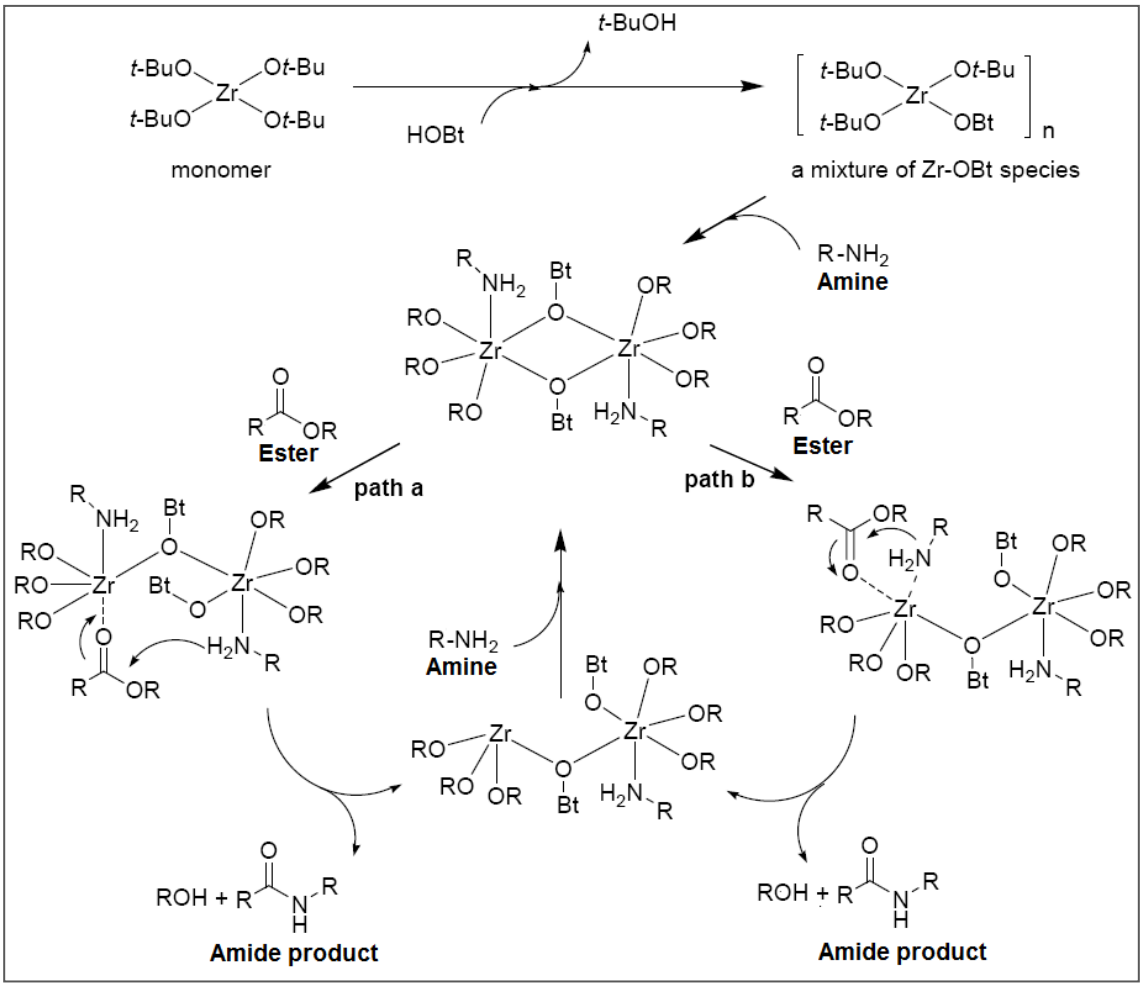

Figure 27 – Amide coupling activation with Zr(Ot-Bu)$_4$/HOBt. Adapted from [74].

The synthetic approach used for the preparation of triazene prodrugs derivatives (**21a-f**, table 2) is shown in figure 28.

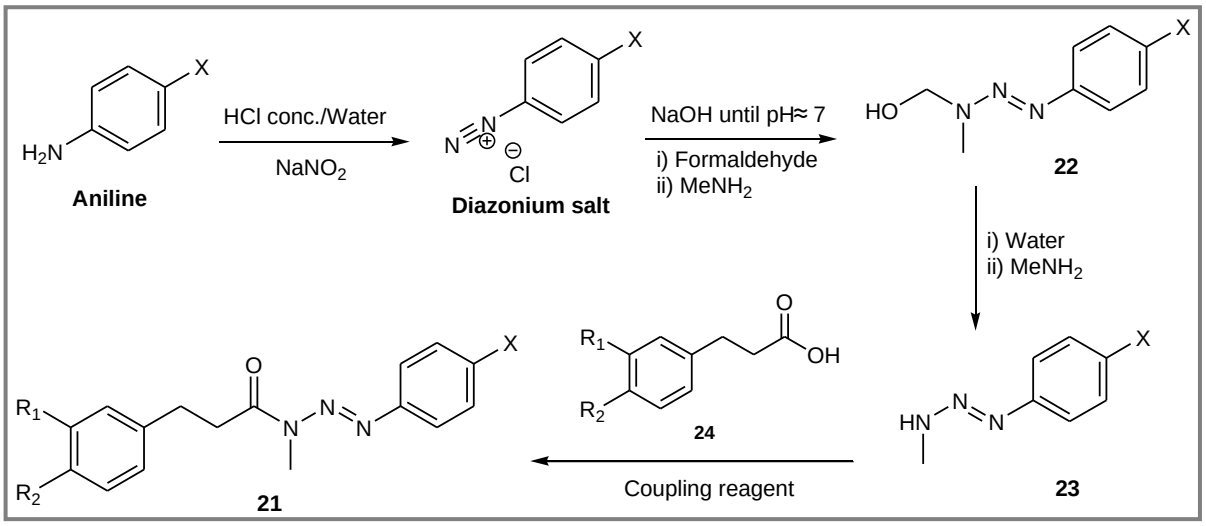

Figure 28 – Synthetic pathway involved in the synthesis of triazene prodrugs 21.

Table 2 – Triazene prodrugs synthesized 21a-f.

Triazene Prodrug	R_1	R_2	Substituent in X
21a	OH	H	$COOCH_3$
21b	OH	H	CN
21c	H	OH	$COOCH_3$
21d	H	OH	CN
21e	H	OH	$COCH_3$
21f	H	OH	$CONH_2$

MMTs **23** were synthesized from the corresponding HMTs **22**. Compound **22** resulted from diazotization of the proper aniline with sodium nitrite and HCl. The diazonium salt obtained reacts further with a conjugate, formed *in situ* between formaldehyde and methylamine, to give the desired HMT derivative **22** [77,78]. HMT derivatives **22** were transformed into MMT derivatives **23** by methylamine catalysis in aqueous medium (figure 23) [79].

As coupling reagents we have tried DCC/DMAP, TBTU, DMTMM, thionyl chloride and zirconium.

Amide coupling was also enhanced with the activation of the amino group, along with the activation of the carboxylic acid **24**. Amino group, in MMT **23**, responsible for the nucleophilic attack, is a secondary amine. In our experiments (figure 29) the secondary amine in MMT **23** was activated with NaH. Sodium hydride behaves as a strong base that promotes the deprotonation of the N-methyl nitrogen atom. This deprotonation process generates a negative charge in nitrogen atom, increasing its nucleophilicity and enhancing the amide coupling between MMT **23** and the activated carboxylic acid **24** [80].

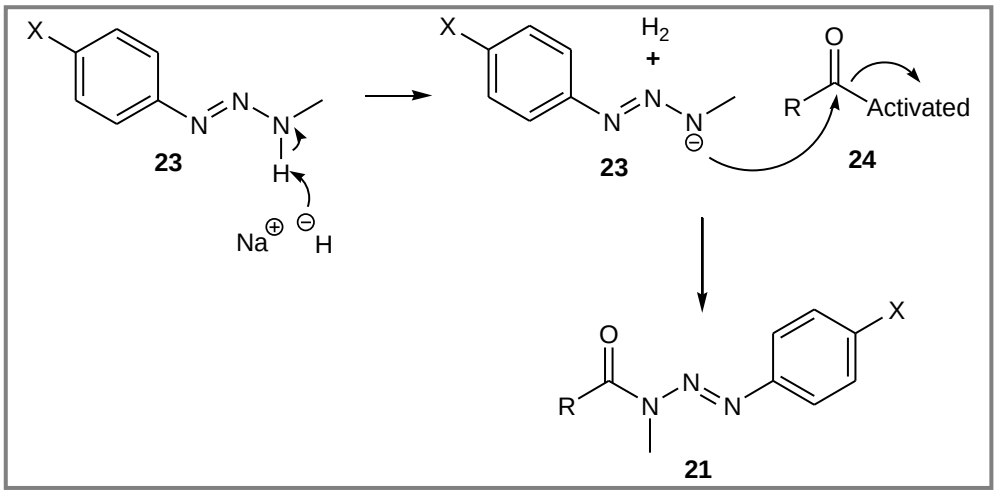

Figure 29 – Amide coupling activation with activation of the amino group.

Sometimes, when the amide coupling was not efficient at room temperature, it was necessary to provide energy in order to accelerate the process. This energy can be provided by two different sources, microwave irradiation or conventional heating.

Microwave irradiation produces a rapid and volumetric heating, where all reaction mixture is heated at the same time. The acceleration of reactions with microwave irradiation results from a combination between thermal and non-thermal effects, which are not usually accessible by conventional heating. Thermal effects are dielectric heating, overheating, hotspots and selective absorption of radiation by polar substances. Non-thermal effects of highly polarizing radiation, also called specific microwave effects, still to be a controversial topic. Microwave-assisted organic synthesis has as main advantages, the achievement of higher yields, the use of milder

conditions and shorter reaction times. Amide coupling assisted by microwave irradiation has been previously reported in literature with success [81,82].

In contrast, the conventional heating source is a slower and a more inefficient process of transferring energy for the reaction. In addition, the temperature gradient formed in the reaction mixture can develop local overheating, which can lead to product or reagent decomposition [81,82].

Microwave irradiation has been described to be efficient in reactions, which do not occur by conventional heating [82,83].

2.2 – Results and Discussion

- Synthesis of triazene prodrugs **21a-f**

Triazene prodrugs **21a-f** (table 3) were synthesized using different methodologies, which are fully described in the chapter 5, section 5.2.2. The yields obtained in the different processes were low and did not exceed 20 % (table 3).

Table 3 – Methodologies applied in the synthesis of triazene prodrugs 21a-f and the yields obtained.

Triazene prodrug	Hydroxyphenylpropionic acid derivative	Substituent X	Method	Yield (%)
21a	3-(3-hydroxyphenyl)propionic acid	$COOCH_3$	DCC/DMAP	< 5
21b	3-(3-hydroxyphenyl)propionic acid	CN	TBTU (MW irradiation)	8 and 20
21c	3-(4-hydroxyphenyl)propionic acid	$COOCH_3$	TBTU (MW irradiation)	< 5
21d	3-(4-hydroxyphenyl)propionic acid	CN	DCC/DMAP	15
21e	3-(4-hydroxyphenyl)propionic acid	$COCH_3$	TBTU (reflux)	< 5
21f	3-(4-hydroxyphenyl)propionic acid	$CONH_2$	DMTMM	< 5

First attempt to synthesize triazene prodrugs **21** was accomplished by DCC/DMAP coupling. This method was the first choice, because in our research group, the synthesis of triazene derivatives with an amide linkage was previously achieved with yields between 21% and 73% [84-86]. This methodology was also used by Chen and co-workers in the synthesis of amide-linked paclitaxel analogs, with yields that ranged from 50% to 71% [87]. With this method the synthesis of triazene prodrugs **21a,d** was accomplished but the yields obtained were substantially lower in comparison with the yields described above. The explanation for these low yields could be in the structure of the hydroxyphenylpropionic acid derivative **24**. Compound **24** has a phenolic moiety that is easily oxidized by different promoters as UV-light or high temperatures [88,89]. Although in this method the amide coupling was performed at room temperature and protected from light, some oxidation in compound **24** must have occurred, thus compromising the yields obtained in the synthesis of prodrugs **21a,d**. Other possible explanation for the lower yields obtained could be in the complex purification process applied in this method, due to formation of DCU, which was partially soluble in the reaction solvent, tetrahydrofuran (THF). This long and complex purification process could have also promoted the oxidation of prodrugs **21a,d**. This method was also attempted with activation of MMT **23** but the results did not improve. Negative charge generated in the N-methyl nitrogen atom, after MMT **23** activation, is involved in resonance (figure 30), thus decreasing its nucleophilic character.

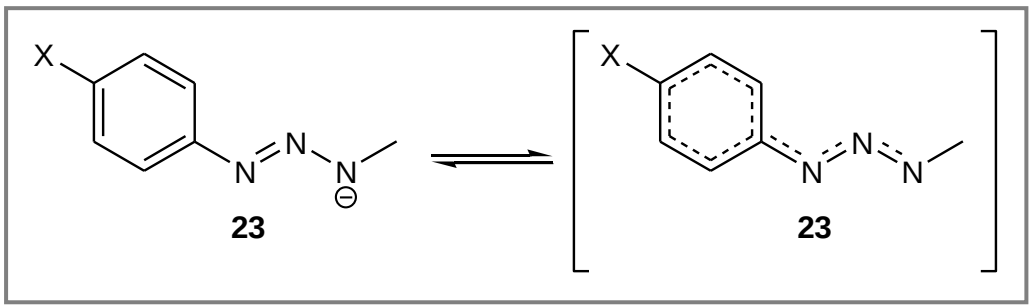

Figure 30 – Resonance process in MMT 23 structure after the formation of the negative charge.

In order to overcome the long reaction time and the complex purification process, another method was applied. By this method the amide coupling occurred with activation of the 3-(4-hydroxyphenyl)propionic acid **24** with DMTMM. This method is a highly rapid strategy for amide coupling at room temperature with an easy purification process. This methodology was successfully applied by Kunishima and co-workers in the amide coupling between several carboxylic acids (e.g: aromatic, sterically hindered, α,β-unsaturated, etc) with primary and secondary amines. The yields obtained ranged between 62% and 92% [90]. Luca and co-workers also applied this method in the preparation of Weinreb amides, which consisted in the coupling between several types of carboxylic acids and *N*,*O*-dimethylhydroxylamine. The yields obtained ranged between 49% and 97% [91]. Another reference in the literature for this method refers the amide coupling done by Bandgar and co-workers in the synthesis of monoacylated piperazine derivatives with yields that ranged from 60% to 95%. One of the amide couplings carried out by them, was between 4-hydroxybenzoic acid (phenolic moiety) and piperazine (secondary amine), with a yield of 92% [92]. In our research work, this method was used to synthesize triazene prodrug **21f**, but the yield obtained was much lower in comparison with the yields previously reported. We could envisage three possible explanations for this low yield:

- MMT derivatives **23** are usually unstable in the reaction conditions, thus hydrolyzing in the corresponding anilines [77];
- N-methyl nitrogen atom of the MMT derivatives **23** is a weak nucleophile;
- We observed during the synthesis some solubility problems, which may negatively influenced the yield obtained.

Synthesis of triazene prodrug **21e** was achieved with activation of 3-(4-hydroxyphenyl)propionic acid **24** with TBTU. In this method, amide coupling was assisted by conventional heating. This method was previously applied with success by Loffredo and co-workers in peptide synthesis [83]. Finaru and co-workers also used this method in the synthesis of 5-carboxamido-*N*-acetyltryptamine derivatives, and the yields obtained ranged from 58% to 100% [93]. The yield obtained in the synthesis of

triazene prodrug **21e** was very poor in comparison with the yields mentioned before. There are some possible explanations for this poor yield:

- As described before the conventional heating source can lead to product and reagent decomposition [81];
- Reaction temperature promoted a dimerization process of the activated 3-(4-hydroxyphenyl)propionic acid **24** before the amide coupling and the result was the emergence of secondary products **25** (figure 31). The same type of process was previously observed by Bejugam and co-workers [94];

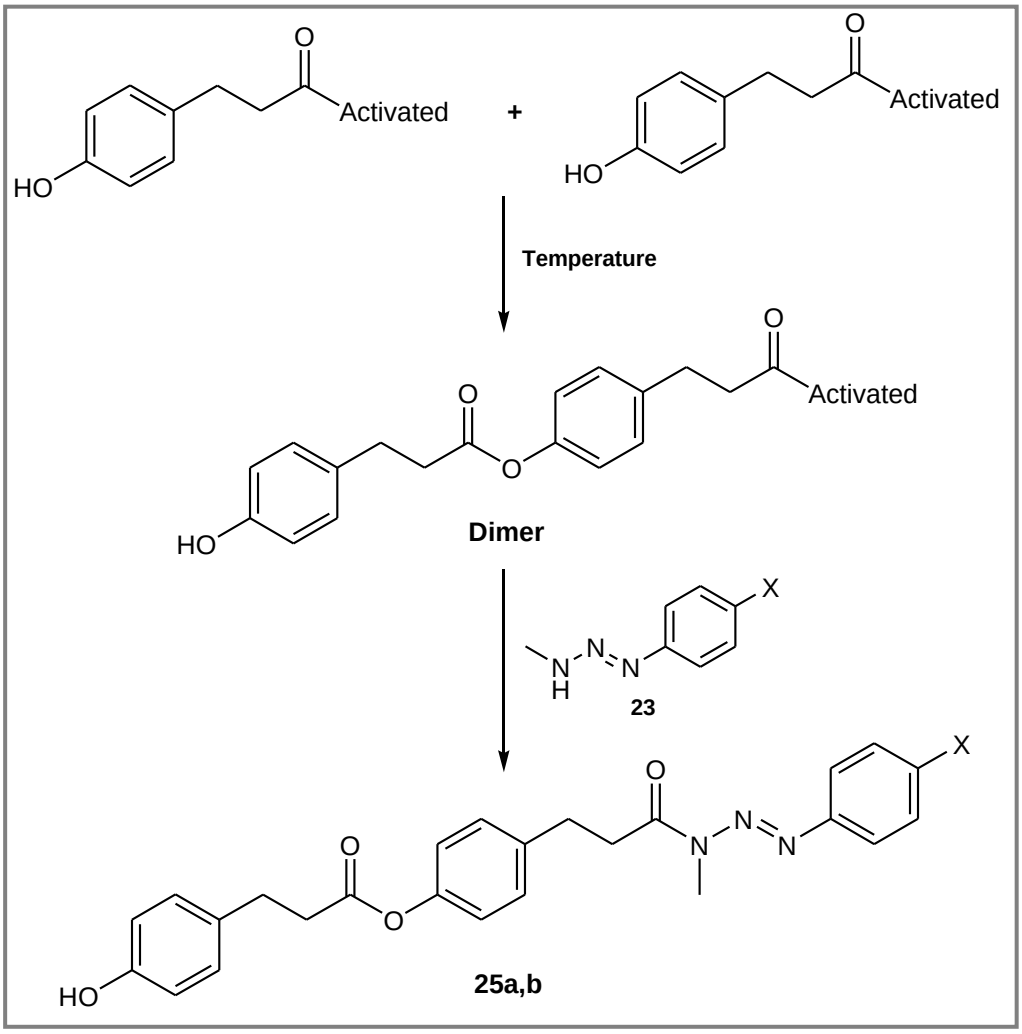

Figure 31 – Dimerization process of two activated molecules of 3-(4-hydroxyphenyl)propionic acid before the amide coupling and formation of compounds 25a,b.
Legend: Compound 25a – X = COOCH3; Compound 25b – X = COCH3.

- A possible side reaction between MMT **23** and TBTU, which promoted the formation of a guanidinium by-product (figure 32) [68];

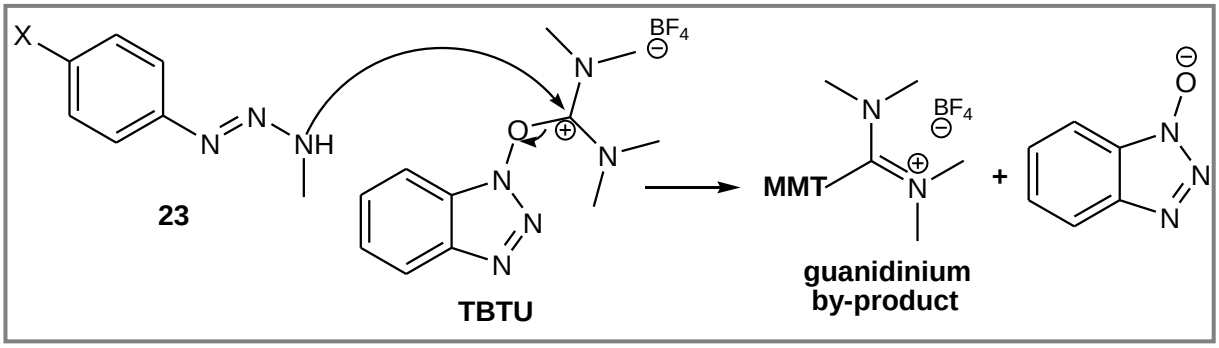

Figure 32 – Guanidinium by-product formation.

- Some amounts of triazene prodrug **21e** were lost during the extraction process used to remove dimethylformamide (DMF).

In order to overcome the decomposition problems caused by the conventional heating, it was attempted the synthesis of triazene prodrugs **21b,c** with microwave irradiation. This method was also applied with sucess by Loffredo and co-workers in peptide synthesis [83]. Synthesis of 5-carboxamido-*N*-acetyltryptamine derivatives was also attempted by Finaru and co-workers and the yields obtained ranged between 80% and 100% [93]. The yields obtained in the synthesis of triazene prodrugs **21b,c** were poor in comparison with the yields described above. We observed that the yield obtained in the synthesis of triazene prodrug **21b**, significantly increased to 20% when the microwave cycle was performed twice. These low yields can be explained by the reasons described in the previous method. The dimerization process (figure 31) have also occurred in the synthesis of triazene prodrug **21c**.

Attempts to synthesize triazene prodrug **21g** lead us to apply activation of carboxylic acid function **24** with thionyl chloride. Cvetovich and co-workers applied this method in the synthesis of acrylanilides, acrylamides and amides with yields between 50% and 98% [95]. This method was also applied in the preparation of *N*-Fmoc α-amino/ peptidyl Weinreb amides by Sureshbabu and co-workers with yields ranging from 76% to 90% [96]. Unfortunately triazene prodrug **21g** was only synthesized in

very small amounts and very impure. The lack of efficiency of this method in this amide coupling can be possibly explained by:

- Activation of 3-(3,4-dihydroxyphenyl)propionic acid **24** with thionyl chloride increased the acidity in the reaction medium, promoting the hydrolysis of the MMT-CN **23** in the corresponding aniline-CN [97];
- A condensation process between two activated molecules of 3-(3,4-dihydroxyphenyl)propionic acid **24**, with formation of a dimer (e.g: figure 31) [98].

Another method tried in the synthesis of prodrug **21g** encompassed the use of a metal coupling catalyst $Zr(Ot\text{-}Bu)_4$ with HOBt. Han and co-workers applied this method in the amide coupling between several types of esters and amines, and the yields obtained ranged between 75% and 95% [74]. The same method was also used by Yang and co-workers and the yields obtained in the amide coupling ranged from 72% to 93% [76]. These results prompt us to think that this method could be advantageous for the synthesis of our prodrugs **21** but in our experiment, amide coupling did not occur. Maybe the extreme temperature (100ºC) applied in this method has decomposed the reactants or even the triazene prodrug **21g**.

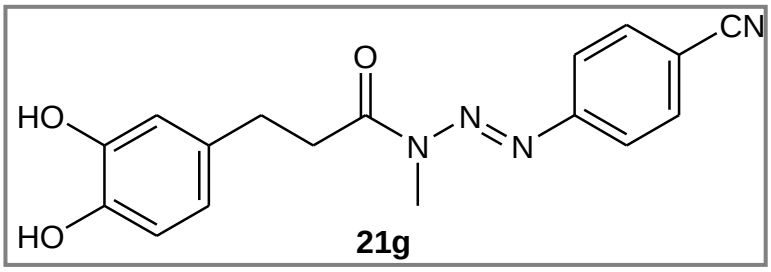

21g

- Structural Identification

Structural identification of triazene prodrugs **21** was carried out by nuclear magnetic resonance (NMR) spectroscopic methods (^{1}H NMR, ^{13}C NMR, heteronuclear multiple quantum correlation (HMQC)), infrared (IR) spectroscopy and electrospray ionization mass spectrometry (ESI-MS). Complete structural identification is shown in chapter 5, section 5.3. HMQC information is shown in the appendices.

- ^{1}H NMR spectroscopy

Table 4 – Summary of the common peaks in the ^{1}H NMR spectra of triazene prodrugs 21a-f.

Triazene Prodrug	C**H**$_2$**'s**	N-C**H**$_3$	O**H**$_{Phenol}$	Ar(C**H's**)$_{Phenol}$	Ar(C**H's**)$_{MMT}$
21a	**3.04** (2H, *t*, *J* = 7.7 Hz) **3.26** (2H, *t*, *J* = 7.7 Hz)	**3.44** (3H, *s*)	**5.31** (1H, *s*)	**6.69** (1H, *dd*, *J* = 7.8, 2.0 Hz) **6.75** (1H, *br s*) **6.81** (1H, *d*, *J* = 7.8 Hz) **7.16** (1H, *t*, *J* = 7.8 Hz)	**7.60** (2H, *AA'*, *J* = 8.4 Hz) **8.11** (2H, *XX'*, *J* = 8.4 Hz)
21b	**3.03** (2H, *t*, *J* = 7.8 Hz) **3.25** (2H, *t*, *J* = 7.8 Hz)	**3.45** (3H, *s*)	**5.39** (1H, *s*)	**6.69** (1H, *dd*, *J* = 7.8, 2.2 Hz) **6.75** (1H, *br s*) **6.80** (1H, *d*, *J* = 7.8 Hz) **7.15** (1H, *t*, *J* = 7.8 Hz)	**7.63** (2H, *AA'*, *J* = 8.4 Hz) **7.73** (2H, *BB'*, *J* = 8.4 Hz)
21c	**3.01** (2H, *t*, *J* = 7.6 Hz) **3.23** (2H, *t*, *J* = 7.6 Hz)	**3.44** (3H, *s*)	**4.97** (1H, *s*)	**6.76** (2H, *AA'*, *J* = 7.8 Hz) **7.11** (2H, *XX'*, *J* = 7.8 Hz)	**7.60** (2H, *AA'*, *J* = 8.2 Hz) **8.11** (2H, *XX'*, *J* = 8.2 Hz)
21d	**3.01** (2H, *t*, *J* = 7.6 Hz) **3.22** (2H, *t*, *J* = 7.6 Hz)	**3.44** (3H, *s*)	**4.74** (1H, *s*)	**6.76** (2H, *AA'*, *J* = 7.6 Hz) **7.11** (2H, *XX'*, *J* = 7.6 Hz)	**7.63** (2H, *AA'*, *J* = 7.8 Hz) **7.73** (2H, *BB'*, *J* = 7.8 Hz)
21e	**3.01** (2H, *t*, *J* = 7.8 Hz) **3.23** (2H, *t*, *J* = 7.8 Hz)	**3.45** (3H, *s*)	**5.15** (1H, *s*)	**6.77** (2H, *AA'*, *J* = 8.6 Hz) **7.11** (2H, *XX'*, *J* = 8.6 Hz)	**7.63** (2H, *AA'*, *J* = 8.8 Hz) **8.03** (2H, *XX'*, *J* = 8.8 Hz)
21f	**2.90** (2H, *t*, *J* = 7.6 Hz) **3.14** (2H, *t*, *J* = 7.6 Hz)	**3.35** (3H, *s*)	nd	**6.65** (2H, *AA'*, *J* = 8 Hz) **6.98** (2H, *XX'*, *J* = 8 Hz)	**7.52** (2H, *AA'*, *J* = 8 Hz) **7.83** (2H, *XX'*, *J* = 8 Hz)

Analysis of table 4 shows that:

- Chemical shifts from the alkyl C**H$_2$'s** are assigned by two triplets in the region between 2.90-3.26 ppm;
- N-C**H$_3$** signal is characterized by a singlet in the region of 3.40 ppm;
- Chemical shift from the aromatic O**H**, when is observed, is characterized by a singlet near 5 ppm;
- In the aromatic C**H's** from MMT **23**, the chemical shifts are assigned by a pair of doublets in the region between 7.52-8.11 ppm. Depending on the substituent X in the MMT derivatives **23**, these aromatic C**H's** can be represented by a *AA'BB'* spin system ($\Delta\nu/J \leq 10$) or by a *AA'XX'* spin system ($\Delta\nu/J > 10$). Only in triazene prodrugs **21b**,**d**, the aromatic C**H's** are represented by a *AA'BB'* spin system;
- In the aromatic C**H's** from the phenolic moiety, the chemical shifts depend on the hydroxyphenylpropionic acid **24** derivative:

  - Triazene prodrugs **21a,b** (3-(3-hydroxyphenyl)propionic acid derivatives) have four different chemical shifts in the region between 6.69-7.16 ppm (H_2 – 6.69; H_1 – 6.75; H_3 – 6.80/6.81; H_4 – 7.15/7.16). The assignment of these chemical shifts is supported by ^{1}H NMR data collected by Takaishi and co-workers from several *m*-alkylphenols [99];

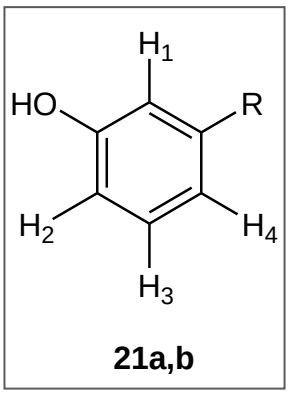

21a,b

  - In triazene prodrugs **21c-f** (3-(4-hydroxyphenyl)propionic acid, these protons are assigned by a pair of doublets in the region between 6.65-7.11 ppm with a *AA'XX'* spin system.

- ^{13}C NMR and HMQC spectroscopic methods

In ^{13}C NMR data of triazene prodrugs **21**, all carbon chemical shifts were detected. HMQC spectra of triazene prodrugs **21** revealed all the expected proton-carbon correlations.

- IR spectroscopy

Table 5 – Summary of the relevant IR absorption bands in triazene prodrugs 21a-f and 25a,b.

	IR absorption bands (cm^{-1})		
Triazene prodrug	**Carbonyl of function amide** 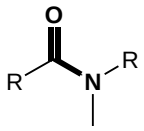	**Substituent X** 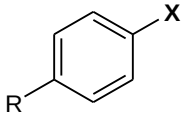	**Carbonyl of function ester** 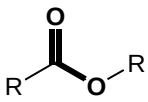
21a	1686	Ester$_{(C=O)}$ - 1713	----------
21b	1684	Cyano$_{(C\equiv N)}$ - 2228	----------
21c	1697	Ester$_{(C=O)}$ - 1728	----------
21d	1711	Cyano$_{(C\equiv N)}$ - 2234	----------
21e	1661	Ketone$_{(C=O)}$ - 1695	----------
21f	1686 / 1670*		----------
25a	1717		1734 / 1749**
25b	1682	Ketone$_{(C=O)}$ - 1703	1754

* two undifferentiated amide functions; ** two undifferentiated ester functions

Analysis of table 5 shows that:

- IR amide band varies from 1661 to 1717 cm^{-1} but the range for tertiary amides referred in the literature varies from 1630 to 1680 cm^{-1} [100]. This discrepancy can be explained by the influence of the vicinity atoms.
- IR absorptions bands of substituent X for compounds **21** and **25** were all identified and in accordance with the literature [100].
- IR carbonyl band from the ester of the dimer was detected in compounds **25a,b**, in addition to the other IR bands.

- ESI-MS

Table 6 – Expected molecular weights and the m/z values for the molecular ion of each triazene prodrug 21a-f.

Triazene prodrug	Expected molecular weight	ESI^+ $[M+Na]^+$	ESI^- $[M-H]^-$
21a	341	364 (**341**+23)	340 (**341**-1)
21b	308	331 (**308**+23)	307 (**308**-1)
21c	341	364 (**341**+23)	340 (**341**-1)
21d	308	331 (**308**+23)	307 (**308**-1)
21e	325	348 (**325**+23)	324 (**325**-1)
21f	326	349 (**326**+23)	325 (**326**-1)

Analysis of table 6 reveals that the expected molecular weights for all triazene prodrugs **21a-f** are confirmed.

2.3 – Conclusions

Although all the difficulties associated with amide coupling, the synthesis, purification and structural identification of a new serie of anti-tumor triazene prodrugs **21** was achieved.

About the different methodologies adopted in the synthesis of prodrugs **21**, it is possible to conclude that:

- The activation methods with DCC/DMAP, TBTU and DMTMM were useful but not efficient, due to the fact that the yields obtained did not exceed 20 %;

- The activation methods with DCC/DMAP and TBTU (MW irradiation) provided the best yields, however in the activation with TBTU (MW irradiation), reaction time and purification process are much shorter;

- Microwave irradiation is more efficient than conventional heating;

- The activation methods with thionyl chloride and zirconium must be further modified in order to become useful in the synthesis of prodrugs **21**;

- The poor yields obtained can also be explained based on the intrinsic reactivity of the main reactants (hydroxyphenylpropionic acid derivatives **24** and MMT derivatives **23)**, which are unstable and can easily suffer decomposition processes in the reaction mediums.

CHAPTER 3 – Evaluation of Triazene Prodrugs for MDEPT Strategy

3.1 – Introduction

In order to study the stability of triazene prodrugs **21** in conditions that mimic physiological environment and to evaluate their activation by mushroom tyrosinase and their efficiency in drug release, several kinetic assays were performed: chemical hydrolysis in PBS (0.01 M, pH 7.4), hydrolysis in 80% of human plasma and oxidation of prodrugs **21** by mushroom tyrosinase.

These assays were all accomplished at 37 ºC and performed by HPLC, by monitoring the loss of substrate and the generation of products. The percentages of these compounds in each assay were calculated using calibration curves (chapter 5, section 5.4.4). Chemical reactions followed pseudo first-order kinetics and were monitored during at least 3 half-lives. Pseudo first-order rate constants (k_{obs}) were calculated from the slopes of plots of ln(Area) vs time (equation 1) and half-lives ($t_{1/2}$) from equation 2. An example of the plots obtained is shown in figure 33.

- Equation 1 – $\mathrm{Ln(Area)} = -k_{obs} \times \mathrm{time} + \mathrm{b}$
- Equation 2 – $t_{1/2} = \frac{\mathrm{Ln}(2)}{k_{obs}}$

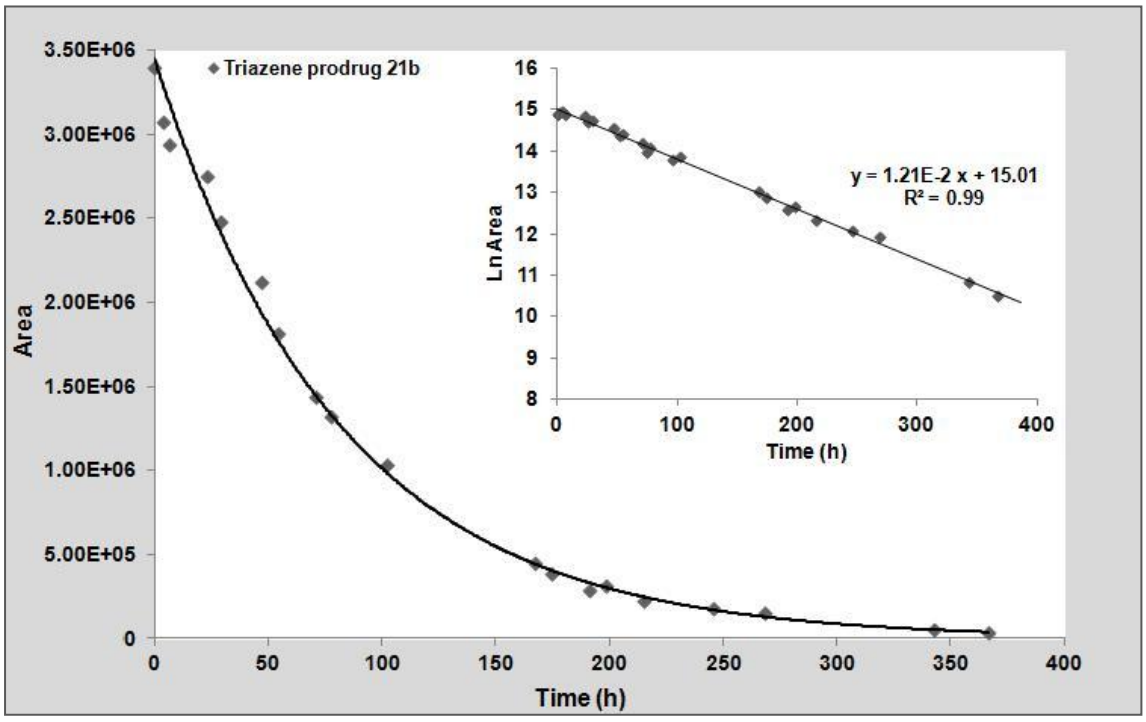

Figure 33 – Plot of the hydrolysis reaction of triazene prodrug 21b in PBS (0.01 M, pH=7.4).

3.2 – Chemical hydrolysis of triazene prodrugs in physiological conditions

Triazene prodrugs **21** suitable for MDEPT strategy must be chemically stable in physiological conditions (37 ºC and pH 7.4) and reach the desired target undecomposed. The assays were performed following the experimental procedure described in the chapter 5, section 5.4.1. The calculated pseudo first-order rate constants (k_{obs}) and half-lives ($t_{1/2}$) for the hydrolysis of triazene prodrugs **21** in PBS are given in table 7.

Table 7 – Results from HPLC analysis of the assays in PBS (0.01 M, pH=7.4) at 37 ºC for triazene prodrugs 21.

Triazene Prodrug	%Prodrug consumption	%Aniline formation	k_{obs} (s^{-1})	R^2	Half-live (h)
21a	97.4 ± 1.5	93.8 ± 0.7	$2.0x10^{-6} \pm 0.2x10^{-6}$	0.99	94.7 ± 10.4
21b	98.4 ± 0.5	92.0 ± 8.6	$3.2x10^{-6} \pm 0.2x10^{-6}$	0.99	60.1 ± 3.9
21c	97.5 ± 3.6	90.1 ± 0.3	$1.9x10^{-6} \pm 0.2x10^{-6}$	0.99	101.5 ± 9.5
21d	93.7 ± 2.7	82.9 ± 0.4	$2.6x10^{-6} \pm 0.3x10^{-6}$	0.99	76.0 ± 9.0
21e	90.6 ± 3.5	81.5 ± 2.1	$1.57x10^{-6} \pm 0.02x10^{-6}$	0.99	122.7 ± 1.9
21f	94.5 ± 2.1	86.7 ± 2.8	$1.63x10^{-6} \pm 0.05x10^{-6}$	0.99	118.2 ± 3.4

Triazene prodrugs **21** decompose in PBS leading to generation of 1-aryl-3-methyltriazenes **23** and hydroxyphenylpropionic acid **24**. Under the reaction conditions, MMTs **23** are also unstable and further hydrolyze into the corresponding anilines (figure 34 and 35) [97].

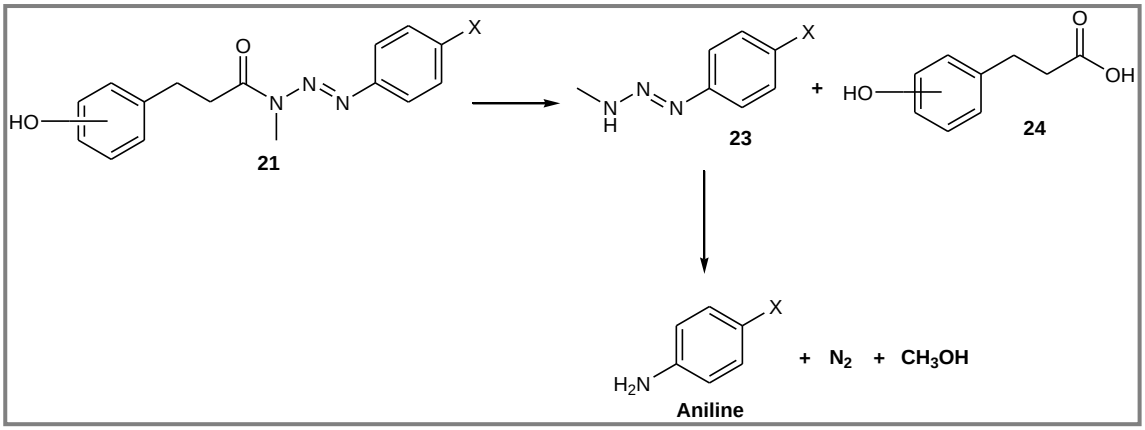

Figure 34 – Chemical hydrolysis reaction of triazene prodrugs 21 and their hydrolysis compounds. Adapted from (97).

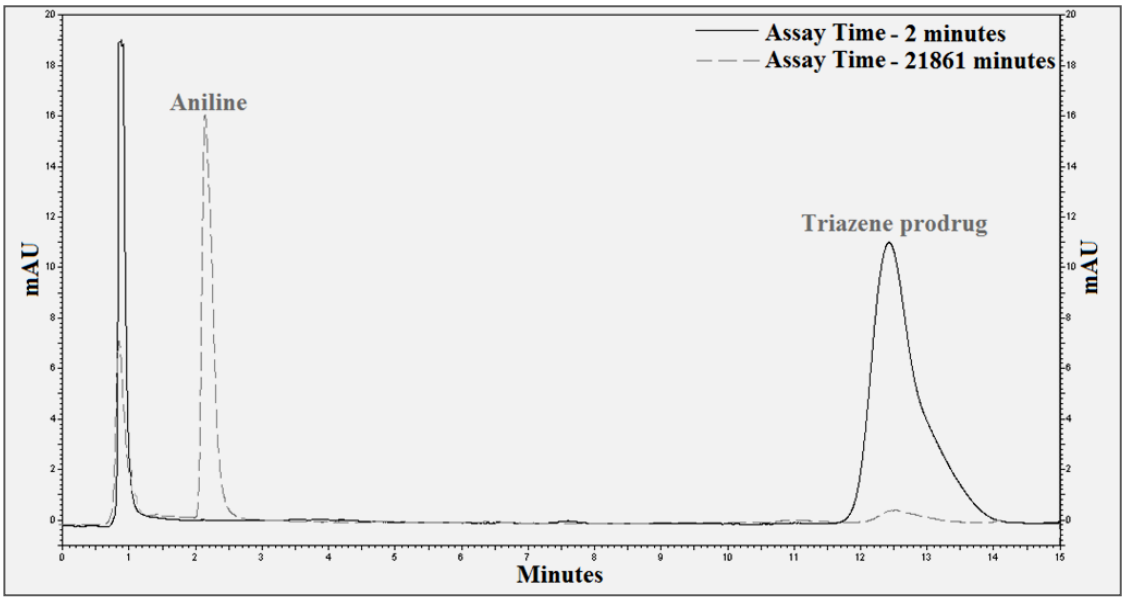

Figure 35 – HPLC chromatograms of the hydrolysis of triazene prodrug 21a in PBS (0.01 M, pH=7.4).

Table 7 shows that triazene prodrugs **21** decompose in this medium with half-lives ranging from 60 to 123 hours, so they are chemically stable in physiological conditions (37 ºC and pH 7.4). When we compare the stability in PBS between triazene prodrugs **21a,b** with **21c,d** respectively, is possible to see that the position of the OH group in the phenolic moiety does not have a significant influence in the chemical hydrolysis of compounds **21**. Complete mass balance was observed for all prodrugs **21** in this assay (table 7 and figure 36).

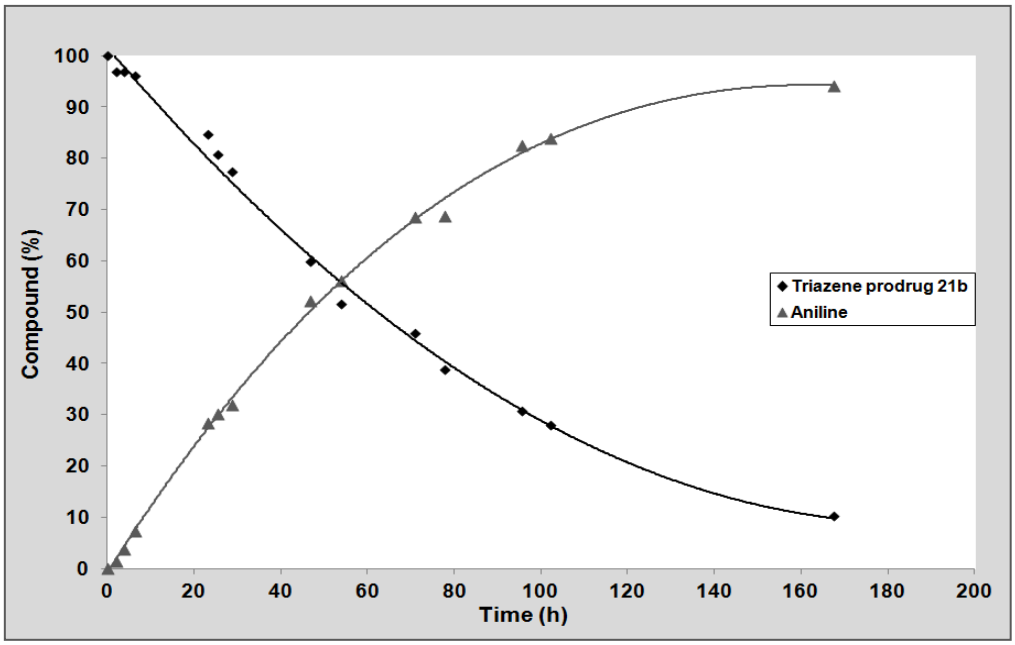

Figure 36 – Time course for the decay of prodrug 21b and generation of aniline.

Carvalho and co-workers analyzed the chemical stability of a range of aminoacyltriazenes **26** in the same conditions. Our prodrugs **21** reveal to be 140 to 240 times more stable in this medium in comparison with compounds **26** [85,86].

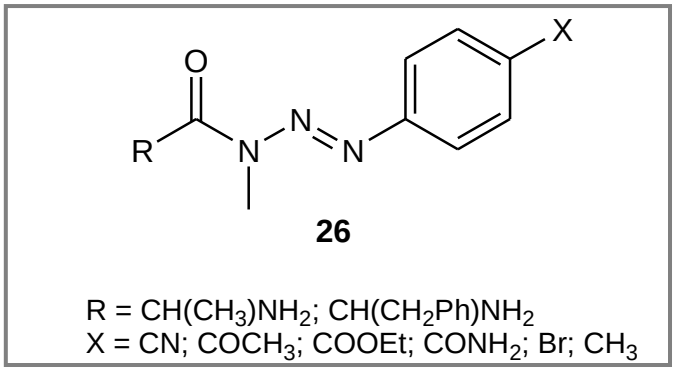

26

R = $CH(CH_3)NH_2$; $CH(CH_2Ph)NH_2$
X = CN; $COCH_3$; COOEt; $CONH_2$; Br; CH_3

Perry and co-workers also evaluated the chemical stability of a range of *N*-acylamino acid derivatives of triazenes **27** in PBS. Although these derivatives **27** gain some stability upon aminoacyl derivatives **26**, they are 6 to 9 times less stable than our prodrugs **21** [84]. Since the only difference between MMT-based prodrugs **21** and MMT-based prodrugs **26** and **27** is in the trigger/carrier unit, is possible to affirm that the hydroxyphenylpropionic acid trigger **24** is more efficient than the amino acid unit in the amide-linker stabilization.

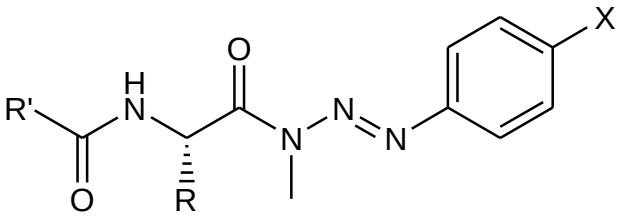

27

R = CH_3; H; CH_2Ph; $CH(CH_3)_2$
R' = CH_3; CH_2CH_3; $CH_2CH_2CH_3$; Ph
X = CN; $COCH_3$; COOEt; $CONH_2$; Br

Our prodrugs **21** also reveal to have an intermediate stability in PBS in comparison with the prodrugs synthesized by Perry, which are a carbamate and an aryl derivatives of prodrugs **26** (Carbamate linker - X = CN, R = OCH_3, $t_{1/2}$ = 46 h; Amide linker - X = CN, R = CH_3, $t_{1/2}$ = 124 h) [97].

Wanner and co-workers synthesized triazene prodrugs **28** with a heterocyclic ring in the triazene moiety. Prodrugs **28a-d** with an amide linkage have half-lives ranging between 22.1 and 58.3 hours and prodrugs **28e-k** (with a carbamate linkage) have half-lives ranging from 0.4 to 58.3 hours. Triazene prodrugs **21** reveal to be more stable in PBS than methyltriazene prodrugs **28** [48].

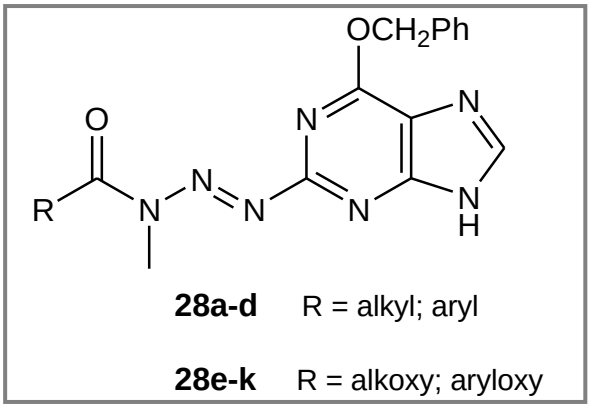

28a-d R = alkyl; aryl

28e-k R = alkoxy; aryloxy

When we compare the stability of our prodrugs **21** with urea and thiourea prodrugs previously synthesized by Knaggs and co-workers for MDEPT strategy (**18a-c** and **19a,b** that practically remained undecomposed after 5 hours of incubation), it is possible to see that prodrugs **21** are at least equal or slightly less stable [39].

Perry and co-workers have also evaluated the stability of potential MDEPT prodrugs **20**, which have an urea linker. Prodrugs **20a-d** are stable in PBS for 15 days and prodrugs **20e-g** have half-lives larger than 15 hours. Triazene prodrugs **21** reveal to be more stable than prodrugs **20e-g** and to have an ideal chemical stability as prodrugs **20a-d** [50].

Prodrugs **21** revealed to be sufficiently stable to reach the tumor cells undecomposed, which allowed further chemical and enzymatic studies.

3.3 – Hydrolysis of triazene prodrugs in human plasma

Blood serum and plasma contain a variety of enzymes that catalyse the hydrolysis of ester and amide functions. Since triazene prodrugs **21** have in their structure an amide function, tests in human plasma were performed in order to evaluate if prodrugs **21** are stable in this medium [84,101].

These assays were performed following the experimental procedure described in the chapter 5, section 5.4.2. The calculated pseudo first-order rate constants (k_{obs}) and half-lives ($t_{1/2}$) for the hydrolysis of prodrugs **21** in human plasma are given in table 8.

Table 8 – Results from HPLC analysis of the assays in human plasma (80% v/v) at 37 ºC for triazene prodrugs 21.

Triazene Prodrug	%Prodrug consumption	%Aniline formation	%MMT formation*	k_{obs} (s^{-1})	R^2	Half-live (h)
21a	98.9 ± 0.2	nd	nd	$2.48x10^{-5} \pm 0.03x10^{-5}$	0.99	7.8 ± 0.1
21b	99.9 ± 0.2	85.4 ± 4.1	38.4 ± 9.2	$7.1x10^{-5} \pm 0.2x10^{-5}$	0.99	2.7 ± 0.1
21c	99.0 ± 0.5	nd	nd	$2.66x10^{-5} \pm 0.09x10^{-5}$	0.99	7.3 ± 0.2
21d	96.1 ± 1.8	85.1 ± 2.9	18.3 ± 2.6	$3.3x10^{-5} \pm 0.1x10^{-5}$	0.99	5.8 ± 0.3
21e	90.7 ± 0.9	82.8 ± 1.2	nd	$1.32x10^{-5} \pm 0.03x10^{-5}$	0.99	14.6 ± 0.4
21f	88.9 ± 0.6	89.7 ± 5.9	nd	$4.0x10^{-6} \pm 0.3x10^{-6}$	0.99	48.5 ± 2.9

*maximum % observed in the assay.

In this assay it was possible to observe for triazene prodrugs **21b,d**, their hydrolysis in the corresponding MMT-CN **23**. Over time MMT-CN **23** began to be hydrolyzed in the corresponding aniline-CN (figure 37). Complete mass balance was observed for prodrugs **21b,d-f** (table 8 and figure 38).

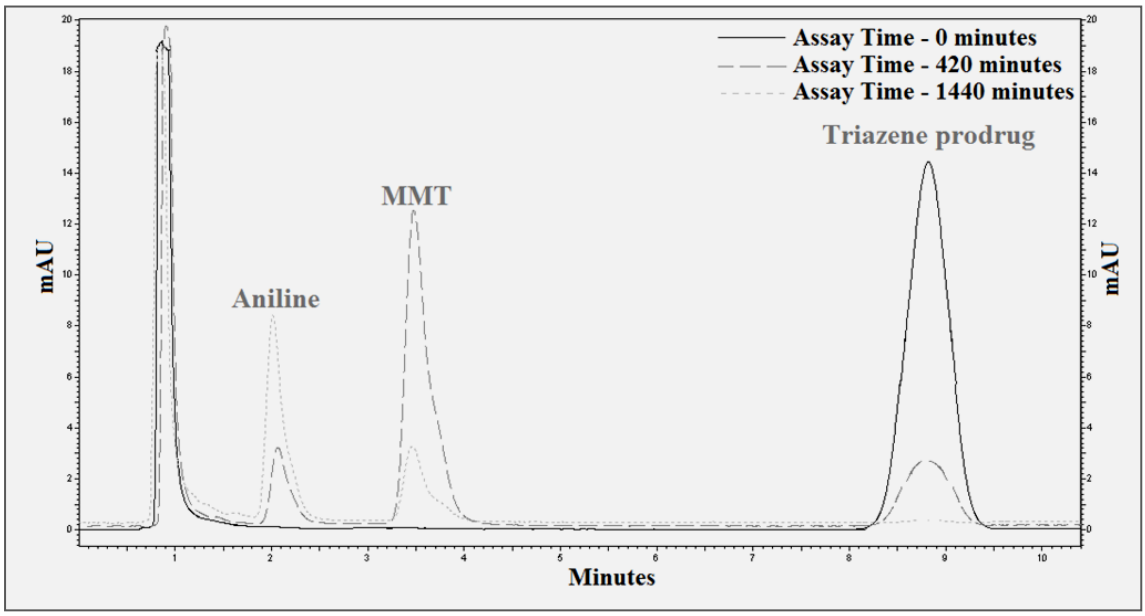

Figure 37 – HPLC chromatograms of the hydrolysis of triazene prodrug 21b in human plasma (80% v/v).

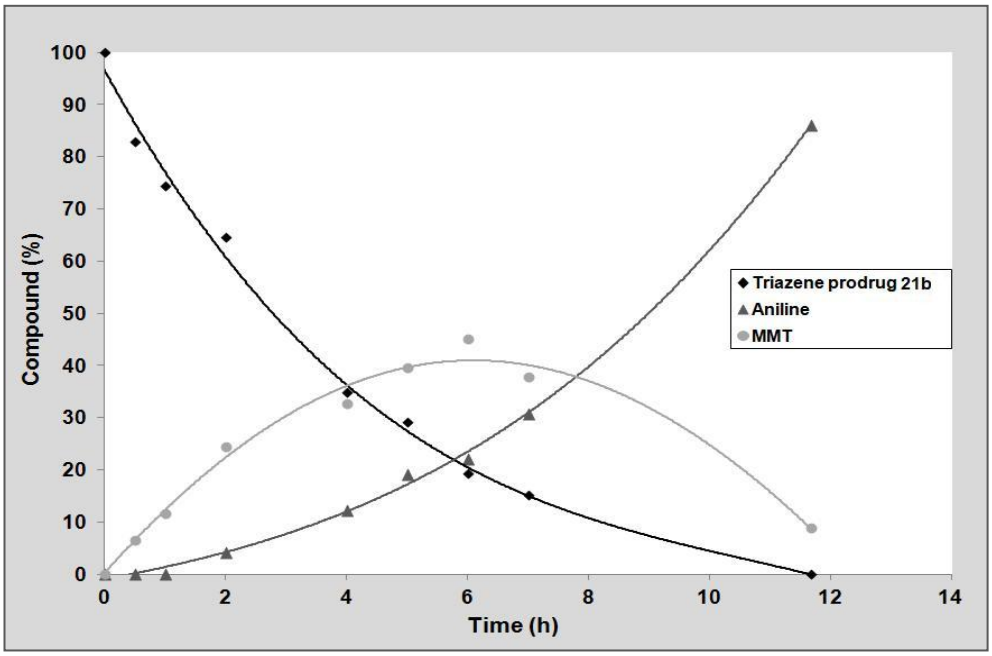

Figure 38 – Time course for the formation and decay of intermediates in the plasma hydrolysis of prodrug 21b.

The half-lives (table 8) obtained in these assays range from 3 to 49 hours. These results clearly show that all prodrugs **21** are substrates for plasma enzymes, because they are hydrolyzed 3 to 22 times faster in plasma than in PBS. When prodrugs **21** are compared with other triazene derivatives with an amide function, it is possible to assess that:

- Triazene prodrugs **21** are 2 to 6.5 times more stable than *N*-acylamino acid derivatives of triazenes **27** [84];
- The low stability of triazene prodrugs **21b,d**, which are derivatives of MMT-CN **23**, in human plasma has been previously observed for aminoacyltriazenes **27** [85];
- Triazene prodrugs **21e,f** reveal to be more stable when compared with the aryl derivative of prodrugs **26** synthesized by Perry (Amide linker - X = CN, R = CH_3, $t_{1/2}$ = 13 h) [97].

Comparison of stability of triazene prodrugs **21** in plasma, with other potential MDEPT prodrugs shows that:

- Amide linker in triazene prodrugs **21** is much more stable than the carbamate linker in prodrug **9** ($t_{1/2}$ = 0.8 h). Prodrug **17**, which have an urea linker, remained undecomposed after 2 hours of incubation in plasma, so it is more stable than prodrugs **21** [51,54];
- In almost all cases, amide linker in triazene prodrugs **21** provides more stability than thiourea linker in prodrugs **18b,d** and **19b** ($t_{1/2} \leq 5$ h). Urea linker in prodrugs **18a,c** and **19a** ($t_{1/2} \geq 5$ h) reveal to be as stable as the amide linker in prodrugs **21** [39];
- Amide linker in triazene prodrugs **21** is as stable as urea linker in prodrugs (**20e-g**, $5.7 \leq t_{1/2}$ (h) ≤ 15), but is less stable than urea linker in prodrugs (**20a-d**, $t_{1/2} \geq 72$ h) [50].

Triazene prodrugs **21**, with the exception of **21b**, have an adequate stability in plasma, so they are suitable for MDEPT strategy.

3.4 – Activation of triazene prodrugs by mushroom tyrosinase

These assays were performed in order to evaluate the ability of triazene prodrugs **21** to act as substrates for tyrosinase and their capacity to release the cytotoxic agent MMT **23** after tyrosinase activation. These assays are fundamental due to the fact that tyrosinase is the target enzyme in MDEPT strategy.

These assays were performed according with the experimental procedure described in the chapter 5, section 5.4.3. The calculated pseudo first-order rate constants (k_{obs}) and half-lives ($t_{1/2}$) for the activation of compounds **21** and **25** by mushroom tyrosinase are given in table 9.

Table 9 – Results from HPLC analysis of the assays performed in the presence of mushroom tyrosinase at 37 ºC for triazene prodrugs 21 and 25.

Triazene prodrugs	Mushroom tyrosinase (units/mL)	%Prodrug consumption	%Aniline formation	%MMT formation	k_{obs} (s^{-1})	R^2	Half-live (h)
21a	300	97.5 ± 3.4	54.9 ± 11.2	2.0 ± 0.2	$9.1x10^{-6} \pm 0.9x10^{-6}$	0.99	21.2 ± 2.0
21b	300	91.1 ± 3.6	68.9 ± 11.4	4.6 ± 0.7	$9.9x10^{-6} \pm 0.9x10^{-6}$	0.99	19.5 ± 1.8
21c	100	100**	36**	5**	$4.7x10^{-3} \pm 0.4x10^{-3}$	0.99	0.041 ± 0.004
21d	100	100**	46**	4**	$7.9x10^{-3} \pm 0.5x10^{-3}$	0.99	0.025 ± 0.002
21e	100	100**	24**	5**	$3.2x10^{-3} \pm 0.3x10^{-3}$	0.99	0.061 ± 0.005
21f	100	100**	20**	4**	$2.5x10^{-3} \pm 0.2x10^{-3}$	0.99	0.077 ± 0.005
25a	100	----------	----------	----------	$1.8x10^{-3}$**	0.99**	0.105**
25b	100	----------	----------	----------	$2.1x10^{-3}$**	0.99**	0.093**

*maximum % observed in the assay; **single assay.

Comparing the results in table 9 with the ones in table 7, we can clearly affirm that triazene prodrugs **21** are substrates of mushroom tyrosinase. Depending on the hydroxyphenylpropionic acid derivative **24**, two different processes were observed:

- After tyrosinase activation, triazene prodrugs **21a,b** (3-(3-hydroxyphenyl)propionic acid derivatives), released the corresponding MMT derivatives **23**. MMT **23** specie remained for a while and then it began to be hydrolyzed in the corresponding aniline over time (figure 39 and 40);

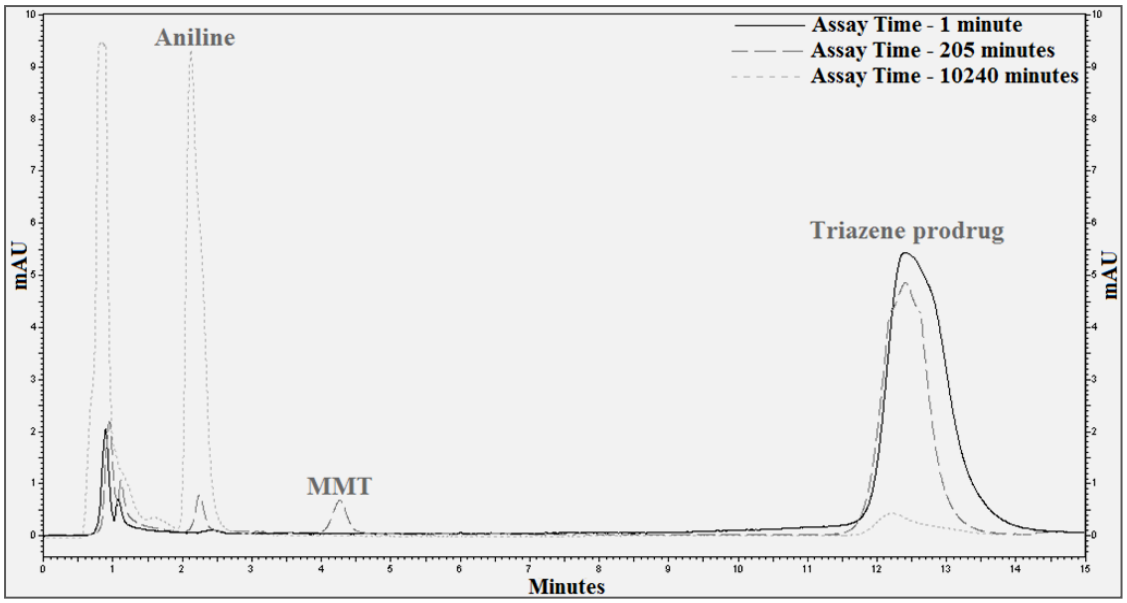

Figure 39 – HPLC chromatograms of the activation of triazene prodrug 21a by mushroom tyrosinase.

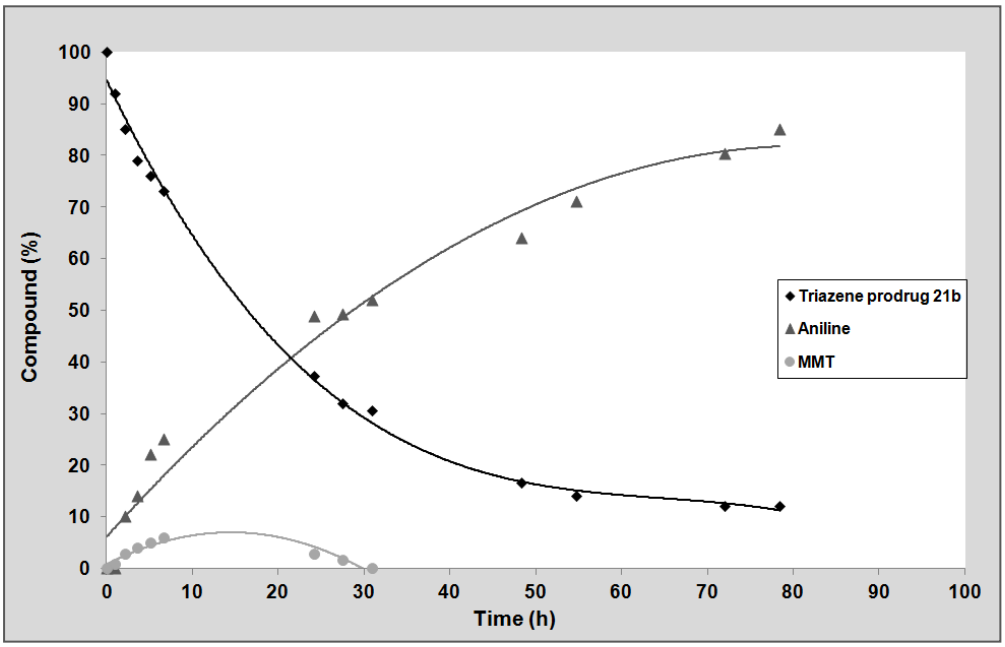

Figure 40 – Time course for the formation and decay of intermediates after activation of prodrug 21b by mushroom tyrosinase.

- Triazene prodrugs **21c-f** (3-(4-hydroxyphenyl)propionic acid derivatives), when exposed to mushroom tyrosinase, are oxidized into an intermediate specie **29** before the MMT **23** release (figure 41 and 42). This intermediate could be a quinone specie that is stable enough to be detected. In the literature is referred the generation of a similar quinone specie when 3-(4-hydroxyphenyl)propionic acid is oxidized by tyrosinase [20]. Actually, it was already observed by Perry

and co-workers, using LC-MS, the generation of a similar intermediate in the oxidation of compounds **20b,c** and **e** promoted by mushroom tyrosinase [50].

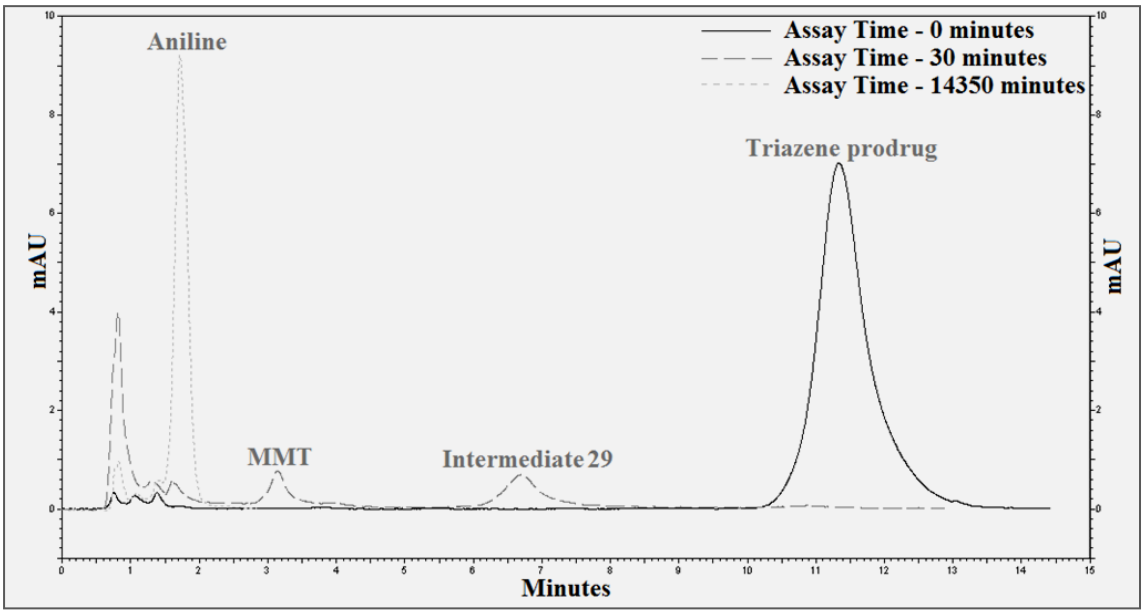

Figure 41 – HPLC chromatograms of the activation of triazene prodrug 21e by mushroom tyrosinase.

With the data collected from the assays of prodrugs **21c-f** in the presence of mushroom tyrosinase, we hypothesized a tyrosinase-dependent mechanism of MMT **23** release (figure 42). In this drug release pathway, triazene prodrugs **21c-f** are oxidized by tyrosinase in the corresponding orthoquinone **29**. Then this specie **29** can initiate an intramolecular cyclization pathway and MMT **23** is released from a reactive intermediate instable in aqueous media.

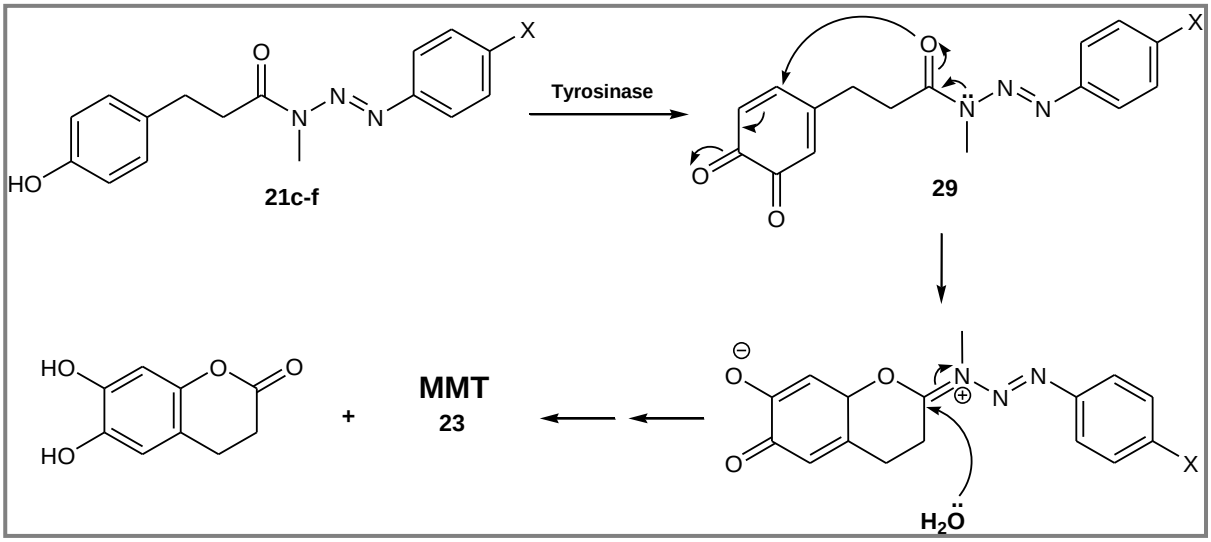

Figure 42 – Hypothetic mechanism for MMT 23 release from prodrugs 21c-f after tyrosinase activation.

The release of MMT **23**, was detected 250 seconds after exposure of triazene prodrugs **21c-f** to mushroom tyrosinase. The maximum percentage of MMT **23** generation that was detected, ranged from 4 to 5 % (figure 43). MMT release from prodrugs **21c-f** is much faster in comparison with other drug release pathways described in the literature for potential MDEPT prodrugs. In prodrugs **9**, **10b** and **17** synthesized by Jordan and co-workers, the drug release after tyrosinase activation was only detected at 10.2, 30 and 30 minutes, respectively [51,52,54].

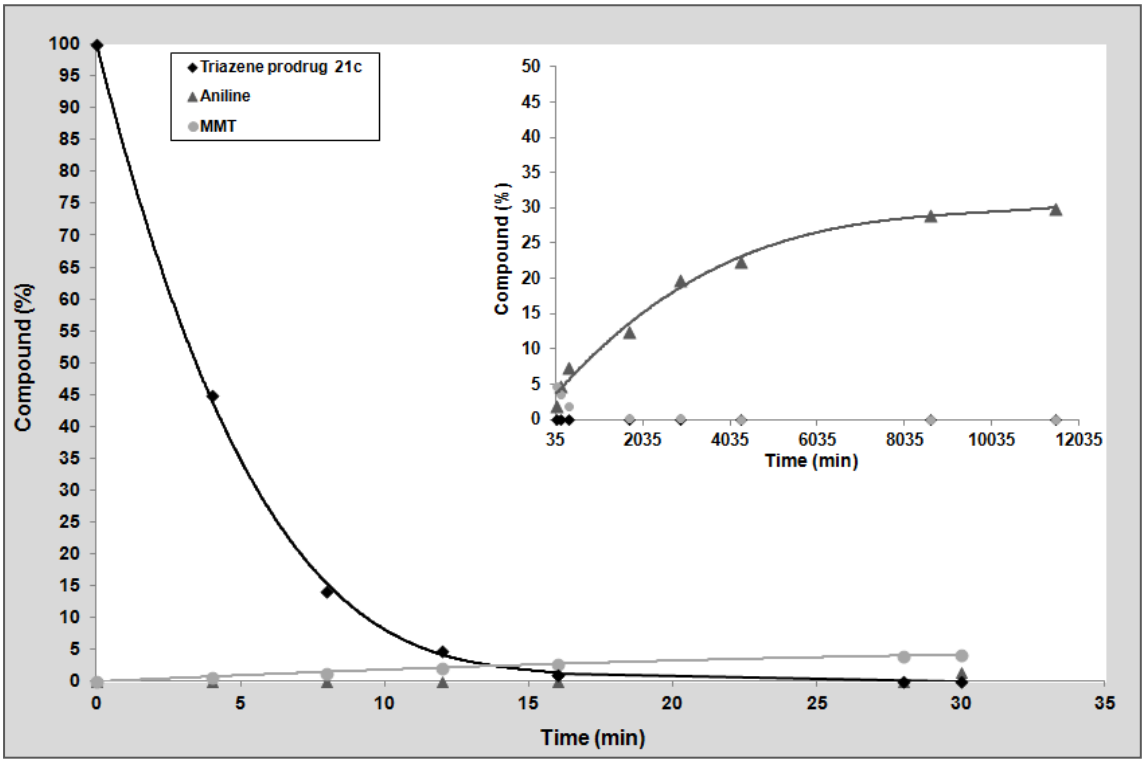

Figure 43 – Time course for the formation and decay of intermediates after activation of prodrug 21c by mushroom tyrosinase.

In these assays, the complete mass balance was not observed because we never saw the total formation of aniline. This situation can be explained by the fact that aromatic amines (e.g: anilines) are also tyrosinase substrates. Toussaint and co-workers have found in a previous research work that several *p*-anilines are oxidized in a two-step mechanism by tyrosinase. Firstly, *p*-anilines suffer an ortho hydroxylation and then they are converted to *o*-quinone imines [102]. The interaction mechanism between *p*-anilines and the active site of tyrosinase was proposed by Munoz-Munoz and co-workers [19]. The formation of this *o*-quinone imine specie can be the main reason by which we did

not observe the expected total concentration of aniline in these mushroom tyrosinase assays.

When the half-lives of triazene prodrugs **21c-f** are compared with the half-lives of triazene prodrugs **21a,b**, it is possible to see that the derivatives of 3-(4-hydroxyphenyl)propionic acid have much more affinity for tyrosinase than the derivatives of 3-(3-hydroxyphenyl)propionic acid. A similar difference has already been observed in a previous work of Fenoll and co-workers, in which they found that the catalytic efficiency of tyrosinase is much higher for 4-hydroxyanisole than for 3-hydroxyanisole [103].

Triazene prodrugs **21c-f** reveal to be excellent tyrosinase substrates with half-lives that range from 1.5 to 5 minutes. These prodrugs **21c-f** have a better affinity for tyrosinase in comparison with other potential MDEPT prodrugs described in the literature because they have shorter half-lives in the presence of mushroom tyrosinase:

- Prodrugs **18a,c** and **19a** synthesized by Knaggs co-workers have, in the presence of 938 units of mushroom tyrosinase per mL, half-lives that range from 58 to 100 minutes [39];
- Triazene prodrugs **20** synthesized by Perry and co-workers have, in the presence of 100 units of mushroom tyrosinase per mL, half-lives that range between 6.1 an 18.2 minutes [50].

Tyrosinase activation in compounds **25a,b** was also evaluated and it was surprisingly found that these compounds are excellent tyrosinase substrates despite of being large molecules. Compounds **25a,b** have a half-live of approximately 6 minutes. In this assay it was possible to observe the generation of two intermediate species **29** and **30** (figure 44 and 45). Intermediate **30** could be the same type of quinone specie already observed during the hydrolysis of prodrugs **21c-f**.

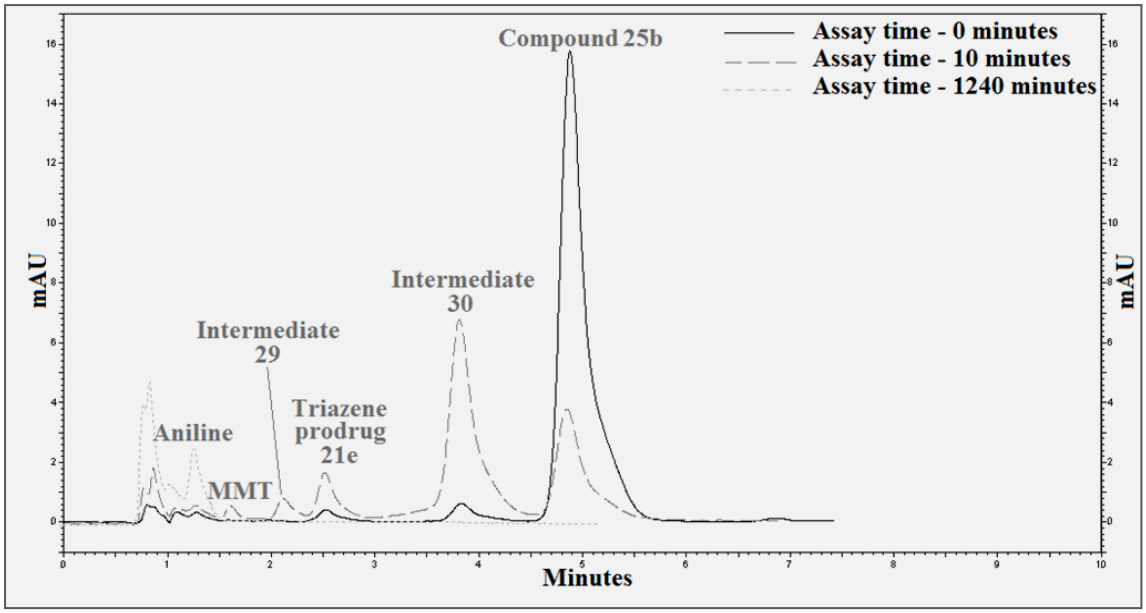

Figure 44 – HPLC chromatograms of the activation of compound 25b by mushroom tyrosinase.

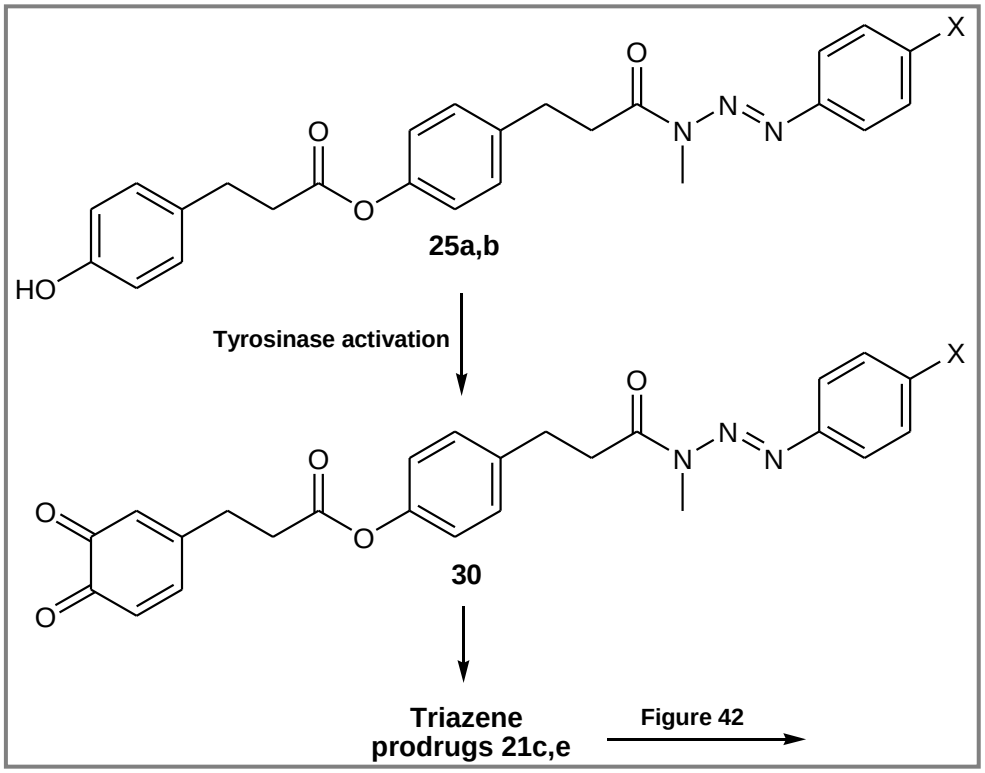

Figure 45 – Formation of a quinone specie 30, after tyrosinase activation in compounds 25a,b.

Since compounds **21c-f** and **25a,b** are excellent tyrosinase substrates, it was calculated the partition coefficients using the ALOPS 2.1 (table 10) and their respective molecular weights (MW) in order to estimate if they have the ability to diffuse across the biological membranes in the malignant melanoma cells [104,105].

Table 10 – Calculated log *P* and MW for triazene prodrugs 21c-f and 25a,b

Triazene prodrugs	Substituent X	Calculated log *P*	MW
21c	$COOCH_3$	3.45 ± 0.63	341.14
21d	CN	3.29 ± 0.67	308.13
21e	$COCH_3$	3.35 ± 0.63	325.14
21f	$CONH_2$	2.63 ± 0.62	326.14
25a	$COOCH_3$	5.09 ± 0.81	489.19
25b	$COCH_3$	5.00 ± 0.80	473.20

Due to the fact that these log *P* were calculated, it is only possible to estimate that:

- Prodrug **21f** has a calculated log *P* near to 2, so it is in the desirable range to diffuse freely across biological membranes. Triazene prodrugs **21c-e** are not definitely excluded because in the literature there are some examples of some successful drugs/prodrugs that have log *P* values outside this desirable range. In terms of MW, prodrugs **21c-f** are in the desirable range (MW < 500 g/mol) to permeate across biological membranes [106,107];
- According to Lipinski rules, compounds **25a,b** will have problems to diffuse freely across biological membranes, because they are too lipophilic (log P > 5) and their MW are near to 500 g/mol [107].

3.5 – Conclusions

Taking into account the results described in this chapter, it is possible to conclude that in terms of stability:

- Triazene prodrugs **21** show to be chemically stable in physiological conditions (37 ºC and pH 7.4) with half-lives between 60 and 123 hours;
- Most of triazene prodrugs **21**, with the exception of triazene prodrug **21b**, show to be stable in human plasma with half-lives between 6 and 49 hours;
- Amide function reveals to be very stable in both mediums;
- It is expected that most of triazene prodrugs **21** reach the malignant melanocytes undecomposed.

In terms of triazene prodrugs **21** activation by mushroom tyrosinase, it is possible to conclude that:

- Triazene prodrugs **21c-f** have much more affinity for tyrosinase than triazene prodrugs **21a,b**;
- Triazene prodrugs **21c-f** reveal to be excellent tyrosinase substrates with half-lives between 1.5 and 5 minutes and they will promote a fast release of the cytotoxic agent MMT **23** after tyrosinase activation.

Despite of being large molecules, compounds **25a,b** reveal to be excellent tyrosinase substrates with half-lives of approximately 6 minutes.

The final conclusion about these results is that triazene prodrugs **21c-f** have the stability, the tyrosinase affinity and the drug release efficiency to be promising for application in MDEPT strategy.

CHAPTER 4 – Hepatotoxicity Assessment of Triazene Prodrugs

4.1 – Introduction

The liver is an important target of prodrugs/drugs toxicity due to its unique metabolism and relationship to the gastrointestinal tract. Hepatotoxicity evaluation of triazene prodrugs **21** is necessary because when these prodrugs, which have in their structure a phenolic moiety, pass through the liver they can possibly be metabolized by liver CYP450 enzymes into cytotoxic quinones that cause liver cell toxicity [108,109]. Benzoquinones and related compounds have the ability to react irreversibly with GSH by conjugate addition, causing GSH depletion.

In terms of phenolic moiety, prodrugs **21** can be considered as analogs of monoalkylphenols. Since the metabolization by CYP450 enzymes in monoalkylphenols, as *p*-cresol and *m*-cresol, are described in the literature, we can hypothesize the type of quinones formed, after CYP450 metabolization in triazene prodrugs **21**.

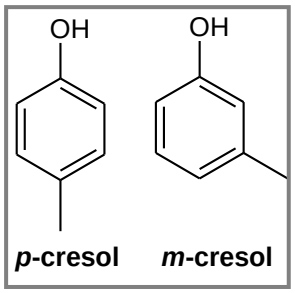

Triazene prodrugs **21a,b** are related with *m*-cresol, because they both are phenolic compounds with a *meta* alkyl group. Sulistyaningdyah and co-workers have found in a previous work that *m*-cresol is metabolized by CYP450 into the corresponding *p*-hydroquinone compound [110]. Based on this information we can theorize the metabolic pathway promoted by liver CYP450 in triazene prodrugs **21a,b** and the following conjugation reactions between the quinone formed and GSH (figure 46).

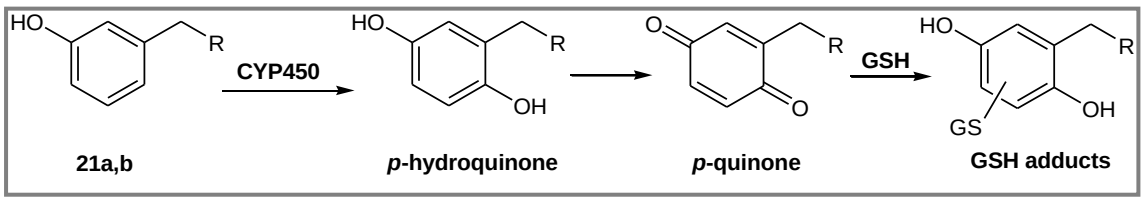

Figure 46 – Possible metabolic activation by liver CYP450 in triazene prodrugs 21a,b.

Since triazene prodrugs **21c-f** are phenolic compounds with a *para* alkyl group, we can compare them with *p*-cresol. In the literature there are references about two metabolic pathways, in which *p*-cresol is metabolized by CYP450 into two different types of quinones. Thompson and co-workers have discovered in a prior work that *p*-cresol is metabolized in a CYP450-dependent metabolism into a quinone methide specie [111]. Later, Yan and co-workers have found that *p*-cresol can also be metabolized by CYP450 into the corresponding *o*-hydroquinone compound [112]. With this information we can hypothesize the metabolic pathways promoted by liver CYP450 activation in triazene prodrugs **21c-f** and the subsequent conjugation reactions between the quinone species generated and GSH (figure 47).

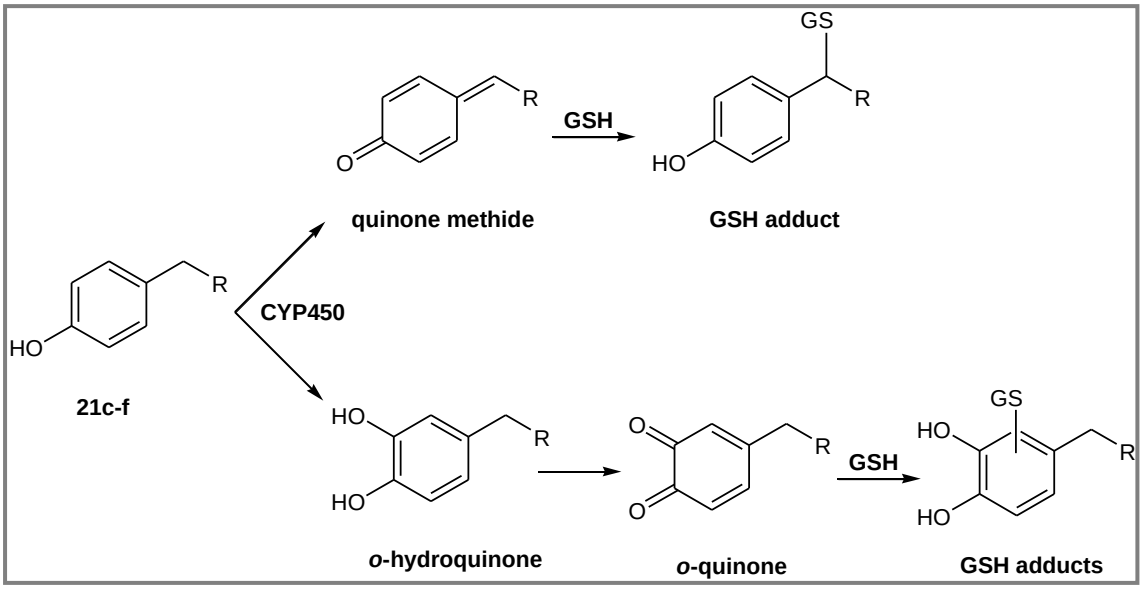

Figure 47 – Possible metabolic pathways promoted by liver CYP450 activation in triazene prodrugs 21c-f.

The methodology used in the hepatotoxicity assessment of triazene prodrugs **21** is based on the experimental procedure developed by Moridani and co-workers (chapter 5, section 5.5) [61]. In this assay is measured the GSH depletion induced by triazene prodrugs **21**, when they are metabolized/oxidized into cytotoxic quinones by a rat liver CYP450 microssomal preparation/NADPH/O_2 system. GSH that is not depleted, will further react and reduce 5,5'-dithiobis-2-nitrobenzoic acid (DTNB) to form 2-nitro-5-thiobenzoic acid, which formation can be followed by UV spectroscopy at 412 nm (figure 48).

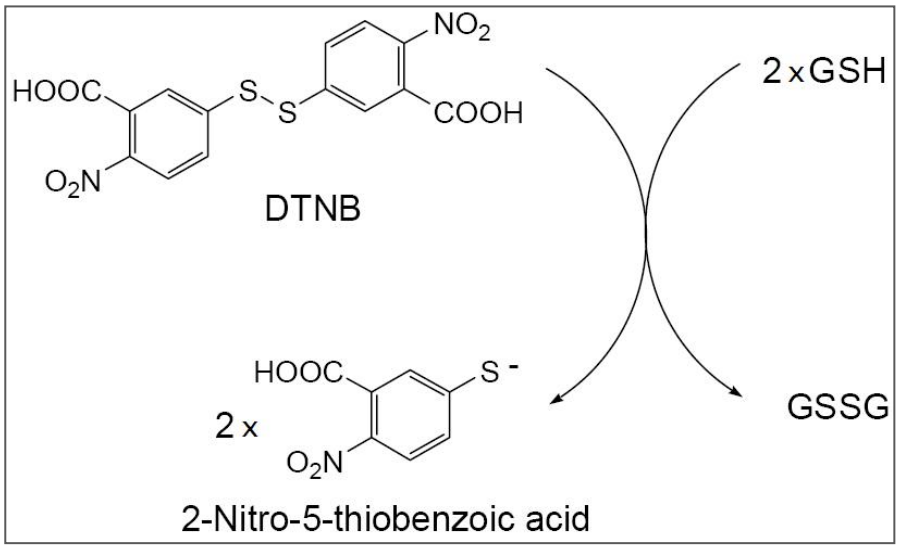

Figure 48 – Calculation of non depleted GSH, following 2-Nitro-5-thiobenzoic acid generation at 412 nm.

The percentage of GSH depletion ($GSH_{depletion}$ (%)) observed in these assays is related with the non depleted GSH by the equation 3:

- Equation 3 –

$$GSH_{depletion}\,(\%) = \left(\frac{\text{Total GSH (n)} - \text{ Non depleted GSH (n)}}{\text{Total GSH (n)}} \times 100\right) \text{x } 2^{*}$$

* The GSH concentration used in these assays was twice as the concentration of triazene prodrugs **21**.

Non depleted GSH was quantified using a calibration curve (chapter 5, section 5.5.1).

4.2 – Results and Discussion

$GSH_{depletion}$ (%) was measured at selected times of incubation (30, 60 and 180 min) and the results obtained for each triazene prodrug **21** are shown in figure 49.

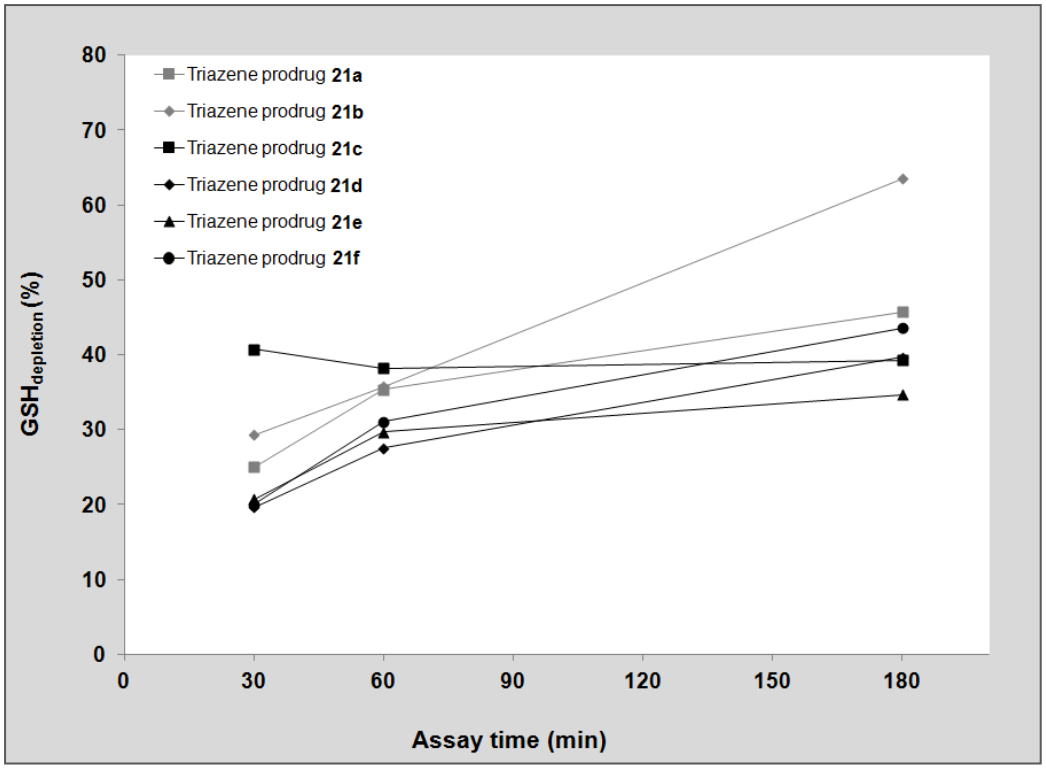

Figure 49 – $GSH_{depletion}$ (%) induced by triazene prodrugs 21 at different times.

By analysis of figure 49 it is possible to see that most of triazene prodrugs **21** promote an increase of $GSH_{depletion}$ (%) in the course of the assay. The maximum $GSH_{depletion}$ (%) induced by each triazene prodrug **21** was detected at 180 min of incubation and is shown in table 11.

Table 11 – $GSH_{depletion}$ (%) induced by triazene prodrugs 21 at 180 min of incubation.

Triazene prodrug	Hydroxyphenylpropionic acid derivative	Substituent X	Maximum $GSH_{depletion}$ (%)
21a	3-(3-hydroxyphenyl)propionic acid	$COOCH_3$	45.7 ± 5.0
21b	3-(3-hydroxyphenyl)propionic acid	CN	63.5 ± 5.0
21c	3-(4-hydroxyphenyl)propionic acid	$COOCH_3$	39.3 ± 1.0
21d	3-(4-hydroxyphenyl)propionic acid	CN	39.6 ± 8.6
21e	3-(4-hydroxyphenyl)propionic acid	$COCH_3$	34.6 ± 8.6
21f	3-(4-hydroxyphenyl)propionic acid	$CONH_2$	43.6 ± 2.0

The maximum $GSH_{depletion}$ (%) induced by prodrugs **21a,b** (3-(3-hydroxyphenyl)propionic acid derivatives) is 45.7 ± 5.0 and 63.5 ± 5.0, respectively. Prodrugs **21c-f** (3-(4-hydroxyphenyl)propionic acid derivatives) promote a maximum $GSH_{depletion}$ (%) from 34.6 ± 8.6 to 43.6 ± 2.0. Comparing the triazene prodrugs **21a,b** with **21c-f**, is possible to see that prodrugs **21a,b** are more hepatotoxic. This result can be possibly explained by the different types of quinones generated that are described in figure 47 and 48. The different rates of quinone generation and their conjugation with GSH, can possibly lead to the differences observed by us.

Vad and co-workers evaluated the $GSH_{depletion}$ (%) caused by some 3- and 4-hydroxy analogs of phenolic agents **31** in the same type of assay. They concluded that there was no distinctive order of metabolism observed for the different phenolic analogs **31** in this assay and that the oxidation state, presence of an electron donating/withdrawing group and position of the functional group on the phenolic moiety have a major role in the metabolization of phenolic compounds. Analysis of their results showed some 3-hydroxy analogs (3-hydroxyacetophenone (3-HAP) and 3-hydroxybenzoic acid (3-HBA)) that are more hepatotoxic than the corresponding 4-hydroxy analogs (4-HAP and 4-HBA) [113].

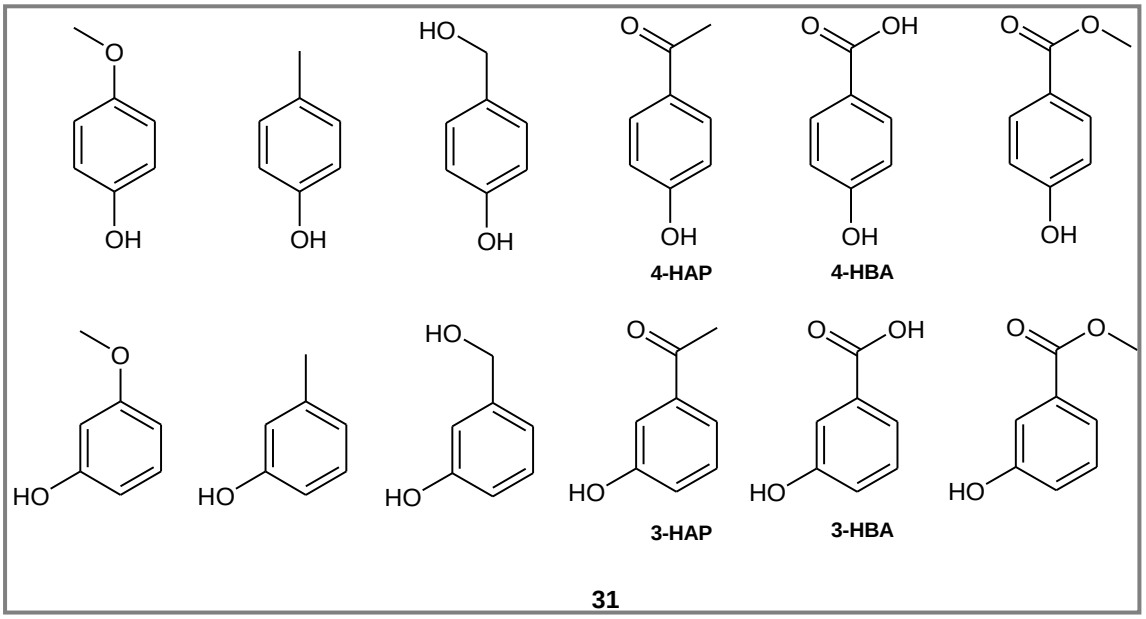

31

In 2010, Kudugunti and co-workers analyzed the $GSH_{depletion}$ (%) induced by several analogs of cinnamic acid **32** in the same type of assay. Compounds **32** promoted $GSH_{depletion}$ (%) between 46 ± 7 and 146 ± 7, which are higher in comparison with $GSH_{depletion}$ (%) induced by triazene prodrugs **21c-f** [114].

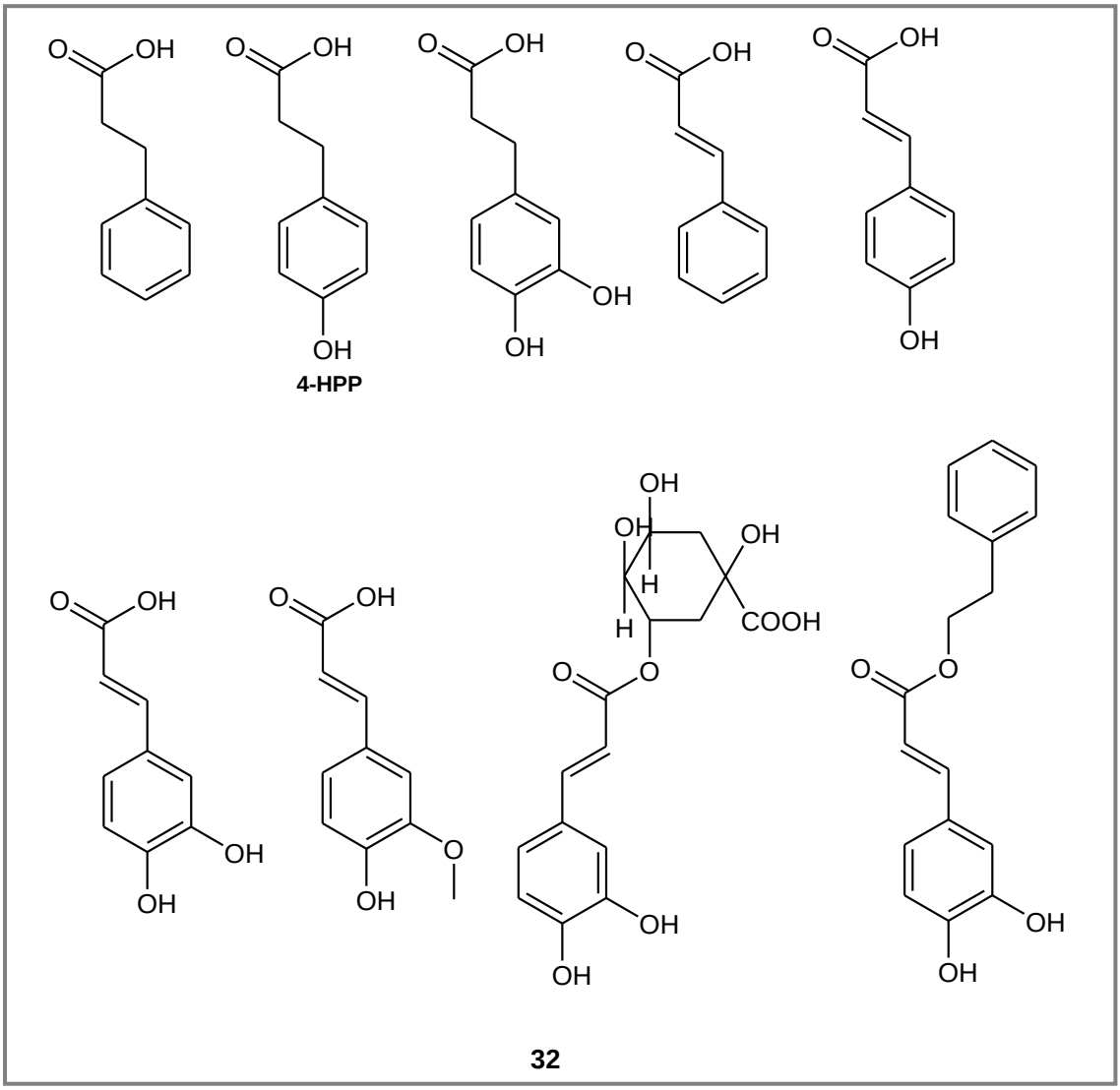

One of compounds **32** was 3-(4-hydroxyphenyl)propionic acid (4-HPP), which is the trigger unit in our triazene prodrugs **21c-f**. The $GSH_{depletion}$ (%) promoted by this compound was 56 ± 4 %, which is higher than the $GSH_{depletion}$ (%) induced by triazene

prodrugs **21c-f** [114]. Based on this result is possible to say that the insertion of MMT **23** in the structure of 3-(4-hydroxyphenyl)propionic acid, decreases its hepatotoxicity.

4-HA, which has a phenolic moiety in its structure was investigated for melanoma treatment in clinical trials, however this compound revealed to be very hepatotoxic [113]. Vad and co-workers have found in a previous research work that the $GSH_{depletion}$ (%) induced by this compound was 88% [53]. When the $GSH_{depletion}$ promoted by triazene prodrugs **21c-f** is compared with this result, it is possible to observe that prodrugs **21c-f** have half of the hepatotoxicity that is induced by 4-HA. With this result we can hypothesize that we are in the right path to reduce the toxicity associated with this type of compounds for MDEPT strategy.

4.3 – Conclusions

With the results obtained in this chapter it is possible to conclude that:

- Prodrugs **21c-f** reveal to be less hepatotoxic than the prodrugs **21a,b**;
- The hepatotoxicity of prodrugs **21c-f** is lower in comparison with most of similar compounds **32** described in the literature;
- The insertion of MMT **23** in the structure of 3-(4-hydroxyphenyl)propionic acid, reduces its hepatotoxicity;
- Since triazene prodrugs **21c-f** have half of the hepatotoxicity induced by 4-HA, we can conclude that they are more suitable for MDEPT strategy.

CHAPTER 5 – Experimental Methodology

5.1 – General information

5.1.1 – Reagents and solvents

- 2-chloro-4,6-dimethoxy-1,3,5-triazine 97% (Sigma-Aldrich)
- 3-(3-hydroxyphenyl)propionic acid 98% (Alfa Aesar)
- 3-(4-hydroxyphenyl)propionic acid 98% (Sigma-Aldrich)
- 3-(3,4-Dihydroxyphenyl)propionic acid 98% (Sigma-Aldrich)
- Acetonitrile (ACN) HPLC (Fisher)
- DCC (Merck)
- DCM (Valente e Ribeiro, Lda)
- Deuterated chloroform (Merck)
- Deuterated methanol (Merck)
- Diethylenetriaminepentaacetic acid (DETAPAC) ≥ 99% (Fluka)
- DMAP ≥ 99% (Sigma-Aldrich)
- DMF anhydrous 99.8% (Sigma-Aldrich)
- Dimethyl sulfoxide (Merck)
- DTNB ≥ 98% (Sigma-Aldrich)
- Ethyl Ether (Panreac)
- Formaldehyde solution puriss. p.a. (Sigma-Aldrich)
- HOBt ≥ 99% (Sigma-Aldrich)
- Hydrochloric acid 1.0 mol (Riedel-de Haën)
- L-Glutathione reduced ≥ 98% (Sigma-Aldrich)
- Methylamine 40% solution in water (Merck)
- Mushroom Tyrosinase (Sigma-Aldrich)
- N-methylmorpholine ≥ 98% (Fluka)
- n-Hexane (Valente e Ribeiro, Lda)
- NADPH regenerating system solution A (31 mM $NADP^+$, 66 mM Glucose-6-phosphate and 66 mM $MgCl_2$ in H_2O) (BD biosciences)

- NADPH regenerating system solution B (40 U/mL Glucose-6-phosphate dehydrogenase in 5 mM sodium citrate) (BD biosciences)
- PBS in tablets (Sigma-Aldrich)
- Petroleum ether B.P. 35ºC to 60ºC (Fisher scientific)
- Pooled rat (Sprague-Dawley) male liver microsomes (BD biosciences)
- Sodium hydride 80% (BDH laboratory reagents)
- Sodium hydroxide 1M (Riedel-de Haën)
- Sodium nitrite (Merck)
- TBTU ≥ 97% (Fluka)
- THF (Fisher scientific)
- Thionyl chloride (Merck)
- Trichloroacetic acid (Merck)
- Triethylamine ≥ 99% (Sigma-Aldrich)
- Tris(hydroxymethyl)aminomethane (Tris) (Merck)
- Water Milli-Q 18MΩcm
- Zirconium (IV) *tert*-butoxide 99.999% (Sigma-Aldrich)

5.1.2 – Equipment

- Thin layer chromatographies (TLC) were performed on silica gel plates from Merck DC Kieselgel 60 F_{254} and were analyzed under a CAMAG UV lamp;
- The reactions performed with microwave irradiation were carried out in a CEM Discover microwave reactor;
- Column chromatographies were performed in glass columns filled with silica gel from Merck Kieselgel 60 (0.040 nm-0.063nm);
- UV spectra were recorded in a spectrophotometer Shimadzu UV-1700 coupled with a Shimadzu CPS-240 thermostatized unit;
- IR spectra were recorded in a Shimadzu FTIR spectometer IRaffinity-1;
- ^{1}H NMR, the ^{13}C NMR and HMQC spectra were recorded in a spectrophotometer Bruker 400 Ultra-Shield. Chemical shifts (δ_H and δ_C) are

given in parts-per-million (ppm) and coupling constants (*J*) are quoted in Hertz (Hz);

- Melting points were determined in a Köfler camera Bock-Monoscop "M" and are uncorrected;
- Mass spectra were obtained by direct infusion on "Full Scan" mode (m/z 60-800) in a Micromass Quattro Micro API benchtop mass spectrometer. Positive and Negative electrospray ionization mode were applied on sample ionization;
- Studies by HPLC were performed in a ELITE LaChrom VWR HITACHI equipment (PUMP L-2130; UV DETECTOR L-2400) with a LiChrospher® 100 RP-18 (5 µm) column;
- Thermostatized bath.

5.2 – Synthesis

WARNING: All the triazenes synthesized and used in this master thesis should be considered as mutagenic and carcinogenic and appropriate care should be taken to handle them safely.

5.2.1 – HMT and MMT derivatives

To a solution of the required aniline (0.046 moles) in 10 mL of HCl 37%, was added 100 mL of cold water. A cold solution of sodium nitrite (3.4 g, 0.049 moles in 5 mL of water) was droppewise to the previous solution. The reaction mixture was stirred for one hour with mechanic stirring at -10 ºC. Then, the reaction mixture was neutralized by addition of NaOH 1M until the pH reach 7. After the neutralization, it was added 60 mL of cold formaldehyde and 9.4 mL of methylamine (Sol. 40%) and the reaction mixture was stirred for 30 minutes. HMT derivatives synthesized were isolated by vacuum filtration and recrystallized.

In the synthesis of each MMT derivative, the proper HMT derivative (0.023 moles) was dissolved in 100 mL of water and then it was added 5.4 mL of methylamine (Sol. 40%) in a $MeNH_2$ 3:1 HMT molar ratio. MMT derivatives synthesized were washed with water and dried out in vacuo.

5.2.2 – Experimental methods used in the synthesis of triazene prodrugs

- **Amide coupling with activation of hydroxyphenylpropionic acid with DCC/DMAP and activation of MMT with NaH**

Hydroxyphenylpropionic acid (1.12 mmol) was dissolved in dried THF (3 mL) and DCC (0.29 g, 1.4 mmol) was added to the solution at room temperature. The reaction mixture was stirred for one hour. Apart, MMT (1.12 mmol) was dissolved in dried THF (2 mL) and NaH (0.027 g, 1.12 mmol) was added to the solution. MMT solution, TEA (0.156 mL, 1.12 mmol) and DMAP (0.014 g, 0.112 mmol) were all added into the reaction mixture. The reaction was stirred at room temperature for 48 hours. Reaction progress was followed by TLC. When the reaction was completed, the reaction mixture was filtered in order to remove DCU, and concentrated under reduce pressure. Triazene prodrugs **21a** (with and without activation of MMT) and **21d** were synthesized by this method.

- **Amide coupling with activation of hydroxyphenylpropionic acid with DMTMM.**

To a solution of 2-chloro-4,6-dimethoxy-1,3,5-triazine (0.176 g, 1 mmol) in 4 mL of dried DCM, was added N-methylmorpholine (0.33 mL, 3 mmol). The reaction mixture was stirred for 30-40 min at 0-5 ºC. Then, 3-(4-hydroxyphenyl)propionic acid (0.166 g , 1 mmol) in 10 mL of dried DCM was added to the reaction mixture. The reaction mixture was stirred at room temperature for one hour. After that, MMT-$CONH_2$ (0.178 g, 1 mmol) was added to the reaction mixture and stirred for 8 hours.

Reaction development was followed by TLC After completion of the reaction, the reaction mixture was washed with 2x5 mL of $NaHCO_3$ (10%) and 3x5 mL of H_2O. The organic phase was dried with anhydrous sodium sulphate and concentrated under reduce pressure. By this method it was synthesized the triazene prodrug **21f**.

- **Amide coupling with activation of hydroxyphenylpropionic acid with TBTU**

3-(4-hydroxyphenyl)propionic acid (0.1 g, 0.6 mmol), MMT-$COCH_3$ (0.117 g, 0.66 mmol) and TBTU (0.202 g, 0.63 mmol) were all dissolved in dried DMF (4 mL). Then, TEA (0.182 mL, 1.3 mmol) was added and the reaction mixture was stirred at 50ºC for one hour. Reaction progress was followed by TLC. When the reaction was completed, it was extracted with a 5% solution of citric acid, a 5% solution of $NaHCO_3$ and a saturated NaCl solution (figure 50). Organic phase was dried with sodium sulphate anhydrous and concentrated under reduce pressure. By this method it was synthesized the triazene prodrug **21e** and **25b**.

- <u>Assisted by microwave irradiation</u>

Hydroxyphenylpropionic acid (0.3 mmol), MMT (0.33 mmol) and TBTU (0.101 g, 0.315 mmol) were dissolved in dried DMF (3 mL) in a microwave tube. After that, TEA (0.088 mL, 0.63 mmol) was added. The resulting mixture was irradiated in a first cycle with 100 W, 50 ºC, 15 min and in a second cycle with 100 W, 55 ºC, 15 min. After completion of the reaction, the work-up described in method TBTU (reflux) was followed. By this method it was synthesized the triazene prodrugs **21b** (with two cycles and with four cycles), **21c** and **25a**.

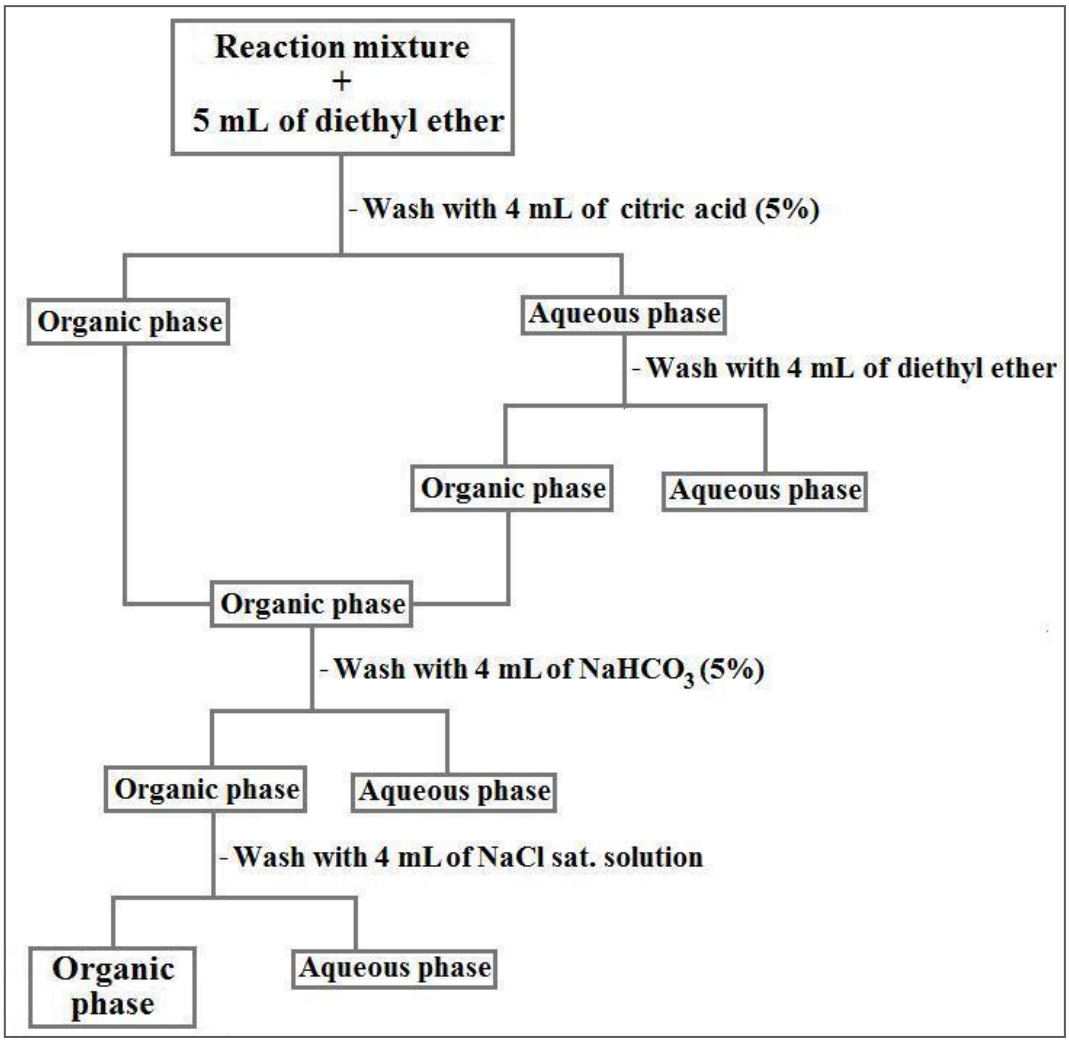

Figure 50 – Extraction process.

- **Amide coupling with activation of hydroxyphenylpropionic acid with thionyl chloride**

To a solution of MMT-CN (0.16 g, 1 mmol) in 2 mL of dried THF, was added 3-(3,4-Dihydroxyphenyl)propionic acid (0.182 g, 1 mmol). The reaction mixture was stirred under ice-cooling. Then, thionyl chloride (0.109 mL, 1.5 mmol) was dropwised into the reaction mixture for 10 min. The reaction mixture continued for 3 hours at room temperature. Reaction development was followed by TLC After completion of the reaction, the reaction mixture was extracted with ethyl acetate and washed with 2 mL of brine. Organic phase was dried over sodium sulphate anhydrous and concentrated under

reduce pressure. Triazene prodrug **21g** was synthesized in small amounts and very impure by this method.

- **Amide coupling activation with $Zr(Ot\text{-}Bu)_4$/HOBt**

The ester was synthesized by dissolving 3-(3,4-Dihydroxyphenyl)propionic acid (0.182 g, 1 mmol) in dried MeOH (1.5 mL) and the reaction mixture was stirred under ice-cooling. Then, thionyl chloride (0.109 mL, 1.5 mmol) was dropwised into the reaction mixture for 10 min. The reaction was stirred for 3 hours at room temperature. After completion, the reaction mixture was extracted with ethyl acetate and washed with 2 mL of brine. The organic phase was dried over sodium sulphate anhydrous and concentrated under reduce pressure [115]. Ester (0.05 g, 0.25 mmol), MMT-CN (0.208 g, 1.3 mmol) and HOBt (0.012 g, 0.086 mmol) were all mixed in a microwave tube and dissolved in dried DMF (4 mL). After dissolution, the zirconium catalyst $Zr(Ot\text{-}Bu)_4$ (0.017 mL, 0.043 mmol) was added. The microwave method used was (100 W, 100ºC, 30 min). After completion of the reaction, the same work-up described in method TBTU (reflux) was followed.

Triazene prodrugs **21** and **25** were purified by column chromatography and in some cases by preparative TLC. These prodrugs were also recrystallized. Experimental conditions are summarized in table 12.

Table 12 – Summary of experimental purification conditions.

Triazene prodrugs	Column chromatography eluent	Preparative chromatography eluent	Recrystallization (rich / poor solvent)
21a	DCM → DCM 9.9 : 0.1 MeOH	It was not necessary	DCM / Petroleum ether
21b	Hexane 7 : 3 Ethyl ether	It was not necessary	DCM / Petroleum ether
21c	DCM → DCM 9.9 : 0.1 MeOH	DCM 9.8 : 0.2 MeOH	DCM / Hexane
21d	DCM	DCM 9.9 : 0.1 MeOH	DCM / Petroleum ether
21e	DCM → DCM 9.9 : 0.1 MeOH	Ethyl ether 7 : 3 Petroleum ether	DCM / Hexane
21f	DCM 9.9 : 0.1 MeOH → DCM 9.5 : 0.5 MeOH	DCM 9 : 1 MeOH	DCM 9 : 1 MeOH / Hexane
25a	DCM → DCM 9.9 : 0.1 MeOH	DCM 9.8 : 0.2 MeOH	DCM / Hexane
25b	DCM → DCM 9.9 : 0.1 MeOH	Ethyl ether 7 : 3 Petroleum ether	Ethyl ether 7 : 3 Petroleum ether
21g	DCM 9.9 : 0.1 MeOH → DCM 9.8 : 0.2 MeOH	----------	----------

5.3 – Structural identification

- **<u>Triazene prodrug 21a</u>**

Yield < 5%; yellow crystals; **m.p** 136-138 ºC; **ν_{max}/cm^{-1}** 1686 (ν C=O_{amide}), 1713 (ν C=O_{ester}), 3410 (ν O-$H_{aromatic}$); **^{1}H NMR (400 MHz, $CDCl_3$):** δ_H/ppm 3.04 (2H, *t*, *J* = 7.7 Hz, C**H_2**), 3.26 (2H, *t*, *J* = 7.7 Hz, C**H_2**), 3.44 (3H, *s*, N-C**H_3**), 3.94 (3H, *s*, COO-C**H_3**), 5.31 (1H, *s*, Ar-O**H)**, 6.69 (1H, *dd*, *J* = 7.8, 2.0 Hz, Ar(C**H**)$_{Phenol}$), 6.75 (1H, *br s*, Ar(C**H**)$_{Phenol}$), 6.81 (1H, *d*, *J* = 7.8 Hz, Ar(C**H**)$_{Phenol}$), 7.16 (1H, *t*, *J* = 7.8 Hz,

Ar(C**H**)$_{Phenol}$), 7.60 (2H, *AA'*, *J* = 8.4 Hz, Ar(C**H's**)$_{MMT}$), 8.11 (2H, *XX'*, *J* = 8.4 Hz, Ar(C**H's**)$_{MMT}$); **^{13}C NMR (101 MHz, CDCl$_3$):** δ_C/ppm 28.14 (N-**C**H$_3$), 30.97 (**C**H$_2$), 35.99 (**C**H$_2$), 52.48 (COO-**C**H$_3$), 113.42 (Ar(**C**H)$_{Phenol}$), 115.57 (Ar(**C**H)$_{Phenol}$), 120.90 (Ar(**C**H)$_{Phenol}$), 122.09 (Ar(**C**H's)$_{MMT}$), 129.89 (Ar(**C**H)$_{Phenol}$), 130.28 (**C**$_{Ar}$), 130.90 (Ar(**C**H's)$_{MMT}$), 142.76 (**C**$_{Ar}$), 152.10 (**C**$_{Ar}$), 155.96 (**C**$_{Ar}$), 166.74 (**C**=O), 175.20 (**C**=O); **ESI$^+$-MS:** m/z 364 ([M+Na]$^+$); **ESI$^-$-MS:** m/z 340 ([M-H]$^-$).

- **Triazene prodrug 21b**

Yield 20%; yellow crystals; **m.p** 119-121 ºC; **ν_{max}/cm^{-1}** 1684 (ν C=O$_{amide}$), 2228 (ν CΞN), 3410 (ν O-H$_{aromatic}$); **^{1}H NMR (400 MHz, CDCl$_3$):** δ_H/ppm 3.03 (2H, *t*, *J* = 7.8 Hz, C**H$_2$**), 3.25 (2H, *t*, *J* = 7.8 Hz, C**H$_2$**), 3.45 (3H, *s*, N-C**H$_3$**), 5.39 (1H, *s*, Ar-O**H**), 6.69 (1H, *dd*, *J* = 7.8, 2.2 Hz, Ar(C**H**)$_{Phenol}$), 6.75 (1H, *br s*, Ar(C**H**)$_{Phenol}$), 6.80 (1H, *d*, *J* = 7.8 Hz, Ar(C**H**)$_{Phenol}$), 7.15 (1H, *t*, *J* = 7.8 Hz, Ar(C**H**)$_{Phenol}$), 7.63 (2H, *AA'*, *J* = 8.4 Hz, Ar(C**H's**)$_{MMT}$), 7.73 (2H, *BB'*, *J* = 8.4 Hz, Ar(C**H's**)$_{MMT}$); **^{13}C NMR (101 MHz, CDCl$_3$):** δ_C/ppm 28.34 (N-**C**H$_3$), 30.88 (**C**H$_2$), 35.95 (**C**H$_2$), 112.18 (**C**$_{Ar}$), 113.46 (Ar(**C**H)$_{Phenol}$), 115.57 (Ar(**C**H)$_{Phenol}$), 118.64 (**C**ΞN), 120.84 (Ar(**C**H)$_{Phenol}$), 122.85 (Ar(**C**H's)$_{MMT}$), 129.89 (Ar(**C**H)$_{Phenol}$), 133.46 (Ar(**C**H's)$_{MMT}$), 142.62 (**C**$_{Ar}$), 151.76 (**C**$_{Ar}$), 156.01 (**C**$_{Ar}$), 175.12 (**C**=O); **ESI$^+$-MS:** m/z 331 ([M+Na]$^+$); **ESI$^-$-MS:** m/z 307 ([M-H]$^-$).

- **Triazene prodrug 21c**

Yield < 5%; yellow crystals; **m.p** 101-103 ºC; **ν_{max}/cm^{-1}** 1697 (ν C=O$_{amide}$), 1728 (ν C=O$_{ester}$), 3368 (ν O-H$_{aromatic}$); **^{1}H NMR (400 MHz, CDCl$_3$):** δ_H/ppm 3.01 (2H, *t*, *J* = 7.6 Hz, C**H$_2$**), 3.23 (2H, *t*, *J* = 7.6 Hz, C**H$_2$**), 3.44 (3H, *s*, N-C**H$_3$**), 3.94 (3H, *s*, COO-C**H$_3$**), 4.97 (1H, *s*, Ar-O**H**), 6.76 (2H, *AA'*, *J* = 7.8 Hz, Ar(C**H's**)$_{Phenol}$), 7.11 (2H, *XX'*, *J* = 7.8 Hz, Ar(C**H's**)$_{Phenol}$), 7.60 (2H, *AA'*, *J* = 8.2 Hz, Ar(C**H's**)$_{MMT}$), 8.11 (2H, *XX'*, *J* = 8.2 Hz, Ar(C**H's**)$_{MMT}$); **^{13}C NMR (101 MHz, CDCl$_3$):** δ_C/ppm 28.10 (N-**C**H$_3$), 30.36 (**C**H$_2$), 36.48 (**C**H$_2$), 52.49 (COO-**C**H$_3$), 115.50 (Ar(**C**H's)$_{Phenol}$), 122.07 (Ar(**C**H's)$_{MMT}$), 122.71 (**C**$_{Ar}$), 129.71 (Ar(**C**H's)$_{Phenol}$), 130.87 (Ar(**C**H's)$_{MMT}$), 132.87

(**C**$_{Ar}$), 152.14 (**C**$_{Ar}$), 154.30 (**C**$_{Ar}$), 166.74 (**C**=O), 175.31 (**C**=O); **ESI$^+$-MS:** m/z 364 ([M+Na]$^+$); **ESI$^-$-MS:** m/z 340 ([M-H]$^-$).

- **Triazene prodrug 21d**

Yield 15%; yellow crystals; **m.p** 140-141 ºC; **ν_{max}/cm^{-1}** 1711 (ν C=O$_{amide}$), 2234 (ν CΞN), 3389 (ν O-H$_{aromatic}$); **^{1}H NMR (400 MHz, CDCl$_3$):** δ_H/ppm 3.01 (2H, *t*, *J* = 7.6 Hz, C**H$_2$**), 3.22 (2H, *t*, *J* = 7.6 Hz, C**H$_2$**), 3.44 (3H, *s*, N-C**H$_3$**), 4.74 (1H, *s*, Ar-O**H**), 6.76 (2H, *AA'*, *J* = 7.6 Hz, Ar(C**H's**)$_{Phenol}$), 7.11 (2H, *XX'*, *J* = 7.6 Hz, Ar(C**H's**)$_{Phenol}$), 7.63 (2H, *AA'*, *J* = 7.8 Hz, Ar(C**H's**)$_{MMT}$), 7.73 (2H, *BB'*, *J* = 7.8 Hz, Ar(C**H's**)$_{MMT}$); **^{13}C NMR (101 MHz, CDCl$_3$):** δ_C/ppm 28.30 (N-**C**H$_3$), 30.24 (**C**H$_2$), 36.42 (**C**H$_2$), 112.16 (**C**$_{Ar}$), 115.53 (Ar(**C**H's)$_{Phenol}$), 118.65 (**C**ΞN), 122.83 (Ar(**C**H's)$_{MMT}$), 129.70 (Ar(**C**H's)$_{Phenol}$), 132.72 (**C**$_{Ar}$), 133.45 (Ar(**C**H's)$_{MMT}$), 151.82 (**C**$_{Ar}$), 154.37 (**C**$_{Ar}$), 175.18 (**C**=O); **ESI$^+$-MS:** m/z 331 ([M+Na]$^+$); **ESI$^-$-MS:** m/z 307 ([M-H]$^-$).

- **Triazene prodrug 21e**

Yield < 5%; yellow crystals; **m.p** 134-136 ºC; **ν_{max}/cm^{-1}** 1661 (ν C=O$_{amide}$), 1695 (ν C=O$_{ketone}$), 3244 (ν O-H$_{aromatic}$); **^{1}H NMR (400 MHz, CDCl$_3$):** δ_H/ppm 2.64 (3H, *s*, O=C-C**H$_3$**), 3.01 (2H, *t*, *J* = 7.8 Hz, C**H$_2$**), 3.23 (2H, *t*, *J* = 7.8 Hz, C**H$_2$**), 3.45 (3H, *s*, N-C**H$_3$**), 5.15 (1H, *s*, Ar-O**H**), 6.77 (2H, *AA'*, *J* = 8.6 Hz, Ar(C**H's**)$_{Phenol}$), 7.11 (2H, *XX'*, *J* = 8.6 Hz, Ar(C**H's**)$_{Phenol}$), 7.63 (2H, *AA'*, *J* = 8.8 Hz, Ar(C**H's**)$_{MMT}$), 8.03 (2H, *XX'*, *J* = 8.8 Hz, Ar(C**H's**)$_{MMT}$); **^{13}C NMR (101 MHz, CDCl$_3$):** δ_C/ppm 26.89 (O=C-**C**H$_3$), 28.14 (N-**C**H$_3$), 30.34 (**C**H$_2$), 36.48 (**C**H$_2$), 115.51 (Ar(**C**H's)$_{Phenol}$), 122.28 (Ar(**C**H's)$_{MMT}$), 129.71 (Ar(**C**H's)$_{Phenol}$), 129.71 (Ar(**C**H's)$_{MMT}$), 132.90 (**C**$_{Ar}$), 137.01 (**C**$_{Ar}$), 152.18 (**C**$_{Ar}$), 154.27 (**C**$_{Ar}$), 175.27 (**C**=O), 197.63 (**C**=O); **ESI$^+$-MS:** m/z 348 ([M+Na]$^+$); **ESI$^-$-MS:** m/z 324 ([M-H]$^-$).

- **Triazene prodrug 21f**

Yield < 5%; yellow crystals; **m.p** 172-174 ºC; **ν_{max}/cm^{-1}** 1670-1686 (ν C=O$_{amide}$), 3306 (ν O-H$_{aromatic}$), 3348-3410 (ν NH$_2$ $_{amide}$); **^{1}H NMR (400 MHz, CDCl$_3$):**

δ_H/ppm 2.90 (2H, *t*, *J* = 7.6 Hz, C**H**$_2$), 3.14 (2H, *t*, *J* = 7.6 Hz, C**H**$_2$), 3.35 (3H, *s*, N-C**H**$_3$), 6.65 (2H, *AA'*, *J* = 8 Hz, Ar(C**H's**)$_{Phenol}$), 6.98 (2H, *XX'*, *J* = 8 Hz, Ar(C**H's**)$_{Phenol}$), 7.52 (2H, *AA'*, *J* = 8 Hz, Ar(C**H's**)$_{MMT}$), 7.83 (2H, *XX'*, *J* = 8 Hz, Ar(C**H's**)$_{MMT}$); **^{13}C NMR (101 MHz, CDCl$_3$):** δ_C/ppm 27.79 (N-**C**H$_3$), 30.41 (**C**H$_2$), 36.44 (**C**H$_2$), 115.29 (Ar(**C**H's)$_{Phenol}$), 122.10 (Ar(**C**H's)$_{MMT}$), 128.61 (Ar(**C**H's)$_{MMT}$), 129.37 (Ar(**C**H's)$_{Phenol}$), 131.64 (**C**$_{Ar}$), 133.26 (**C**$_{Ar}$), 151.30 (**C**$_{Ar}$), 155.13 (**C**$_{Ar}$), 175.66 (**C**=O); **ESI$^+$-MS:** m/z 349 ([M+Na]$^+$); **ESI$^+$-MS:** m/z 325 ([M-H]$^-$).

- **Triazene prodrug 25a**

Yield < 5%; yellow crystals; **m.p** 156-158 ºC; **ν_{max}/cm^{-1}** 1717 (ν C=O$_{amide}$), 1734 (ν C=O$_{ester}$), 1749 (ν C=O$_{ester}$), 3438 (ν O-H$_{aromatic}$); **^{1}H NMR (400 MHz, CDCl$_3$):** δ_H/ppm 2.83 (2H, *t*, *J* = 7.5 Hz, C**H**$_2$), 3.00 (2H, *t*, *J* = 7.7 Hz, C**H**$_2$), 3.06 (2H, *t*, *J* = 7.5 Hz, C**H**$_2$), 3.24 (2H, *t*, *J* = 7.7 Hz, C**H**$_2$), 3.45 (3H, *s*, N-C**H**$_3$), 3.95 (3H, *s*, COO-C**H**$_3$), 5.09 (1H, *s*, Ar-O**H**), 6.79 (2H, *AA'*, *J* = 8.4 Hz, Ar(C**H's**)), 6.90 (2H, *AA'*, *J* = 8.4 Hz, Ar(C**H's**)), 7.13 (2H, *XX'*, *J* = 8.4 Hz, Ar(C**H's**)), 7.23 (2H, *XX'*, *J* = 8.4 Hz, Ar(C**H's**)), 7.61 (2H, *AA'*, *J* = 8.6 Hz, Ar(C**H's**)$_{MMT}$), 8.11 (2H, *XX'*, *J* = 8.6 Hz, Ar(C**H's**)$_{MMT}$).

- **Triazene prodrug 25b**

Yield < 5%; yellow crystals; **m.p** 189-191 ºC; **ν_{max}/cm^{-1}** 1682 (ν C=O$_{amide}$), 1703 (ν C=O$_{cetone}$), 1754 (ν C=O$_{ester}$), 3397 (ν O-H$_{aromatic}$); **^{1}H NMR (400 MHz, CDCl$_3$):** δ_H/ppm 2.64 (3H, *s*, O=C-C**H**$_3$), 2.83 (2H, *t*, *J* = 7.6 Hz, C**H**$_2$), 3.00 (2H, *t*, *J* = 7.6 Hz, C**H**$_2$), 3.06 (2H, *t*, *J* = 7.6 Hz, C**H**$_2$), 3.24 (2H, *t*, *J* = 7.6 Hz, C**H**$_2$), 3.45 (3H, *s*, N-C**H**$_3$), 5.01 (1H, *s*, Ar-O**H**), 6.79 (2H, *AA'*, *J* = 8.4 Hz, Ar(C**H's**)), 6.90 (2H, *AA'*, *J* = 8.4 Hz, Ar(C**H's**)), 7.13 (2H, *XX'*, *J* = 8.4 Hz, Ar(C**H's**)), 7.23 (2H, *XX'*, *J* = 8.4 Hz, Ar(C**H's**)), 7.63 (2H, *AA'*, *J* = 8.4 Hz, Ar(C**H's**)$_{MMT}$), 8.04 (2H, *XX'*, *J* = 8.4 Hz, Ar(C**H's**)$_{MMT}$).

5.4 – Kinetic studies

5.4.1 – PBS (0.01 M, pH=7.4)

A 30 μL aliquot of a 10^{-2} M stock solution of prodrug **21a-f** in ACN was added to 10 mL of PBS (0.01 M, pH 7.4) at 37 ºC. At different times, several aliquots of the reaction mixture were taken and analyzed by HPLC at λ = 300 nm.

5.4.2 – Human plasma (80% v/v)

Human plasma was collected from several healthy donors in sodium heparinate, and stored at -70ºC until required.

A mixture of 2 mL of human plasma and 0.5 mL of PBS (0.01 M, pH 7.4) was thermostatized at 37 ºC. To this mixture was added 10 μL of a 10^{-2} M stock solution of prodrug **21a-f** in ACN. Several aliquots (200 μL) of the reaction mixture were taken at different times, and added to eppendorfs with 400 μL of cold ACN. Eppendorfs were centrifuged at 14000 rpm for 5 min and the supernatant was analyzed by HPLC at λ = 300 nm.

5.4.3 – Mushroom tyrosinase

Mushroom tyrosinase (89.4 μL, 900 units / 29.8 μL, 300 units) was added in a solution of 2.4 mL of PBS (0.01 M, pH=7.4) and 0.6 mL of DMSO at 37 ºC. To this mixture was added 10 μL of a 10^{-2} M stock solution of triazene prodrugs **21a-f** or **25a,b** in ACN. Several aliquots (200 μL) of the reaction mixture were collected at selected times and added to eppendorfs with 400 μL of cold ACN. Eppendorfs were centrifuged at 14000 rpm for 5 min and the supernatant was analyzed by HPLC at λ = 300 nm.

The conditions applied for each compound in HPLC analysis are summarized in table 13.

Table 13 – Mobile phases applied and retention times observed for each compound in HPLC analysis.

		Retention times (min)			
Triazene prodrug	**Compound**	**PBS**	**Human plasma**	**Mushroom tyrosinase**	**Mobile phase**
21a	Aniline-$COOCH_3$	2.18	-------	2.21	45% ACN + 55% H_2O
	MMT-$COOCH_3$	-------	-------	4.24	
	Prodrug **21a**	12.19	11.95	12.41	
21b	Aniline-CN	1.85	1.98	1.96	45% ACN + 55% H_2O
	MMT-CN	-------	3.38	3.36	
	Prodrug **21b**	7.43	8.85	8.70	
21c	Aniline-$COOCH_3$	2.32	-------	2.05	45% ACN + 55% H_2O
	MMT-$COOCH_3$	-------	-------	3.92	
	Intermediate **29**	-------	-------	7.92	
	Prodrug **21c**	10.39	9.57	10.66	
21d	Aniline-CN	1.83	1.99	1.97	50% ACN + 50% H_2O
	MMT-CN	-------	3.38	3.18	
	Intermediate **29**	-------	-------	4.17	
	Prodrug **21d**	5.48	6.15	5.65	
21e	Aniline-$COCH_3$	1.84	1.78	1.66	40% ACN + 60% H_2O
	MMT- $COCH_3$	-------	-------	3.19	
	Intermediate **29**	-------	-------	6.87	
	Prodrug **21e**	12.09	11.71	11.33	
21f	Aniline-$CONH_2$	1.31	1.03	1.03	30% ACN + 70% H_2O
	MMT- $CONH_2$	-------	-------	1.47	
	Intermediate **29**	-------	-------	4.04	
	Prodrug **21f**	8.03	7.98	7.62	
25a	Aniline-$COOCH_3$	-------	-------	1.53	60% ACN + 40% H_2O
	MMT-$COOCH_3$	-------	-------	2.14	
	Intermediate **29**	-------	-------	2.68	
	Prodrug **21c**	-------	-------	3.35	
	Intermediate **30**	-------	-------	5.29	
	Compound **25a**	-------	-------	6.85	
25b	Aniline-$COCH_3$	-------	-------	1.26	60% ACN + 40% H_2O
	MMT-$COCH_3$	-------	-------	1.71	
	Intermediate **29**	-------	-------	2.12	
	Prodrug **21e**	-------	-------	2.52	
	Intermediate **30**	-------	-------	3.81	
	Compound **25b**	-------	-------	4.83	

5.4.4 – Calibration Curves

These calibration curves (e.g: figure 51-53) were made by HPLC analysis at λ = 300 nm of known concentrations of aniline, MMT **23** or triazene prodrug **21**. The slopes obtained are shown in table 14.

Table 14 – Slopes and correlation factors (R^2).

	Aniline		MMT		Prodrug	
Triazene Prodrug	**Slope (m)**	**R^2**	**Slope (m)**	**R^2**	**Slope (m)**	**R^2**
21a	9.184×10^{10}	0.991	1.568×10^{11}	0.997	1.103×10^{11}	0.997
21b	2.943×10^{10}	0.996	1.212×10^{11}	0.996	1.156×10^{11}	0.999
21c	9.184×10^{10}	0.991	1.568×10^{11}	0.997	1.015×10^{11}	0.999
21d	6.970×10^{9}	0.998	3.077×10^{10}	0.991	2.143×10^{10}	0.998
21e	9.125×10^{10}	0.999	7.115×10^{10}	0.996	1.019×10^{11}	0.999
21f	3.549×10^{10}	0.998	9.053×10^{10}	0.997	7.849×10^{10}	0.998

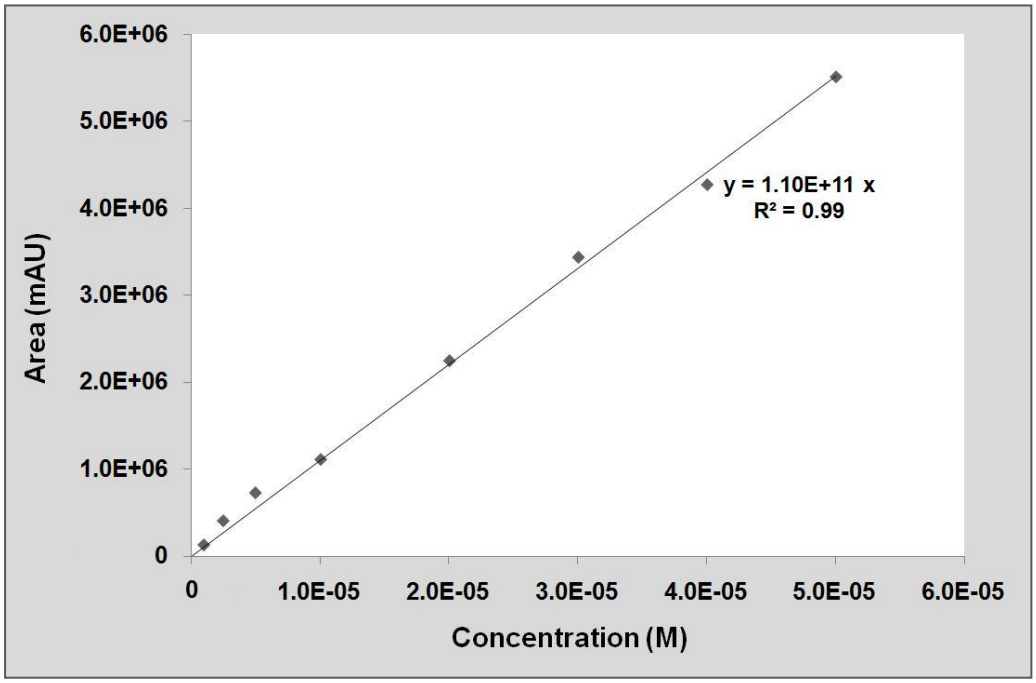

Figure 51 – Graphic plot of the calibration curve of triazene prodrug 21a.

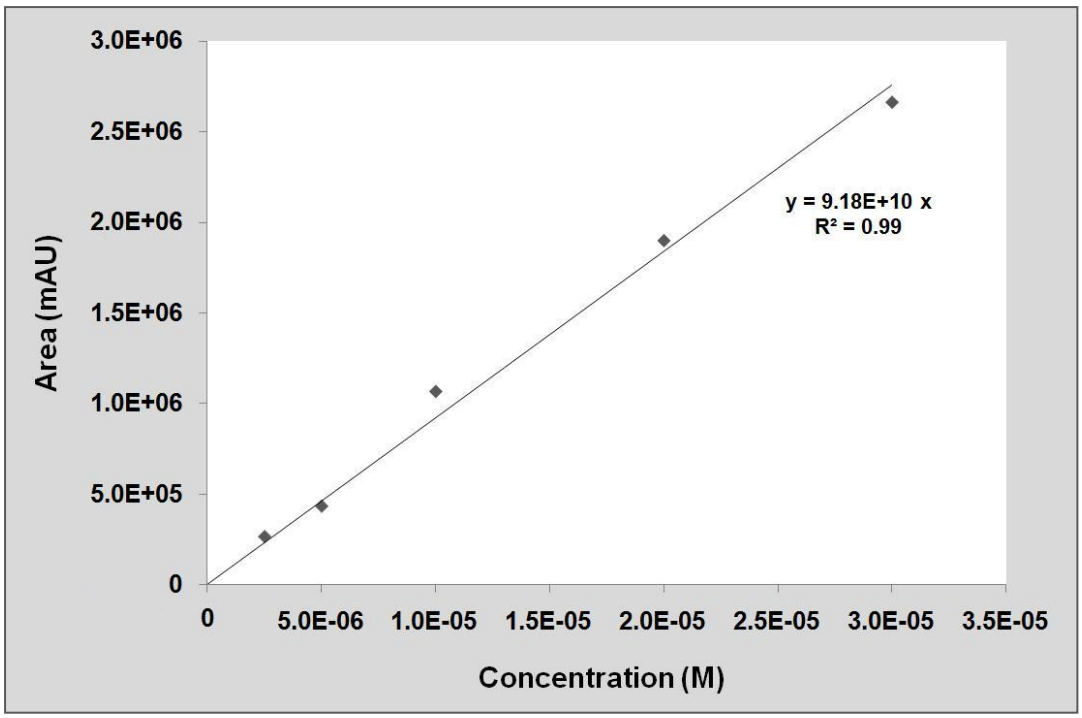

Figure 52 – Graphic plot of the calibration curve of aniline-$COOCH_3$.

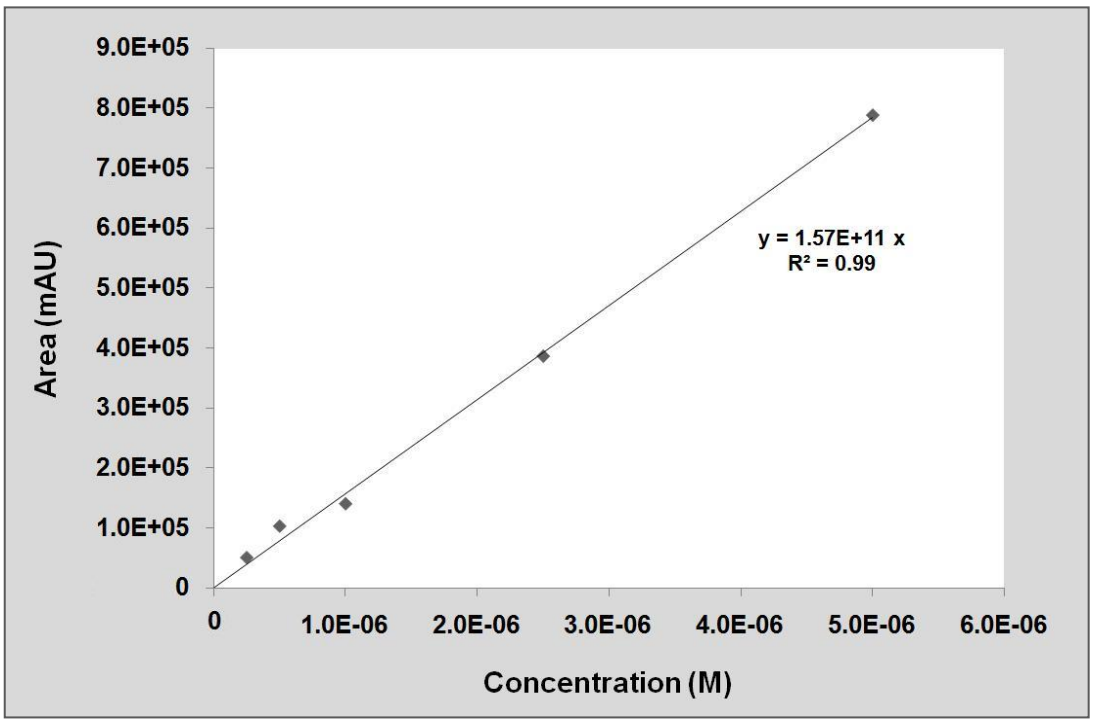

Figure 53 – Graphic plot of the calibration curve of MMT-$COOCH_3$.

5.5 – Hepatotoxicity assessment

Incubation mixture contained 881 μL of phosphate buffer (0.1M, pH 7.4, DETAPAC 1mM), 50 μL of rat liver microsomes solution (20 mg/mL), 20 μL of GSH solution (10 mM), 32.5 μL of NADPH solution A (31 mM $NADP^+$, 66 mM Glucose-6-phosphate and 66 mM $MgCl_2$ in H_2O), 6.5 μL of NADPH solution B (40 U/mL Glucose-6-phosphate dehydrogenase in 5 mM sodium citrate) and 10 μL of a 10^{-2} M stock solution of prodrug **21a-f** in a final volume of 1 mL. The mixture was gently mixed at 37 ºC. Then, three aliquots of 250 μL were taken at different times (30, 60, 180 min) and added to eppendorfs with 25 μL of trichloroacetic acid (30% w/v). Reaction mixture was centrifuged at 14000 rpm for 5 min. GSH levels of a 100 μL aliquot of the supernatant was determined by the addition of 875 μL of Tris/HCl buffer (0.1 M, pH 8.9) and 25 μL of DTNB solution (2 mg/mL). The absorbance of the solution was measured at λ = 412 nm.

5.5.1 – Calibration Curve

Calibration curve (figure 54) was made by adding known concentrations of GSH (100 μL) with 875 μL of Tris/HCl buffer (0.1 M, pH 8.9) and 25 μL of DTNB solution (2 mg/mL). The absorbance of this mixture was also determined by UV at λ = 412 nm.

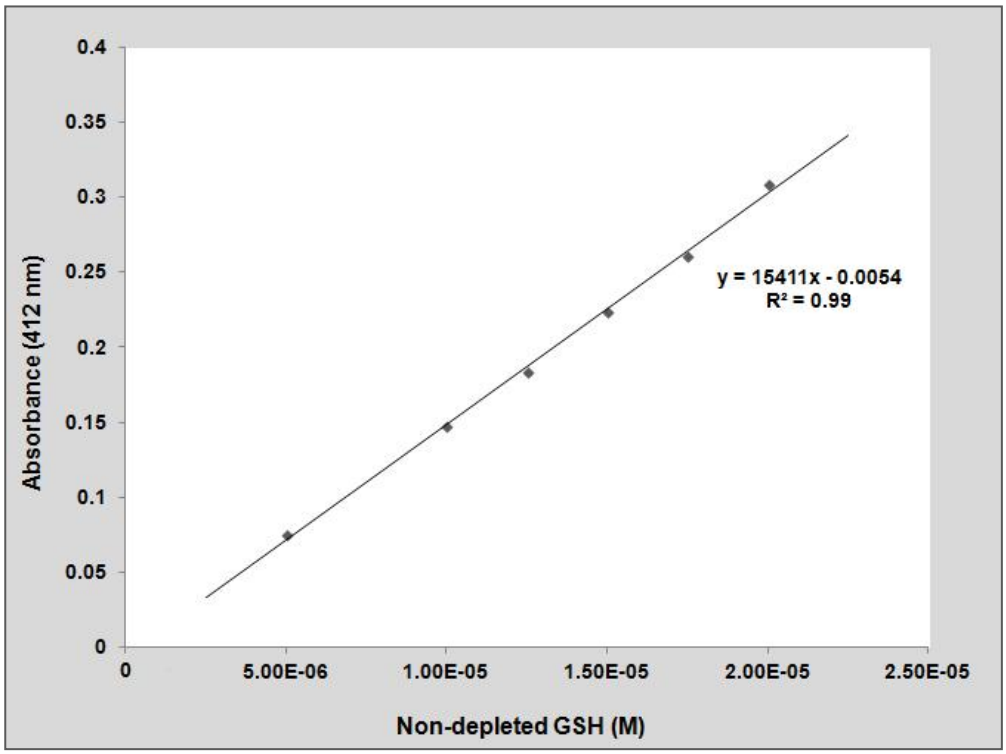

Figure 54 – Calibration curve applied in the hepatotoxicity assessment.

BIBLIOGRAPHY

1. Jawaid, S., Osborn, H.M.I., Williams, N.A.O., "Fighting skin cancer with prodrugs", Education in Chemistry, **(2007)**, vol. 44, pp. 77-81.
2. http://www.who.int/uv/faq/skincancer/en/index1.html, (01/08/2011)
3. http://www.skin212.com/melanocyte3.jpg, (01/08/2011)
4. Jawaid, S., Khan, T.H., Osborn, H.M.I., Williams, N.A.O., "Tyrosinase activated melanoma prodrugs", Anti-Cancer Agents in Medicinal Chemistry, **(2009)**, vol. 9, pp. 717-27.
5. http://www.roche.pt/sites-tematicos/infocancro/index.cfm/tipos/melanoma/, (01/08/2011)
6. Miller, A.J., Mihm, M.C., "Mechanisms of disease-Melanoma", New England Journal of Medicine, **(2006)**, vol. 355, pp. 51-65.
7. Park, H.Y., Kosmadaki, M., Yaar, M., Gilchrest, B.A., "Cellular mechanisms regulating human melanogenesis", Cellular and Molecular Life Sciences, **(2009)**, vol. 66, pp. 1493-1506.
8. Gray-Schopfer, V., Wellbrock, C., Marais, R., "Melanoma biology and new targeted therapy", Nature, **(2007)**, vol. 445, pp. 851-7.
9. Riley, P.A., "Melanogenesis and melanoma", Pigment Cell Research, **(2003)**, vol. 16, pp. 548-52.
10. Bonjoch, J., Drew, M.G., González, A., Greco, F., Jawaid, S., Osborn, H.M.I., Williams, N.A.O., Yaqoob, P., "Synthesis and evaluation of novel boron-containing complexes of potential use for the selective treatment of malignant melanoma", Journal of Medicinal Chemistry, **(2008)**, vol. 51, pp. 6604-8.
11. García-Borrón, J.C., Solano, F., "Molecular anatomy of tyrosinase and its related proteins: beyond the histidine-bound metal catalytic center", Pigment Cell Research, **(2002)**, vol. 15, pp. 162-73.
12. García-Molina, F., Muñoz, J.L., García-Ruíz, P.A., Rodríguez-López, J.N., García-Cánovas, F., Tudela, J., "A further step in the kinetic characterisation of the tyrosinase enzymatic system", Journal of Mathematical Chemistry, **(2007)**, vol. 41, pp. 393-406.

13. Olivares, C., Solano, F., "New insights into the active site structure and catalytic mechanism of tyrosinase and its related proteins", Pigment Cell Melanoma Research, **(2009)**, vol. 22, pp. 750-60.
14. Rolff, M., Schottenheim, J., Tuczek, F., "Monooxygenation of external phenolic substrates in small-molecule dicopper complexes: implications on the reaction mechanism of tyrosinase", Journal of Coordination Chemistry, **(2010)**, vol. 63, pp. 2382-99.
15. Simonova, M., Wall, A., Weissleder, R., "Tyrosinase mutants are capable of prodrug activation in transfected nonmelanotic cells", Cancer Research, **(2000)**, vol. 60, pp. 6656-62.
16. Prezioso, J.A., Wang, N., Bloomer, W.D., "Thymidylate synthase as a target enzyme for the melanoma-specific toxicity of 4-S-cysteaminylphenol and N-acetyl-4-S-cysteaminylphenol", Cancer Chemotherapy and Pharmacology, **(1992)**, vol. 30, pp. 394-400.
17. Rescigno, A., Bruyneel, F., Padiglia, A., Sollai, F., Salis, A., Marchand-Brynaert, J., Sanjust, E., "Structure-activity relationships of various amino-hydroxy-benzenesulfonic acids and sulfonamides as tyrosinase substrates", Biochimica et Biophysica Acta, **(2011)**, vol. 1810, pp. 799-807.
18. Gasowska, B., Kafarski, P., Wojtasek, H., "Interaction of mushroom tyrosinase with aromatic amines, *o*-diamines and *o*-aminophenols", Biochimica et Biophysica Acta, **(2004)**, vol. 1673, pp. 170-7.
19. Munoz-Munoz, J.L., Garcia-Molina, F., Garcia-Ruiz, P.A., Varon, R., Tudela, J., Rodriguez-Lopez, J.N., Garcia-Canovas, F., "Catalytic oxidation of *o*-aminophenols and aromatic amines by mushroom tyrosinase", Biochimica et Biophysica Acta, **(2011)**, vol. 1814, pp. 1974-83.
20. Riley, P.A., Cooksey, C.J., Johnson, C.I., Land, E.J., Latter, A.M., Ramsden, C.A., "Melanogenesis-targeted anti-melanoma pro-drug development: effect of side-chain variations on the cytotoxicity of tyrosinase-generated ortho-quinones in a model screening system", European Journal of Cancer, **(1997)**, vol. 33, pp. 135-43.

21. Chen, Y.M., Chavin, W., "Melanogenesis in human melanomas", Cancer Research, **(1975)**, vol. 35, pp. 606-12.
22. Rooseboom, M., Commandeur, J.N.M., Vermeulen, N.P.E., "Enzyme-catalyzed activation of anticancer prodrugs", Pharmacological Reviews, **(2004)**, vol. 56, pp. 53-102.
23. Chen, Y.M., Chavin, W., "Tyrosinase activity in a highly pigmented human melanoma and in negro skin", Experimental Biology and Medicine, **(1974)**, vol. 145, pp. 695-98.
24. Silverman, R.B., "The organic chemistry of drug design and drug action", Hayhurst. J., Elsevier, 2nd ed., Oxford, **(2004)**, Elsevier, pp. 323-89 & 498-549.
25. Stella, V.J., "A case for prodrugs" in Prodrugs: challenges and rewards - part 1, Stella, V.J., Borchardt, R.T., Hageman, M.J., Oliyai, R., Maag, H., Tilley, J.W., Springer, 1st ed., Kansas, (**2007**), pp. 4-29.
26. Ettmayer, P., Amidon, G.L., Clement, B., Testa, B., "Lessons learned from marketed and investigation prodrugs", American Chemical Society, **(2004)**, vol. 47, pp. 2393-404.
27. Verma, A., Verma, B., Prajapati, S.K., Tripathi, K., "Prodrugs as a chemical delivery system: A review", Asian Journal of Research in Chemistry, **(2009)**, vol. 2, pp. 100-3.
28. Zovko, M., Zorc, B., Novak, P., Tepes, P., Cetina-Cizmek, B., Horvat, M., "Macromolecular prodrugs: XI. Synthesis and characterization of polymer–estradiol conjugate", International Journal of Pharmaceutics, **(2004)**, vol. 285, pp. 35-41.
29. Mahato, R., Tai, W., Cheng, K., "Prodrugs for improving tumor targetability and efficiency", Advanced drug delivery reviews, **(2011)**, vol. 63, pp. 659-70.
30. Ohlan, S., Nanda, S., Pathak, D.P., Jagia, M., "Mutual prodrugs - A swot analysis", International Journal of Pharmaceutical Sciences and Research, **(2011)**, vol. 2, pp. 719-29.
31. Kratz, F., Müller, I.A., Ryppa, C., Warnecke, A., "Prodrug strategies in anticancer chemotherapy", ChemMedChem, **(2008)**, vol. 3, pp. 20-53.

32. Goskonda, V.R., Ghandehari, H., Reddy, I.K., "Novel site-specific chemical delivery system as a potential mydriatic agent: Formation of phenylephrine in the iris-ciliary body from phenylephrone chemical delivery systems", Journal of Pharmaceutical Sciences, **(2001)**, vol. 90, pp. 12-22.

33. Chen, Y., Hu, L., "Design of anticancer prodrugs for reductive activation", Medicinal Research Reviews, **(2009)**, vol. 29, pp. 29-64.

34. Denny, W.A., "Synthetic DNA-targeted chemotherapeutic agents and related tumor-activated prodrugs" in Burger's medicinal chemistry and drug discovery Volume 5: Chemotherapeutic agents, Abraham, D. J., John Wiley and Sons, 6th ed., Virginia, **(2003)**, pp. 52-92.

35. Denny, W.A., "Tumor-activated prodrugs - a new approach to cancer therapy", Cancer Investigation, **(2004)**, vol. 22, pp. 604-19.

36. Denny, W.A., "The contribution of synthetic organic chemistry to anticancer drug development" in Anticancer drug development, Baguley, B.C., Kerr, D.J., Academic Press, 1st ed., Florida, **(2002)**, pp. 187-99.

37. Hubbard, R.D., Fidanze, S., "Alkylating and platinum antitumor compounds" in Comprehensive medicinal chemistry II Volume 7: Therapeutic areas II: Cancer, infectious diseases, inflammation & immunology and dermatology, Taylor, J.B., Triggle, D.J., Elsevier, 1st ed., **(2006)**, pp. 136-8.

38. Francisco, A.P., Perry, M.J., Mendes, E., Moreira, R., "Alkylating agents" in Anticancer therapeutics, Missailidis, S., John Wiley and Sons, 1st ed., Chichester, **(2008)**, pp.133-49.

39. Knaggs, S., Malkin, H., Osborn, H.M.I., Williams, N.A.O., Yaqoob, P., "New prodrugs derived from 6-aminodopamine and 4-aminophenol as candidates for melanocyte-directed enzyme prodrug therapy (MDEPT)", Organic and Biomolecular Chemistry, **(2005)**, vol. 3, pp. 4002-10.

40. Marchesi, F., Turriziani, M., Tortorelli, G., Avvisati, G., Torino, F., De Vecchis, L., "Triazene compounds: Mechanism of action and related DNA repair systems", Pharmacological Research, **(2007)**, vol. 56, pp. 275-87.

41. Nifontov, V.I., Bel'skaya, N.P., Shtokareva, E.A., "Manufacture methods of synthesizing triazenes", Pharmaceutical Chemistry Journal, **(1993)**, vol. 27, pp. 652-65.

42. Griess, P., "Ueber eine neue klasse organischer verbindungen, in denen wasserstoff durch stickstoff vertreten ist", Liebigs Annalen der Chemie, **(1862)**, vol. 121, pp. 257-80.

43. Kimball, D.B., Haley, M.M., "Triazenes: A versatile tool in organic chemistry", Angewandte Chemie International Edition, (**2002**), vol. 41, pp. 3338-51.

44. Clarke, D.A., Barclay, R.K., Stock, C.C., Rondestvedt, C.S., "Triazenes as inhibitors of mouse sarcoma 180", Experimental Biology and Medicine, **(1955)**, vol. 90, pp. 484-9.

45. Carvalho, E., Francisco, A.P., Iley, J., Rosa, E., "Triazene drug metabolites Part 17: Synthesis and plasma hydrolysis of acyloxymethyl carbamate derivatives of antitumour triazenes", Bioorganic & Medicinal Chemistry, **(2000)**, vol. 8, pp. 1719-25.

46. Bhatia, S., Tykodi, S.S., Thompson, J.A., "Treatment of metastatic melanoma: An overview", Oncology, **(2009)**, vol. 23, pp. 488-96.

47. Nifontov, V.I., Bel'skaya, N.P., Shtokareva, E.A., "The reactivity and mechanism of action of triazenes", Pharmaceutical Chemistry Journal, **(1994)**, vol. 28, pp. 687-706.

48. Wanner, M.J., Koch, M., Koomen, G.J., "Synthesis and antitumor activity of methyltriazene prodrugs simultaneously releasing DNA-methylating agents and the antiresistance drug O(6)-benzylguanine", Journal of Medicinal Chemistry, **(2004)**, vol. 47, pp. 6875-83.

49. Middleton, M.R., Grob, J.J., Aaronson, N., Fierlbeck G., Tilgen, W., Seiter, S., Gore, M., Aamdal, S., Cebon, J., Coates, A., Dreno, B., Henz, M., Schadendorf, D., Kapp, A., Weiss, J., Fraass, U., Statkevich, P., Muller, M., Thatcher, N., "Randomized phase III study of temozolomide versus dacarbazine in the treatment of patients with advanced metastatic malignant melanoma", Journal of the American Society of Clinical Oncology, **(2000)**, vol. 18, pp. 158-66.

50. Perry, M.J., Mendes, E., Simplício, A.L., Coelho, A., Soares, R.V., Iley, J., Moreira, R., Francisco, A.P., "Dopamine- and tyramine-based derivatives of triazenes: Activation by tyrosinase and implications for prodrug design", European Journal of Medicinal Chemistry, **(2009)**, vol. 44, pp. 3228-34.

51. Jordan, A.M., Khan, T.H., Osborn, H.M.I., Photiou, A., Riley, P.A., "Melanocyte-directed enzyme prodrug therapy (MDEPT): Development of a targeted treatment for malignant melanoma", Bioorganic & Medicinal Chemistry, **(1999)**, vol. 7, pp. 1775-80.

52. Jordan, A.M., Khan, T.H., Malkin, H., Osborn, H.M.I., Photiou, A., Riley, P.A., "Melanocyte-directed enzyme prodrug therapy (MDEPT): Development of second generation prodrugs for targeted treatment of malignant melanoma", Bioorganic & Medicinal Chemistry, **(2001)**, vol. 9, pp. 1549-58.

53. Vad, N.M., Shaik, I.M., Mehvar, R., Moridani, M.Y., "Metabolic bioactivation and toxicity of ethyl 4-hydroxybenzoate in human sk-mel-28 melanoma cells", Journal of Pharmaceutical Sciences, **(2008)**, vol. 97, 1934-45

54. Jordan, A.M., Khan, T.H., Malkin, H., Osborn, H.M.I., "Synthesis and analysis of urea and carbamate prodrugs as candidates for melanocyte-directed enzyme prodrug therapy (MDEPT)", Bioorganic & Medicinal Chemistry, **(2002)**, vol. 10, pp. 2625-33.

55. Osborn, H.M.I., Williams, N.A.O., "Development of tyrosinase labile protecting groups for amines", Organic Letters, **(2004)**, vol. 6, pp. 3111-3.

56. Napolitano, A., d'Ischia, M., Costantini, C., Prota, G., "A new oxidation pathway of the neurotoxin 6-aminodopamine. Isolation and characterisation of a dimer with a tetrahydro[3,4a]iminoethanophenoxazine ring system", Tetrahedron, **(1992)**, vol. 48, pp. 8515-22.

57. Borovansky, J., Edge, R., Land, E.J., Navaratnam, S., Pavel, S., Ramsden, C.A., Riley, P.A., Smit, N.P.M., "Mechanistic studies of melanogenesis: the influence of N-substitution on dopamine quinone cyclization", Pigment Cell Research, **(2006)**, vol. 19, pp. 170-8.

58. Ishihara, Y., Shimamoto, N., "A role of cytochrome P450 in quinone-induced hepatotoxicity" in Hepatotoxicity, Sahu, S.C., John Wiley and Sons, 1st, Kagawa, **(2008)**, pp. 1-11.

59. Bolton, J.L., Trush, M.A., Penning, T.M., Dryhurst, G., Monks, T.J., "Role of quinones in toxicology", American Chemical Society, **(2000)**, vol. 13, pp. 135-60.

60. Toxopeus, C., van Holsteijn I., Thuring, J.W.F., Blaauboer, B.J., Noordhoek, J., "Cytotoxicity of menadione and related quinones in freshly isolated rat hepatocytes: effects on thiol homeostasis and energy charge", Archives of Toxicology, **(1993)**, vol. 67, pp. 674-9.

61. Moridani, M.Y., Moore, M., Bartsch, R.A., Yang, Y., Heibati-Sadati, S., "Structural toxicity relationship of 4-alkoxyphenols' cytotoxicity towards murine B16-F0 melanoma cell line", Journal of Pharmacy and pharmaceutical sciences, **(2005)**, vol. 8, pp. 348-60.

62. Moridani, M.Y., Siraki, A., O'Brien, P.J., "Quantitative structure toxicity relationships for phenols in isolated rat hepatocytes", Chemico-Biological Interactions, **(2003)**, vol. 145, pp. 213-23.

63. Moridani, M.Y., Siraki, A., Chevaldina, T., Scobie, H., O'Brien, P.J., "Quantitative structure toxicity relationships for catechols in isolated rat hepatocytes", Chemico-Biological Interactions, **(2004)**, vol. 147, pp. 297-307.

64. Moridani, M.Y., "Biochemical basis of 4-hydroxyanisole induced cell toxicity towards B16-F0 melanoma cells", Cancer Letters, **(2006)**, vol. 243, pp. 235-45.

65. Montalbetti, C.A.G.N., Falque, V., "Amide bond formation and peptide coupling", Tetrahedron, **(2005)**, vol. 61, pp. 10827-52.

66. Niculescu-Duvaz, D., Negoita-Giras, G., Niculescu-Duvaz, I., Hedley, D., Springer, C.J., "Directed enzyme prodrug therapies" in Prodrugs and targeted delivery: Towards better ADME properties, Rautio, J., Wiley-VCH, 1st ed., Weinheim, **(2011)**, pp. 298.

67. D'Souza, A.J.M., Topp, E.M., "Release from polymeric prodrugs: Linkages and their degradation", Journal of Pharmaceutical Sciences, **(2004)**, vol. 93, pp. 1962-79.

68. Valeur, E., Bradley, M., "Amide bond formation: beyond the myth of coupling reagents", Chemical Society Reviews, **(2009)**, vol. 38, pp. 606-31.

69. Sheehan, J.C., Cruickshank, P.A., "A convenient synthesis of water-soluble carbodiimides", The Journal of Organic Chemistry, **(1961)**, vol. 26, pp. 2525-28.

70. Iwasawa, T., Wash, P., Gibson, C., Rebek, J., "Reaction of an introverted carboxylic acid with carbodiimide", Tetrahedron, **(2007)**, vol. 63, pp. 6506-11.

71. Balalaie, S., Mahdidous, M., Eshaghi-Najafabadi, R., "2-(1H-Benzotriazole-1-yl)-1,1,3,3-tetramethyluronium tetrafluoroborate as an efficient coupling reagent for the amidation and phenylhydrazation of carboxylic acids at room temperature", Journal of the Iranian Chemical Society, **(2007)**, vol. 4, pp. 364-69.

72. Falchi, A., Giacomelli, G., Porcheddu, A., Taddei, M., "4-(4,6-Dimethoxy[1,3,5]triazin-2-yl)-4-methyl-morpholinium chloride (DMTMM): A valuable alternative to PyBOP for solid phase peptide synthesis", Synlett, **(2000)**, vol. 275, pp. 275-7.

73. Ragnarsson, U., Grehn, L., "Novel amine chemistry based on DMAP-catalyzed Acylation", Accounts of Chemical Research, **(1998)**, vol. 31, pp. 494-501.

74. Han, C., Lee, J.P., Lobkovsky, E., Porco, J.A., "Catalytic ester-amide exchange using group (IV) metal alkoxide-activator complexes", Journal of the American Chemical Society, **(2005)**, vol. 127, pp. 10039-44.

75. Negishi, E., "Organozirconium chemistry" in Organometallics in synthesis: a manual, Schlosser, M., Wiley, 2nd ed., **(2002)**.

76. Yang, D., Kwon, M., Jang, Y., Jeon, H.B., "A convenient and efficient synthesis of C-carbamoyl-1,2,3-triazoles from alkyl bromide by a one-pot sequential addition: conversion of ester to amide using $Zr(Ot\text{-}Bu)_4$", Tetrahedron Letters, **(2010)**, vol. 51, pp. 3691-95.

77. Fernandes, M.L.S., "Química dos Hidroximetiltriazenos", Tese de Doutoramento - Faculdade de Farmácia da Universidade de Lisboa, **(1987)**.

78. Ahern, T.P., Fong, H., Vaughan, K., "Open-chain nitrogen compounds. Part II. Preparation, characterization, and degradation of 1(3)-Aryl-3(1)-methyltriazenes; the effect of substituents on the reaction of diazonium salts with methylamine", Canadian Journal of Chemistry, **(1977)**, vol. 55, pp. 1701-9.

79. Cheng, S.C., Iley, J., "Synthesis of 1-aryl-3-methyltriazenes by based-promoted decomposition of 1-aryl-3-hydroxymethyl-3-methyltriazene", Journal of Chemical Research (S), **(1983)**, pp. 320-1.

80. Hesek, D., Lee, M., Noll, B.C., Fisher, J.F., Mobashery, S., "Complications from dual roles of sodium hydride as a base and as a reducing agent", The Journal of Organic Chemistry, **(2009)**, vol. 74, pp. 2567-70.

81. Kappe, C.O., Stadler, A., "Microwave theory" in Microwaves in organic and medicinal chemistry, Mannhold, R., Kubinyi, H., Folkers, G., Wiley-VCH, 1st ed., Weinheim, **(2005)**, pp. 9-24.

82. Hoz, A., Díaz-Ortiz, A., Moreno, A., "Microwaves in organic synthesis. Thermal and non-thermal microwave effects", Chemical Society Reviews, **(2005)**, vol. 34, pp. 164-78.

83. Loffredo, C., Assunção, N.A., Gerhardt, J., Miranda, M.T.M., "Microwave-assisted solid-phase peptide synthesis at 60 degrees C: alternative conditions with low enantiomerization", Journal of Peptide Science, **(2009)**, vol. 15, pp. 808-17.

84. Perry, M.J., Carvalho, E., Rosa, E., Iley, J., "Towards an efficient prodrug of the alkylating metabolite monomethyltriazene: Synthesis and stability of N-acylamino acid derivatives of triazenes", European Journal of Medicinal Chemistry, **(2009)**, vol. 44, pp. 1049-56.

85. Carvalho, E., Iley, J., Perry, M.J., Rosa, E., "Triazene drug metabolites: Part 15 Synthesis and plasma hydrolysis of anticancer triazenes containing amino acid carriers", Pharmaceutical Research, **(1998)**, vol. 15, pp. 931-35

86. Carvalho, E., Iley, J., Perry, M.J., Rosa, E., "Triazene drug metabolites. Part 16. Kinetics and mechanism of the hydrolysis of aminoacyltriazenes", Journal of The Chemical Society, Perkin Trans. 2, **(1998)**, pp. 2735-80.

87. Chen, S.H., Farina, V., Vyas, D.M., Doyle, T.W., "Synthesis and biological evaluation of C-13 amide-linked paclitaxel (Taxol) analogs", The Journal of Organic Chemistry, **(1996)**, vol. 61, pp. 2065-70.

88. de Gaulejac, N.V., Vivas, N., Nonier M-F., Absalon, C., Bourgeois, G., "Study and quantification of monomeric flavan-3-ol and dimeric procyanidin quinonic forms by HPLC/ESI-MS. Application to red wine oxidation", Journal of the Science of Food and Agriculture, **(2001)**, vol. 81, pp. 1172-79.

89. Dai, J., Mumper, R.J., "Plant phenolics: Extraction, analysis and their antioxidant and anticancer properties", Molecules, **(2010)**, vol. 15, pp. 7313-52.

90. Kunishima, M., Kawachi, C., Morita, J., Terao, K., Iwasaki, F., Tani, S., "4-(4,6-Dimethoxy-1,3,5-triazin-2-yl)-4-methyl-morpholinium chloride: An efficient condensing agent leading to the formation of amides and esters", Tetrahedron, **(1999)**, vol. 55, pp. 13159-70.

91. Luca, L., Giacomelli, G., Taddei, M., "An easy and convenient synthesis of Weinreb amides and hydroxamates", The Journal of Organic Chemistry, **(2001)**, vol. 66, pp. 2534-37.

92. Bandgar, B.P., Pandit, S.S., "Highly rapid and direct synthesis of monoacylated piperazine derivatives from carboxylic acids under mild conditions", Tetrahedron Letters, **(2003)**, vol. 44, pp. 3855-58.

93. Finaru, A., Berthault, A., Besson, T., Guillaumet, G., Berteina-Raboin, S., "Microwave-assisted solid-phase synthesis of 5-carboxamido-N-acetyltryptamine derivatives", Organic Letters, **(2002)**, vol. 4, pp. 2613-15.

94. Bejugam, M., Flitsch, S.L., "An efficient synthetic route to glycoamino acid building blocks for glycopeptide synthesis", Organic Letters, **(2004)**, vol. 6, pp. 4001-4.

95. Cvetovich, R.J., DiMichele, L., "Formation of acrylanilides, acrylamides, and amides directly from carboxylic acids using thionyl chloride in

dimethylacetamide in the absence of bases", Organic Process Research & Development, **(2006)**, vol. 10, pp. 944-6.

96. Sureshbabu, V.V., Hemantha, H.P., "A facile synthesis of N-Fmoc protected amino/peptidyl Weinreb amides employing acid chlorides as key intermediates", Arkivoc, **(2008)**, vol. 2, pp. 243-49.
97. Perry, M.J., "Desenvolvimento de pró-fármacos de triazenos anti-tumorais usando amino-ácidos como transportadores", Tese de Doutoramento - Faculdade de Farmácia da Universidade de Lisboa, **(2002)**.
98. Elias, H.G., Warner, R.J., "Polyesters by thionyl chloride activated polycondensation", Die Makromolekulare Chemie, **(1981)**, vol. 182, pp. 681-86.
99. Takaishi, K., Alen, Y., Kawazu, K., Baba, N., Nakajima, S., "Synthesis and antinematodal activity of 3-n-alkylphenols", Bioscience, Biotechnology and Biochemistry, **(2004)**, vol. 68, pp. 2398-400.
100. Silverstein, R.M., Webster, F.X., Kiemle, D.J., "Spectrometric identification of organic compounds", John Wiley and Sons, 7th ed., Hoboken, **(2005)**, pp. 72-126
101. Simplício, A.L., Clancy, J.M., Gilmer, J.F., "Prodrugs for amines", Molecules, **(2008)**, vol. 13, pp. 519-47.
102. Toussaint, O., Lerch, K., "Catalytic oxidation of 2-aminophenols and ortho hydroxylation of aromatic amines by tyrosinase", Biochemistry, **(1987)**, vol. 26, pp. 8567-71.
103. Fenoll, L.G., Rodríguez-López, J.N., Varón, R., García-Ruiz, P.A., García-Cánovas, F., Tudela, J., "Kinetic study of the oxidation of 3-hydroxyanisole catalysed by tyrosinase", Biophysical Chemistry, **(2000)**, vol. 84, pp. 65-76.
104. Jambhekar, S.S., "Physicochemical and biopharmaceutical properties of drug substances and pharmacokinetics" in Foye's principles of medicinal chemistry, Lemke, T.L., Williams, D.A., Lippincott Williams & Wilkins, 6th ed., Philadelphia, **(2008)**, pp. 210-52.
105. http://www.vcclab.org/lab/alogps/, (01/11/2011)

106. Pandit, N.K., "Introduction to the pharmaceutical sciences", Lippincott Williams & Wilkins, 1st ed., Philadelphia, **(2007)**, pp. 27-42.

107. Reichman, M., Gill, H., "Automated drug screening for ADMET properties" in Drug metabolism handbook concepts and applications, Nassar, A.F., Hollenberg, P.F., Scatina, J., John Wiley and Sons, 1st ed., New Jersey, **(2009)**, pp. 127-66.

108. Jaeschke, H., Gores, G.J., Cederbaum, A.I., Hinson, J.A., Pessayre, D., Lemasters, J.J., "Mechanisms of hepatotoxicity", Toxicological sciences, **(2002)**, vol. 65, pp. 166-76.

109. Vad, N.M., Yount, G., Moore, D., Weidanz, J., Moridani, M.Y., "Biochemical mechanism of acetaminophen (APAP) induced toxicity in melanoma cell lines", Journal of Pharmaceutical Sciences, **(2009)**, vol. 98, pp. 1409-25.

110. Sulistyaningdyah, W.T., Ogawa, J., Li, Q., Maeda, C., Yano, Y., Schmid, R.D., Shimizu, S., "Hydroxylation activity of P450 BM-3 mutant F87V towards aromatic compounds and its application to the synthesis of hydroquinone derivatives from phenolic compounds", Applied Microbiology and Biotechnology, **(2005)**, vol. 67, pp. 556-62.

111. Thompson, D.C., Perera, K., London, R., "Quinone methide formation from para isomers of methylphenol (cresol), ethylphenol, and isopropylphenol: relationship to toxicity", Chemical Research in Toxicology, **(1995)**, vol. 8, pp. 55-60.

112. Yan, Z., Zhong, H.M., Maher, N., Torres, R., Leo, G.C., Cadwell, G.W., Huebert, N., "Bioactivation of 4-methylphenol (p-cresol) via cytochrome P450-mediated aromatic oxidation in human liver microsomes", Drug Metabolism and Disposition, **(2005)**, vol. 33, pp. 1867-76.

113. Vad, N.M., Kandala, P.K., Srivastava, S.K., Moridani, M.Y., "Structure-toxicity relationship of phenolic analogs as anti-melanoma agents: An enzyme directed prodrug approach", Chemico-Biological Interactions, **(2010)**, vol. 183, pp. 462-71.

114. Kudugunti, S.K., Vad, N.M., Whiteside, A.J., Naik, B.U., Yusuf, M.A., Srivenugopal, K.S., Moridani, M.Y., "Biochemical mechanism of caffeic acid

phenylethyl ester (CAPE) selective toxicity towards melanoma cell lines", Chemico-Biological Interactions, **(2010)**, vol. 188, pp. 1-14.

115. Hosangadi, B.D., Dave, R.H., "An efficient general method for esterification of aromatic carboxylic acids", Tetrahedron Letters, **(1996)**, vol. 37, pp. 6375-78.

APPENDICES

Appendix 1 – Triazene prodrug 21a

- ^{1}H NMR

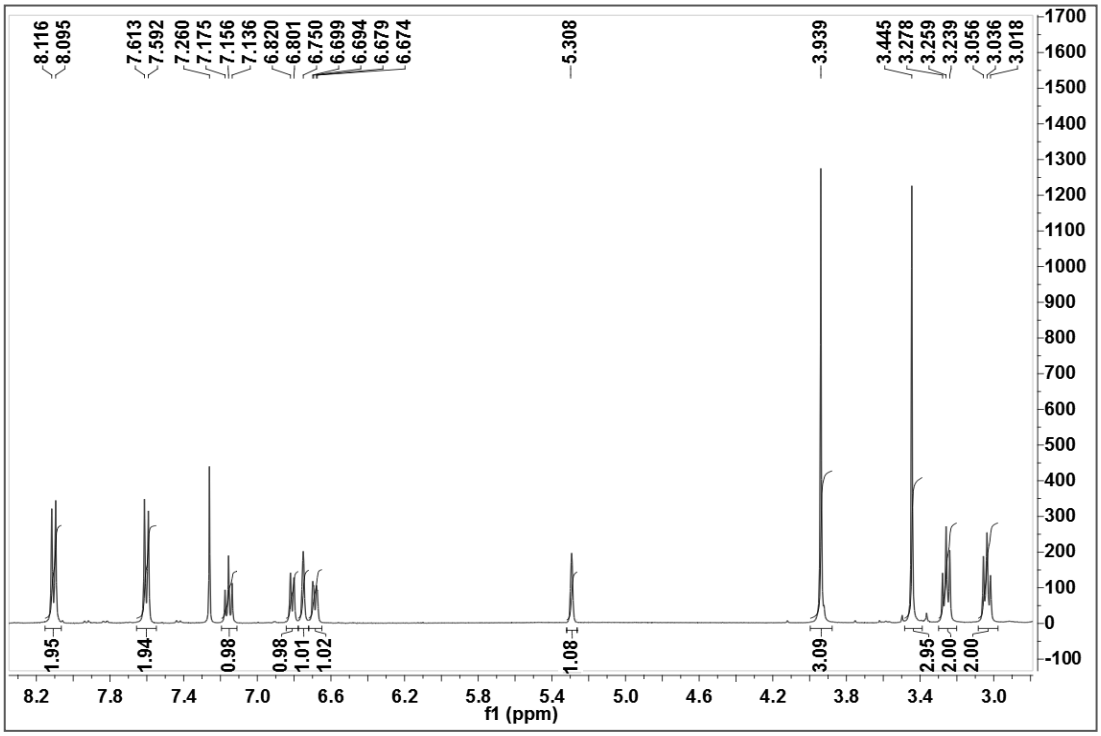

- ^{13}C NMR

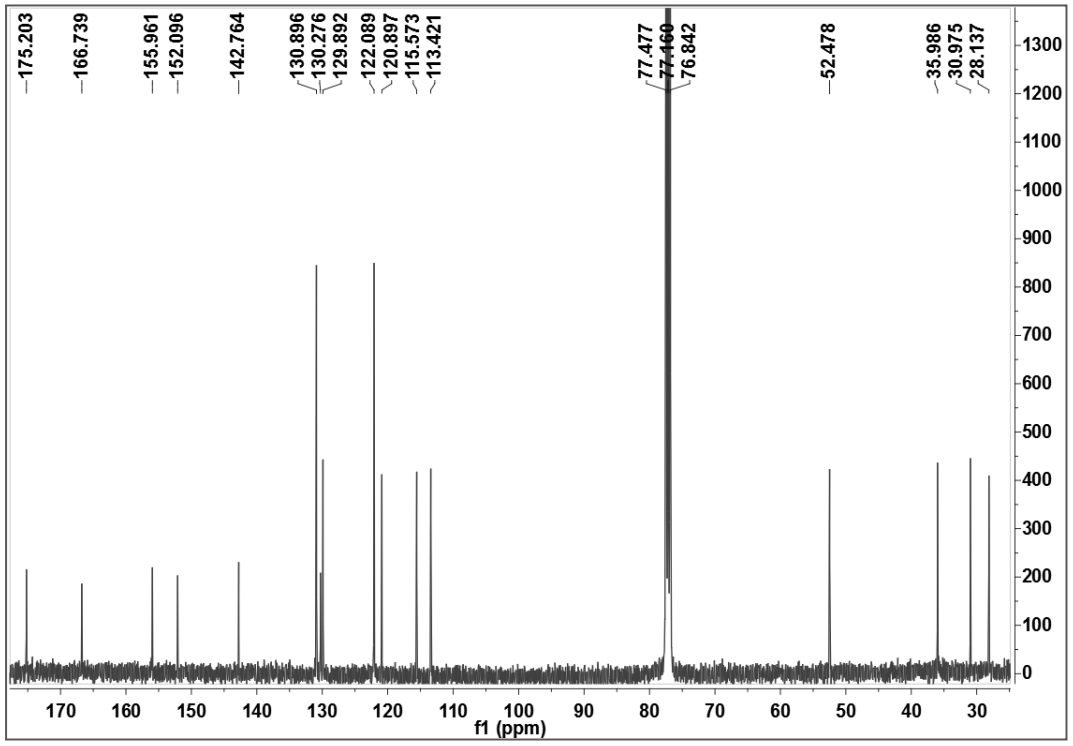

- HMQC

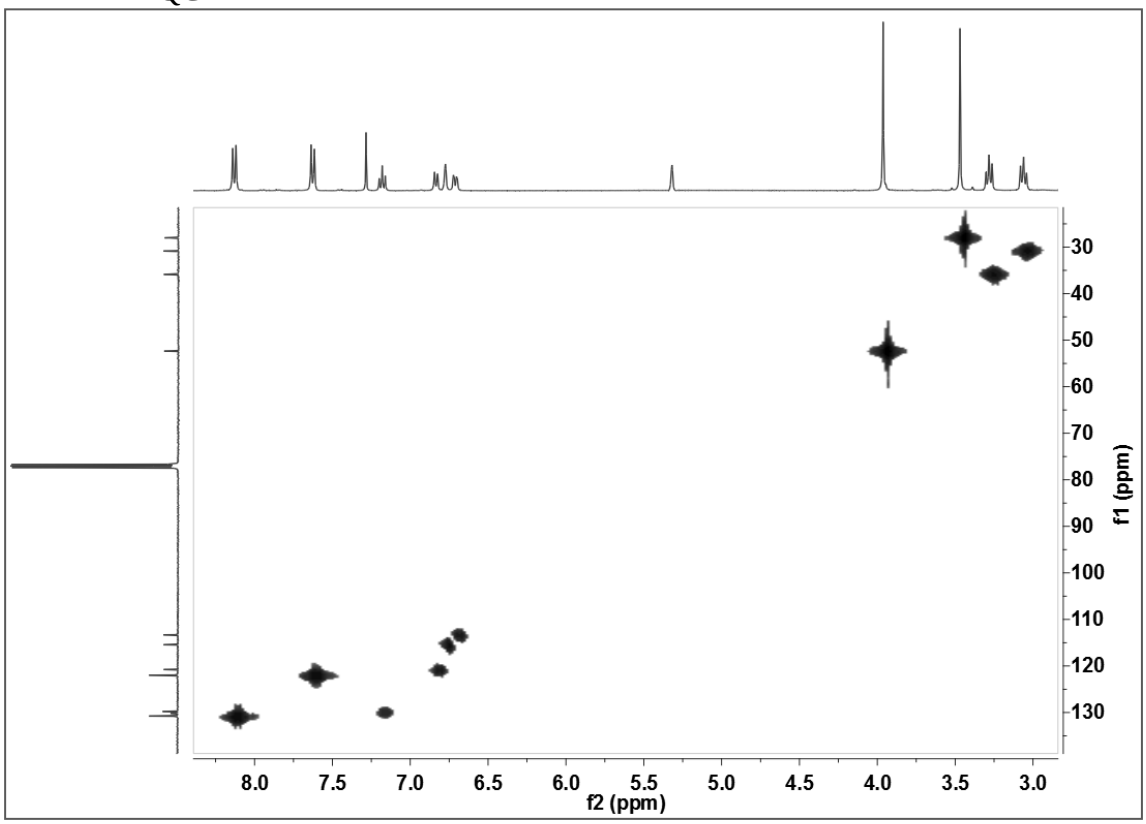
f2 (ppm)
f1 (ppm)
8.0
7.5
7.0
6.5
6.0
5.5
5.0
4.5
4.0
3.5
3.0
30
40
50
60
70
80
90
100
110
120
130

- IR

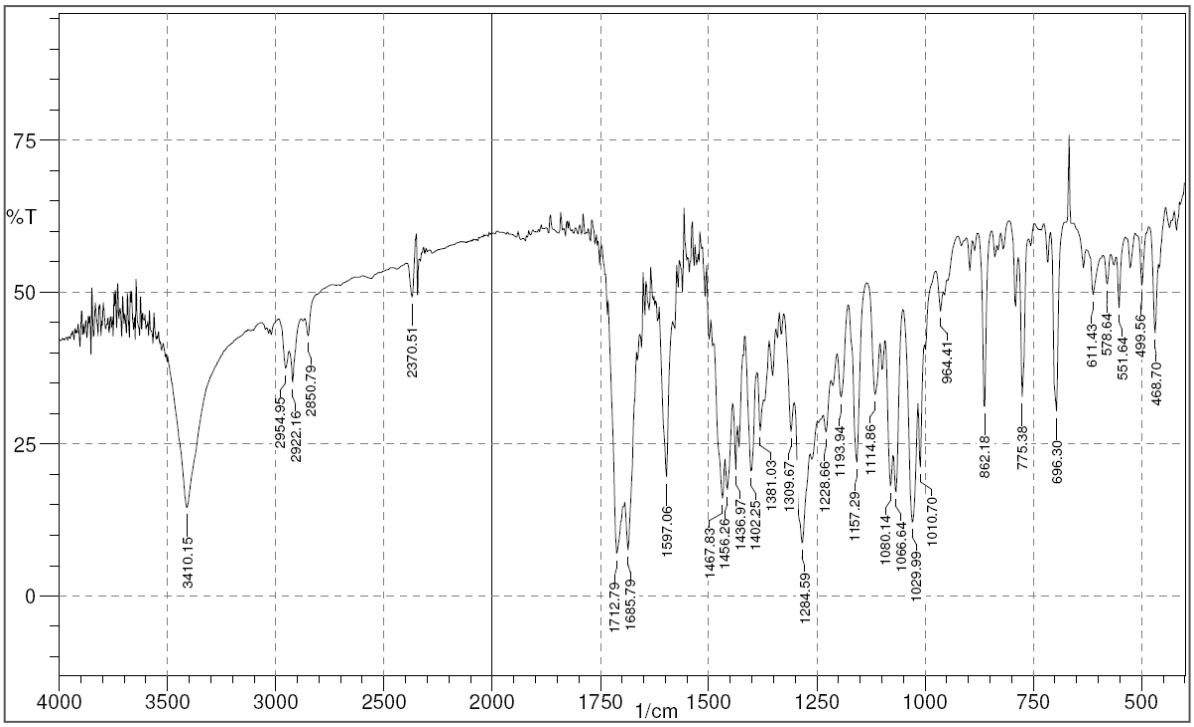
%T
75
50
25
0
4000
3500
3000
2500
2000
1750
1500
1250
1000
750
500
1/cm
3410.15
2954.95
2922.16
2850.79
2370.51
1712.79
1685.79
1597.06
1467.83
1456.26
1436.97
1402.25
1381.03
1309.67
1284.59
1228.66
1193.94
1157.29
1114.86
1080.14
1066.64
1029.99
1010.70
964.41
862.18
775.38
696.30
611.43
578.64
551.64
499.56
468.70

- UV

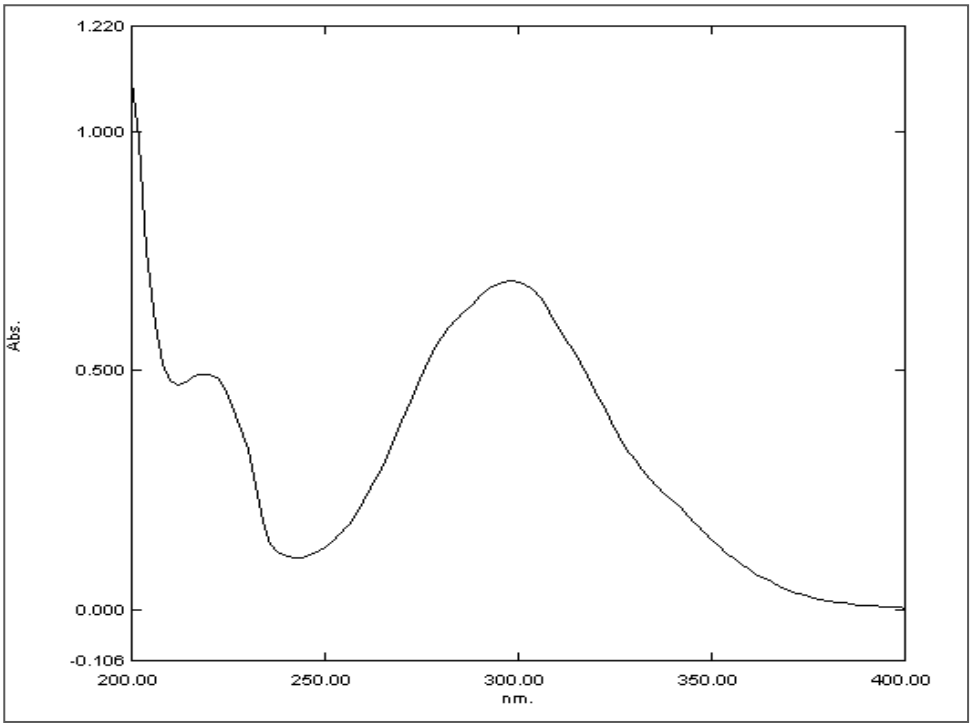
1.220
1.000
0.500
0.000
-0.106
Abs.
200.00
250.00
300.00
350.00
400.00
nm.

- MASS (ESI^+)

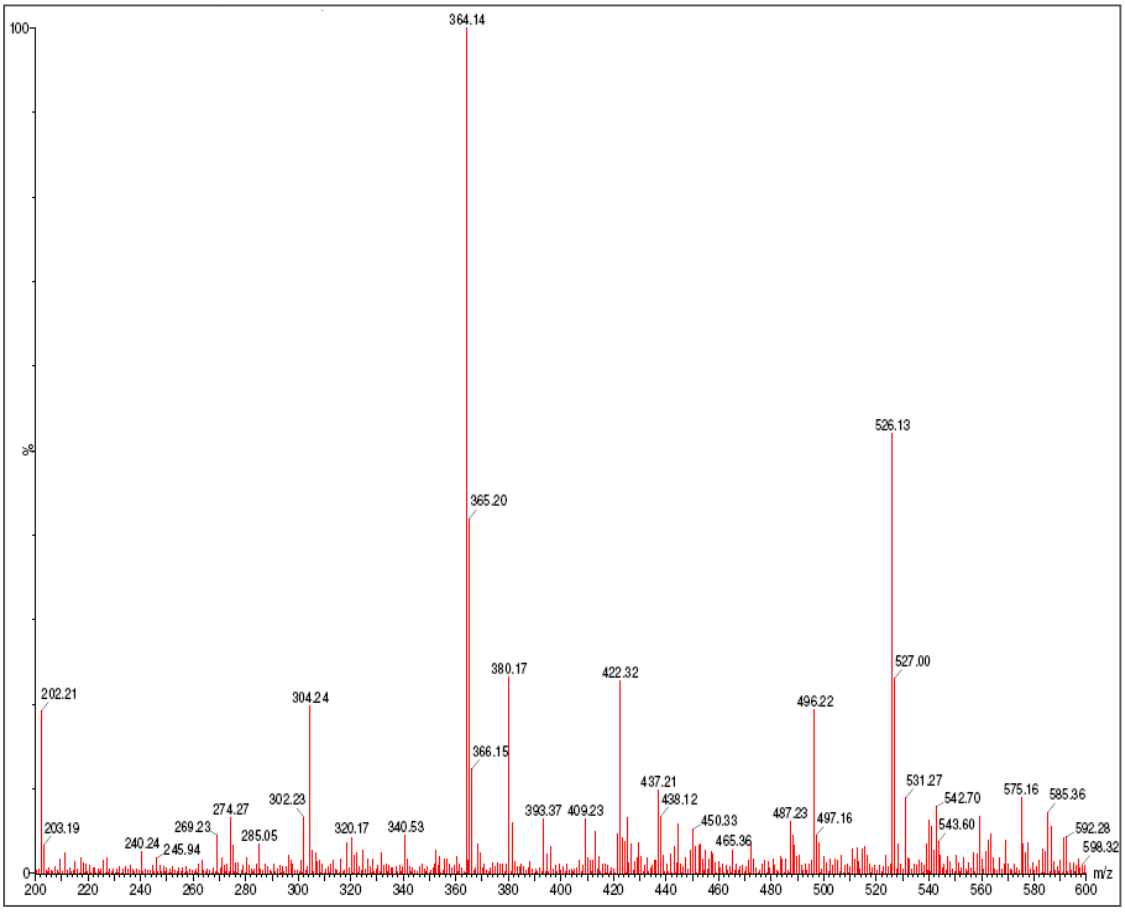
100
%
0
364.14
365.20
526.13
527.00
380.17
422.32
202.21
304.24
496.22
366.15
437.21
438.12
531.27
542.70
575.16
585.36
543.60
592.28
598.32
203.19
240.24
245.94
269.23
274.27
285.05
302.23
320.17
340.53
393.37
409.23
450.33
465.36
487.23
497.16
200
220
240
260
280
300
320
340
360
380
400
420
440
460
480
500
520
540
560
580
600
m/z

Appendix 2 – Triazene prodrug 21b

- ^{1}H NMR

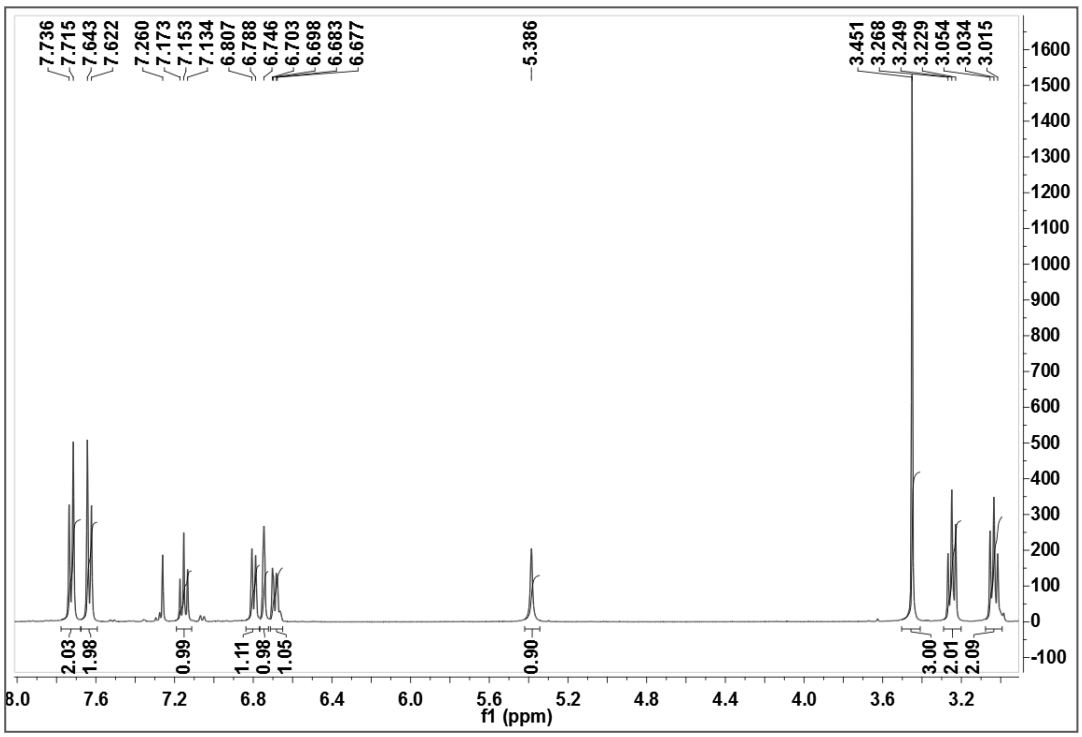

- ^{13}C NMR

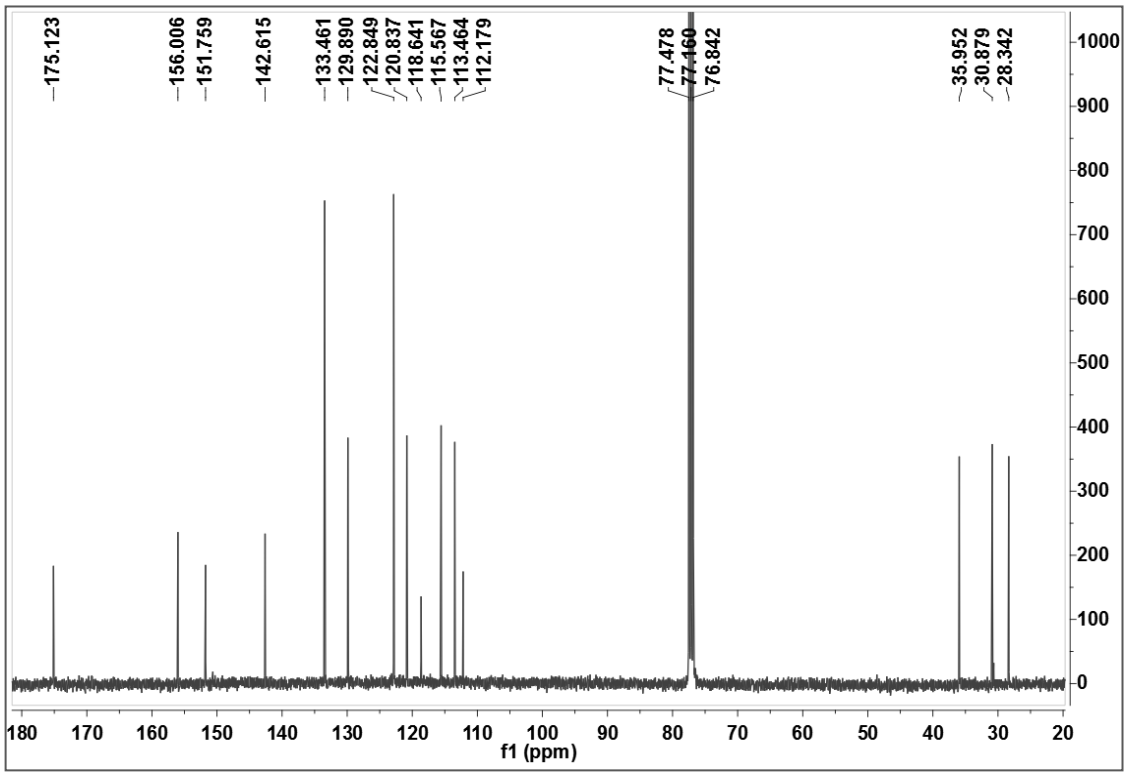

- HMQC

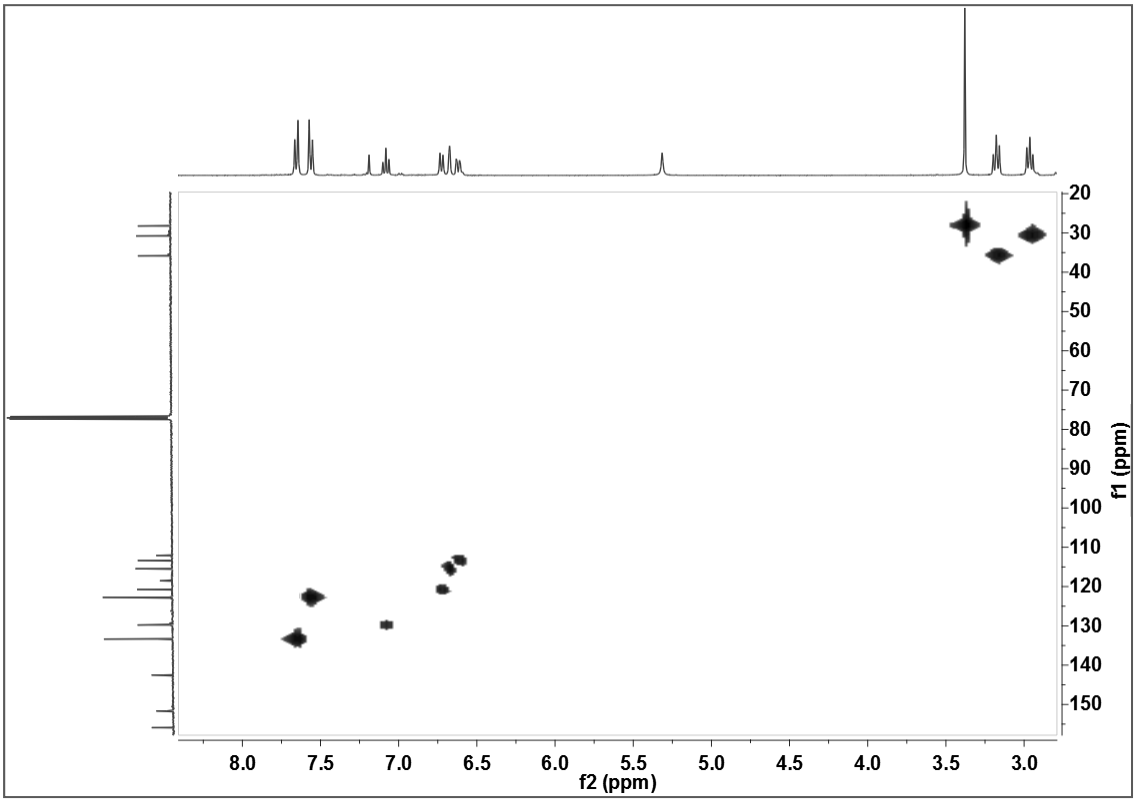
f2 (ppm)
f1 (ppm)

- IR

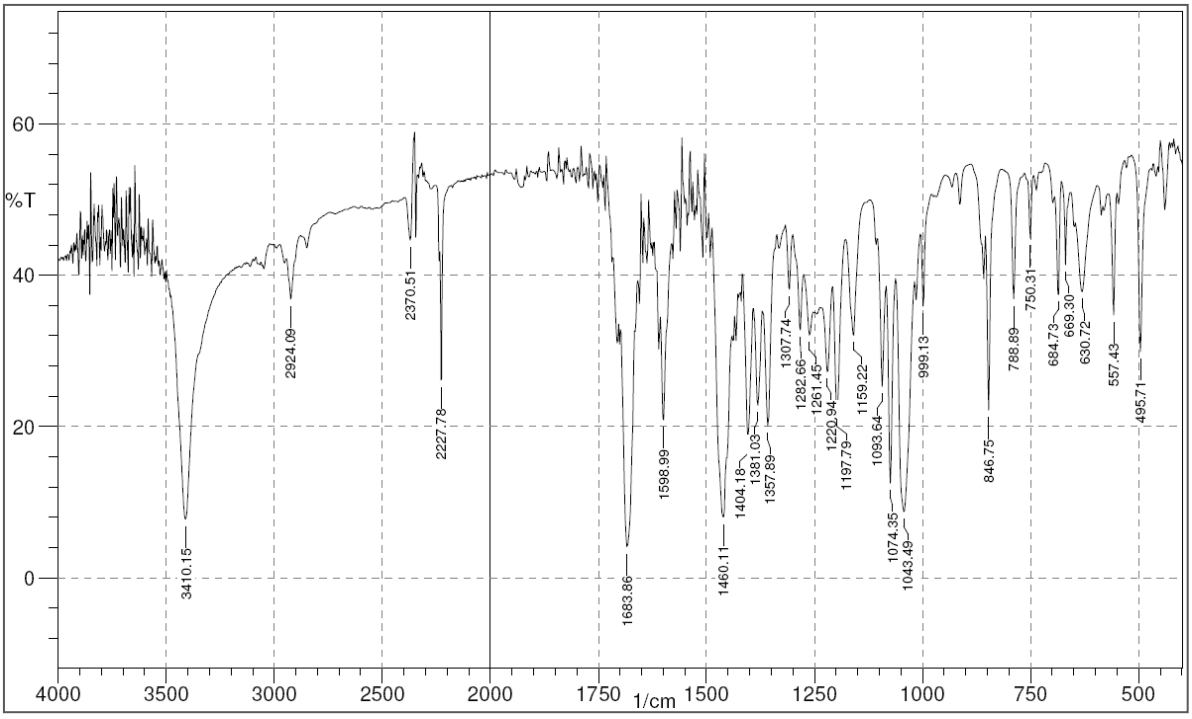
%T
1/cm
3410.15
2924.09
2370.51
2227.78
1683.86
1598.99
1460.11
1404.18
1381.03
1357.89
1307.74
1282.66
1261.45
1220.94
1197.79
1159.22
1093.64
1074.35
1043.49
999.13
846.75
788.89
750.31
684.73
669.30
630.72
557.43
495.71

- UV

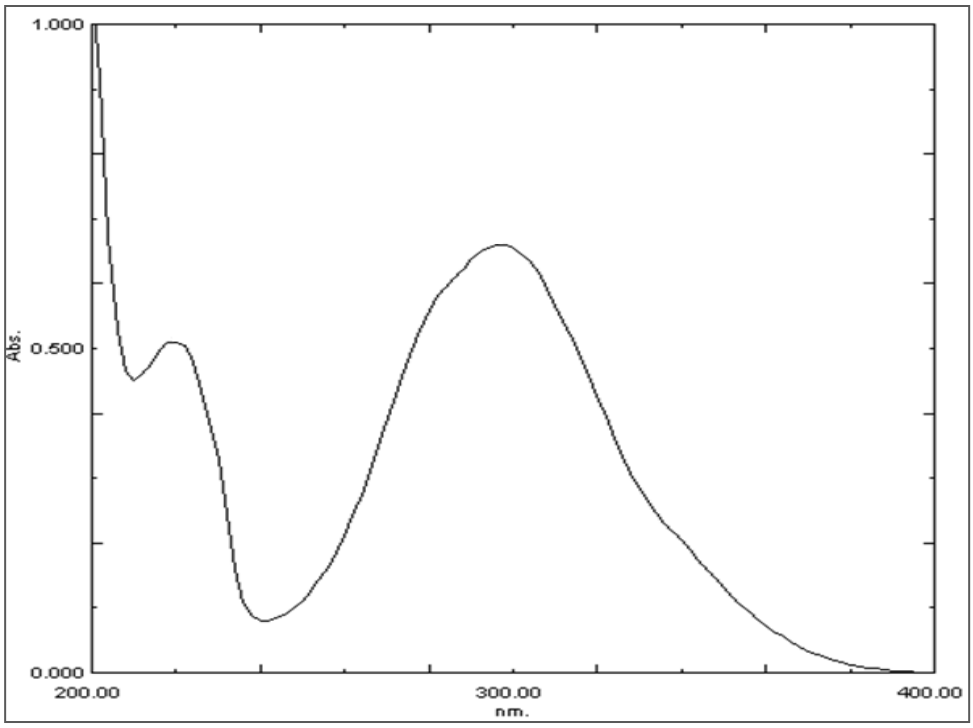
1.000
0.500
0.000
Abs.
200.00
300.00
400.00
nm.

- MASS (ESI)

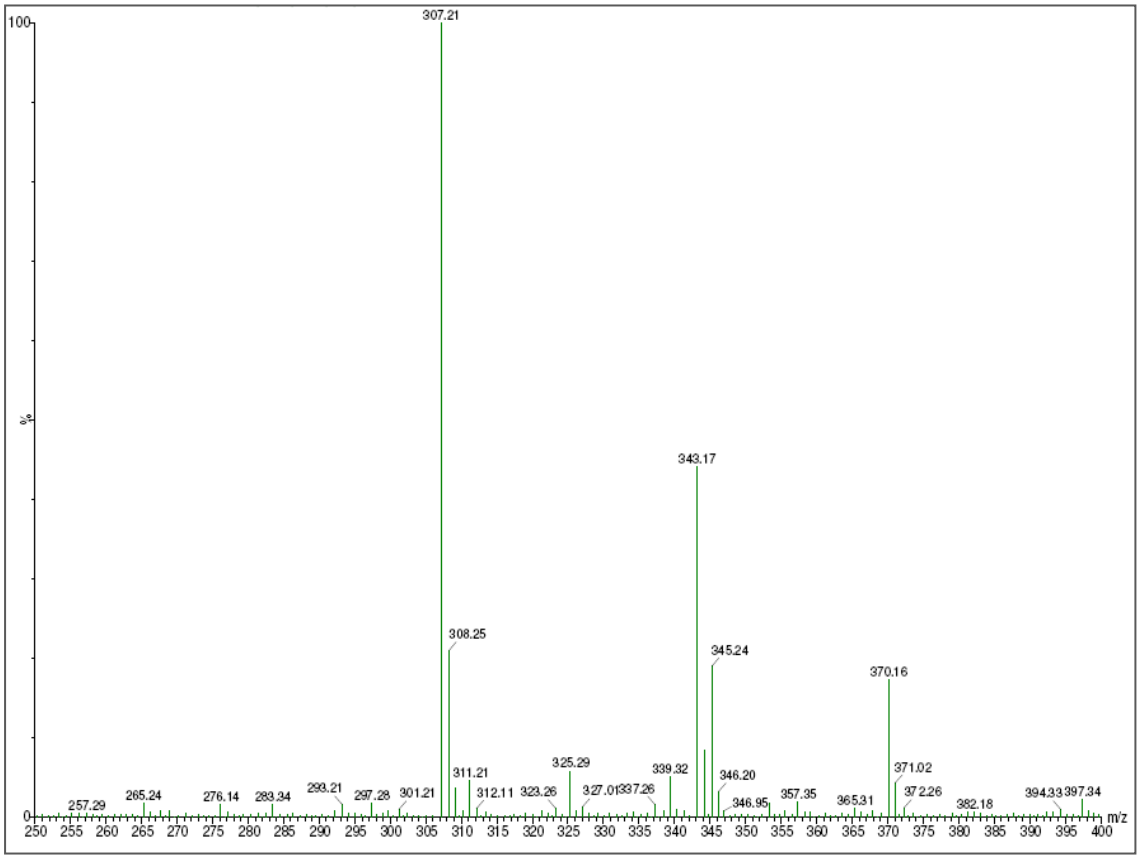
100
%
0
307.21
343.17
308.25
345.24
370.16
325.29
339.32
311.21
346.20
371.02
257.29
265.24
276.14
283.34
293.21
297.28
301.21
312.11
323.26
327.01
337.26
346.95
357.35
365.31
372.26
382.18
394.33
397.34
250 255 260 265 270 275 280 285 290 295 300 305 310 315 320 325 330 335 340 345 350 355 360 365 370 375 380 385 390 395 400
m/z

Appendix 3 – Triazene prodrug 21c

- ^{1}H NMR

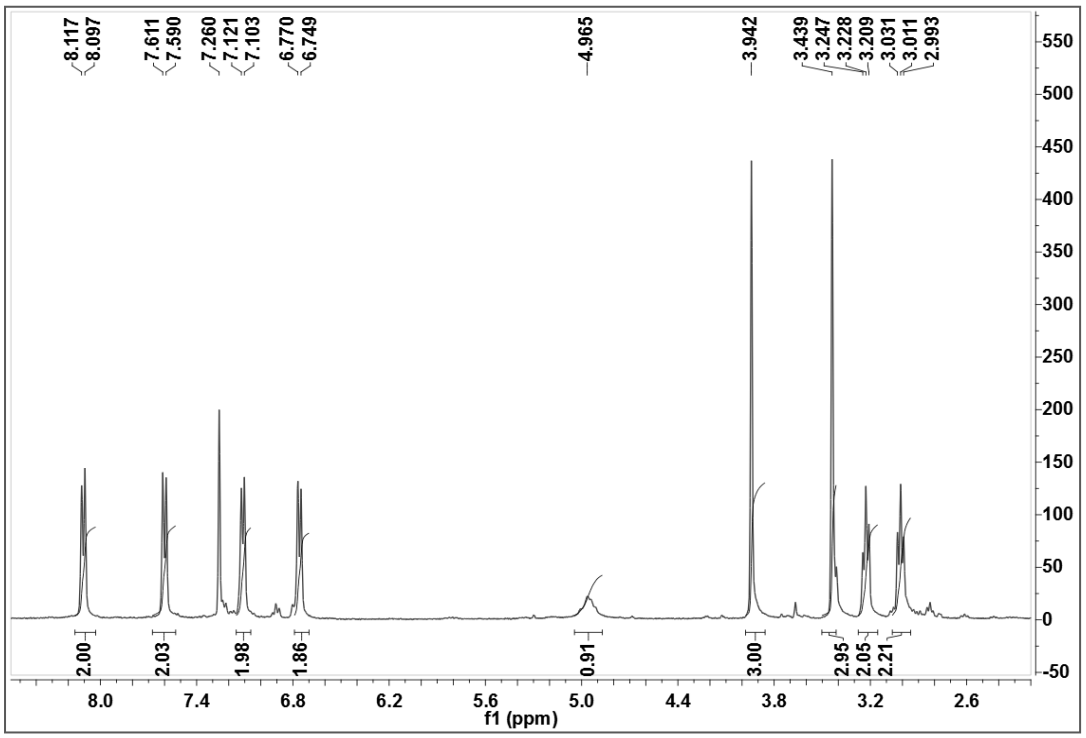

- ^{13}C NMR

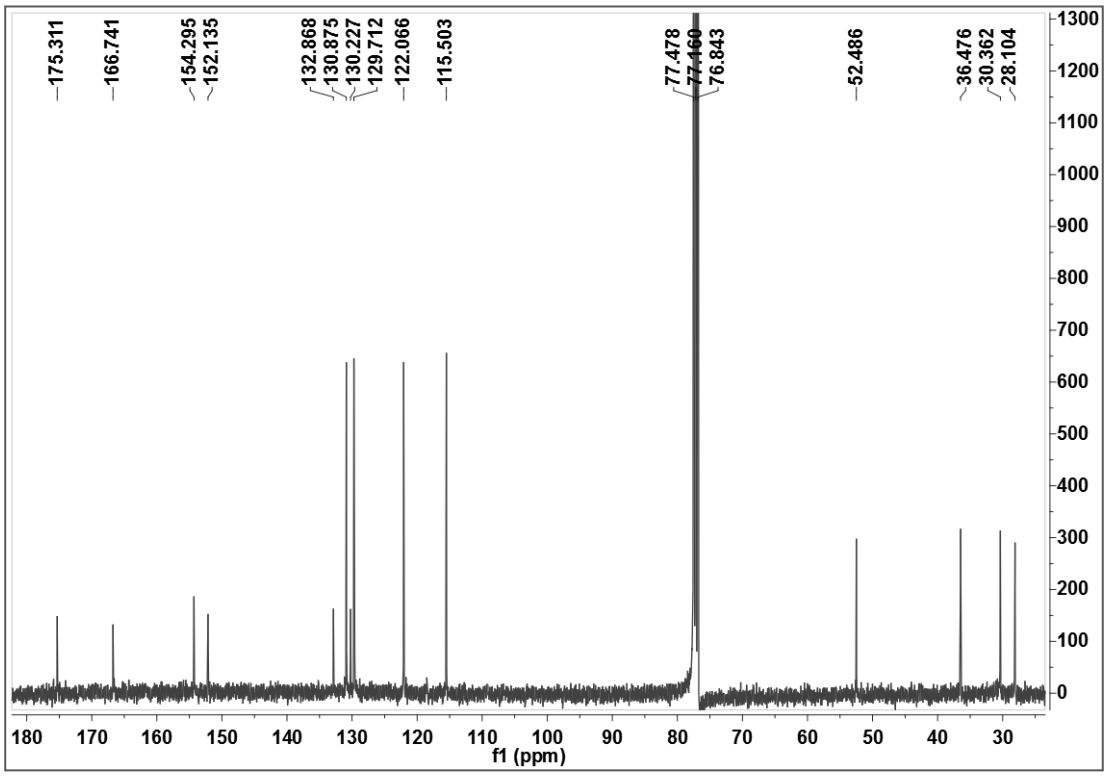

- HMQC

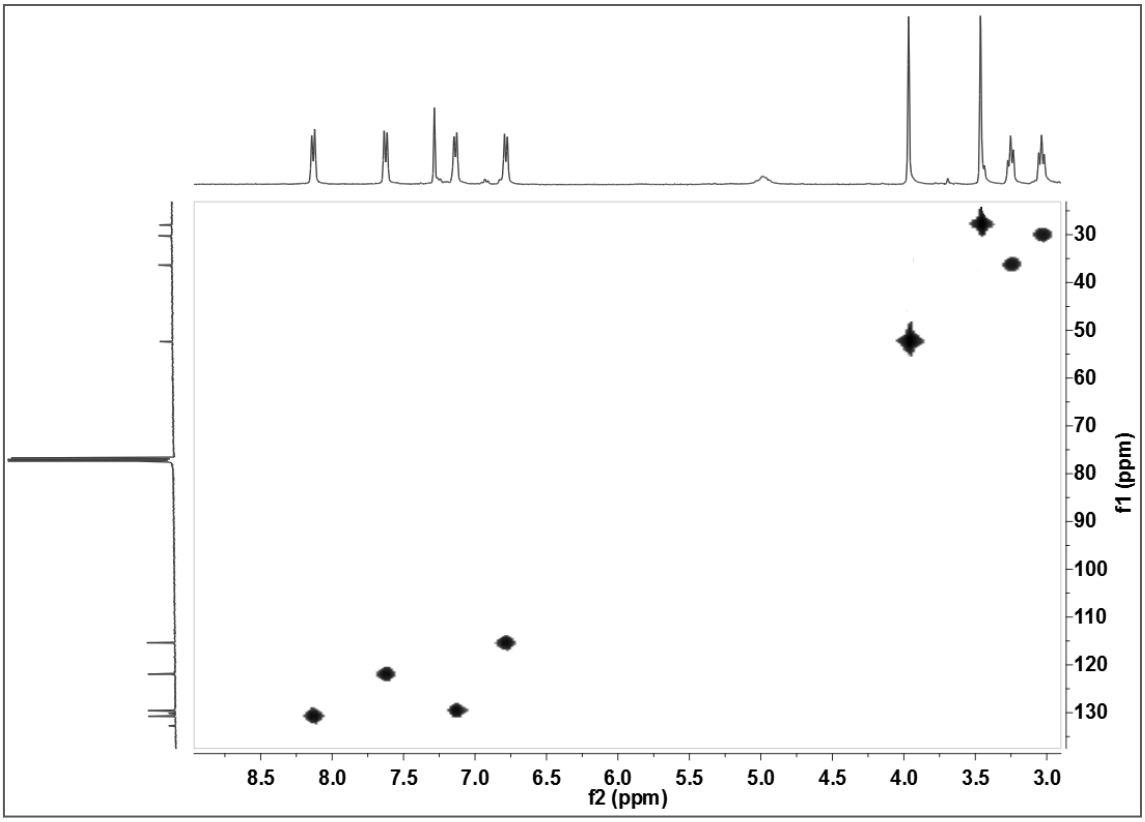
f1 (ppm)
f2 (ppm)
8.5
8.0
7.5
7.0
6.5
6.0
5.5
5.0
4.5
4.0
3.5
3.0
30
40
50
60
70
80
90
100
110
120
130

- IR

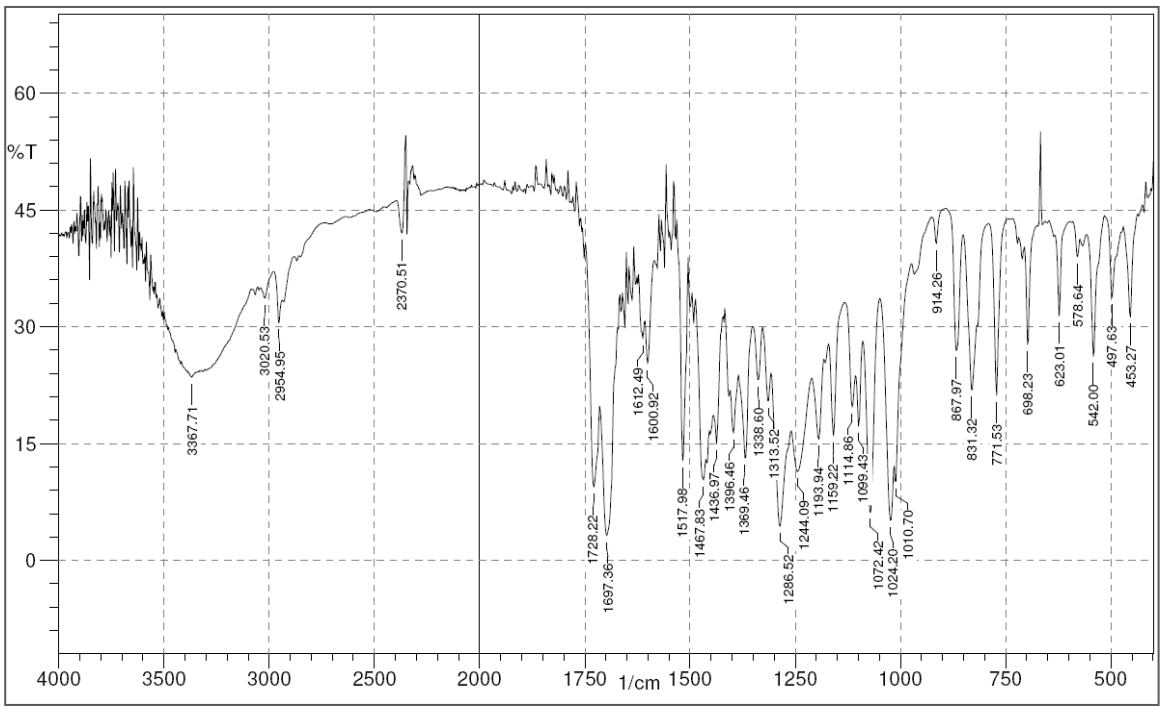
%T
60
45
30
15
0
4000
3500
3000
2500
2000
1750
1/cm
1500
1250
1000
750
500
3367.71
3020.53
2954.95
2370.51
1728.22
1697.36
1612.49
1600.92
1517.98
1467.83
1436.97
1396.46
1369.46
1338.60
1313.52
1286.52
1244.09
1193.94
1159.22
1114.86
1099.43
1072.42
1024.20
1010.70
914.26
867.97
831.32
771.53
698.23
623.01
578.64
542.00
497.63
453.27

- UV

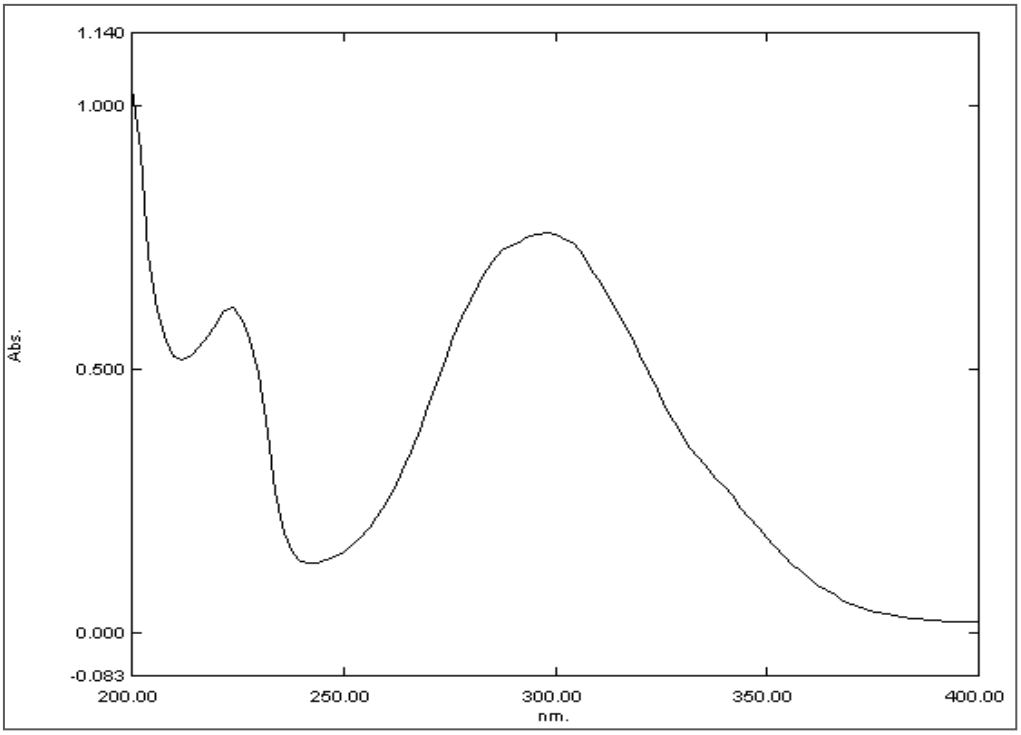
1.140
1.000
0.500
0.000
-0.083
Abs.
200.00
250.00
300.00
350.00
400.00
nm.

- MASS (ESI-)

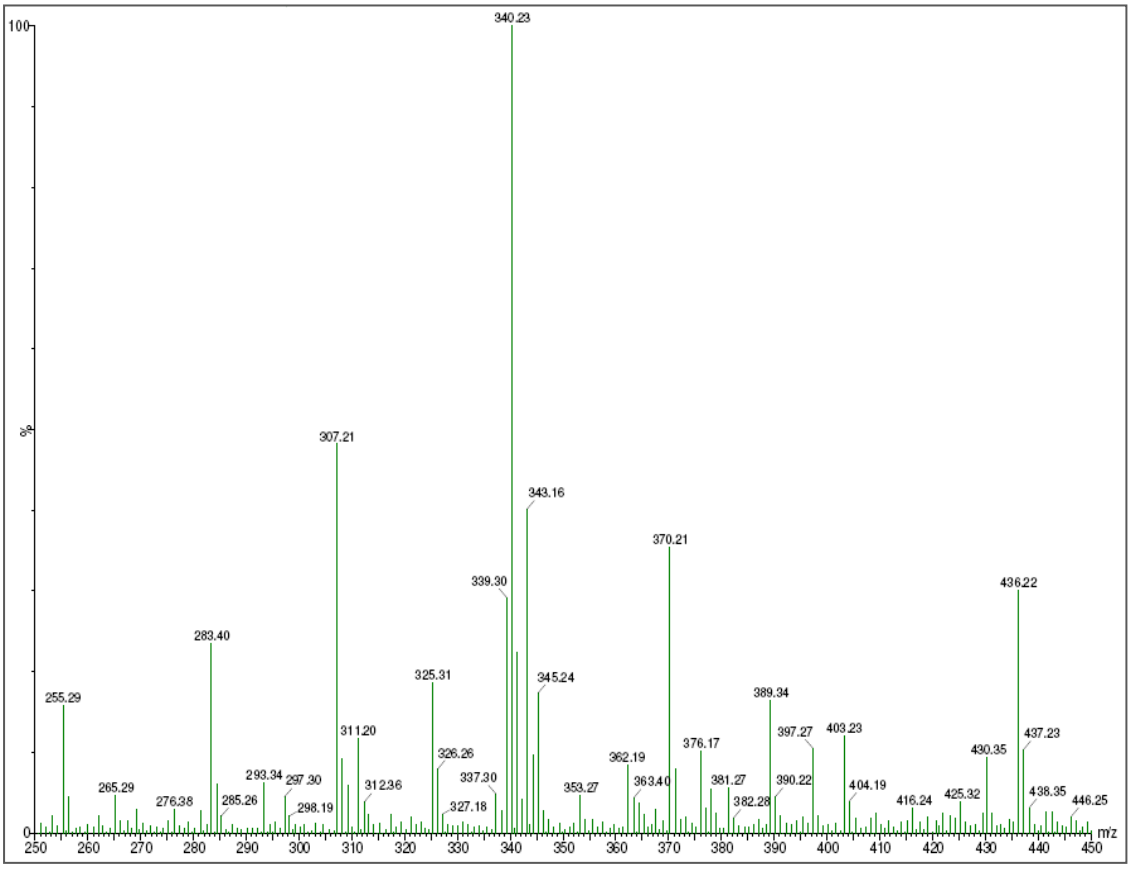
100
%
0
340.23
307.21
343.16
370.21
339.30
436.22
283.40
325.31
345.24
389.34
255.29
311.20
326.26
376.17
397.27
403.23
362.19
437.23
430.35
293.34
297.30
337.30
381.27
390.22
265.29
312.36
363.40
404.19
438.35
276.38
285.26
298.19
327.18
353.27
382.28
416.24
425.32
446.25
250
260
270
280
290
300
310
320
330
340
350
360
370
380
390
400
410
420
430
440
450
m/z

Appendix 4 – Triazene prodrug 21d

- ^{1}H NMR

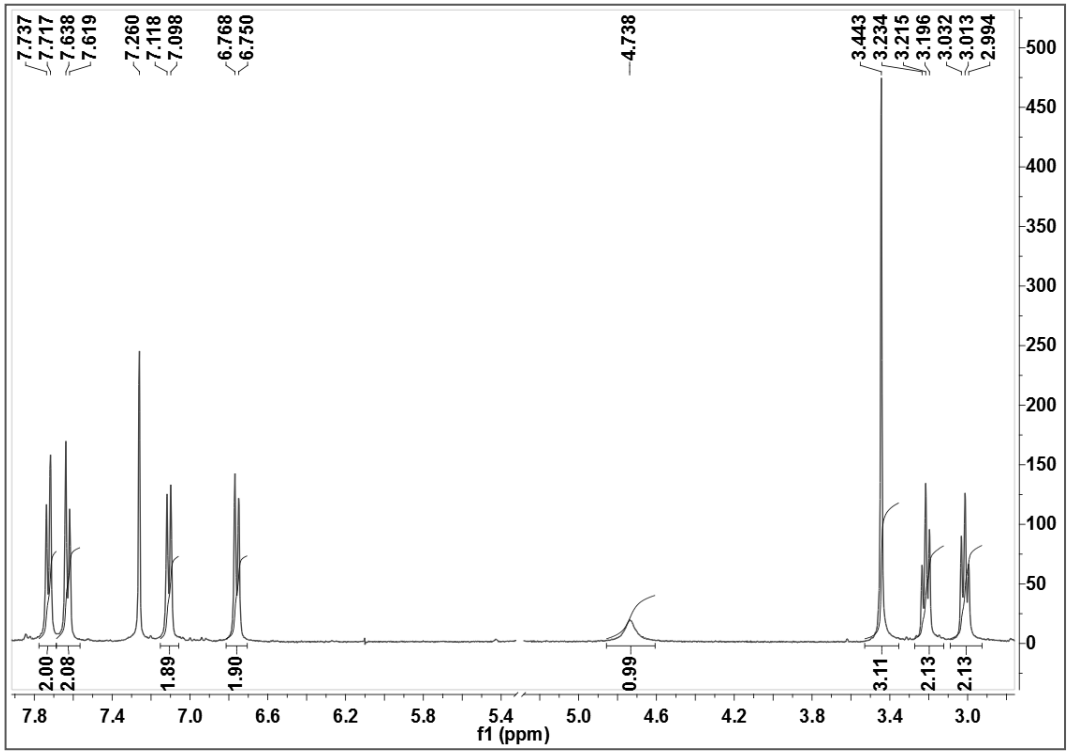

- ^{13}C NMR

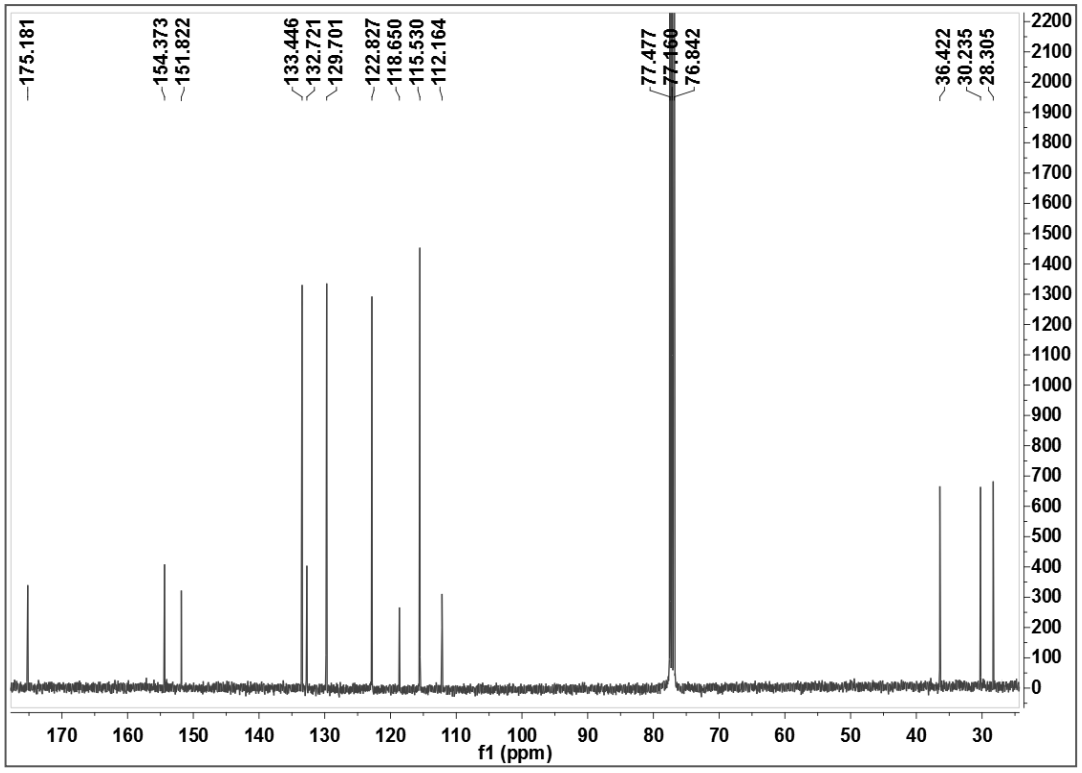

- HMQC

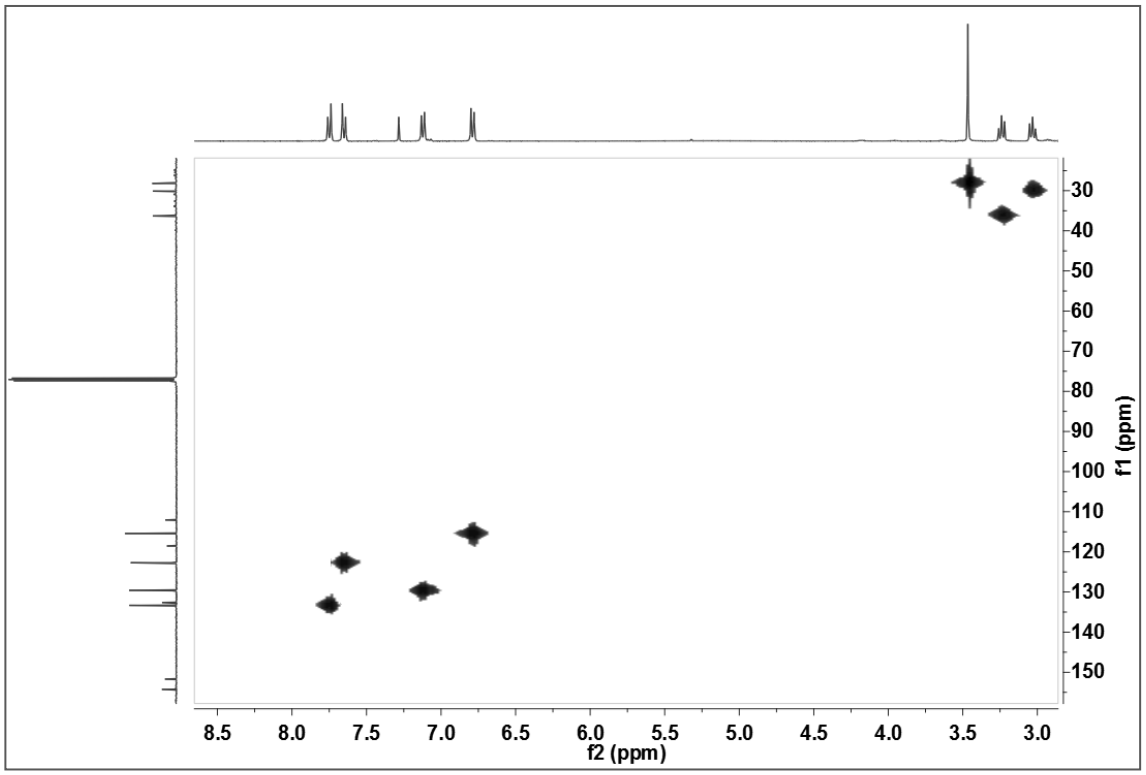
f1 (ppm)
f2 (ppm)
8.5
8.0
7.5
7.0
6.5
6.0
5.5
5.0
4.5
4.0
3.5
3.0
30
40
50
60
70
80
90
100
110
120
130
140
150

- IR

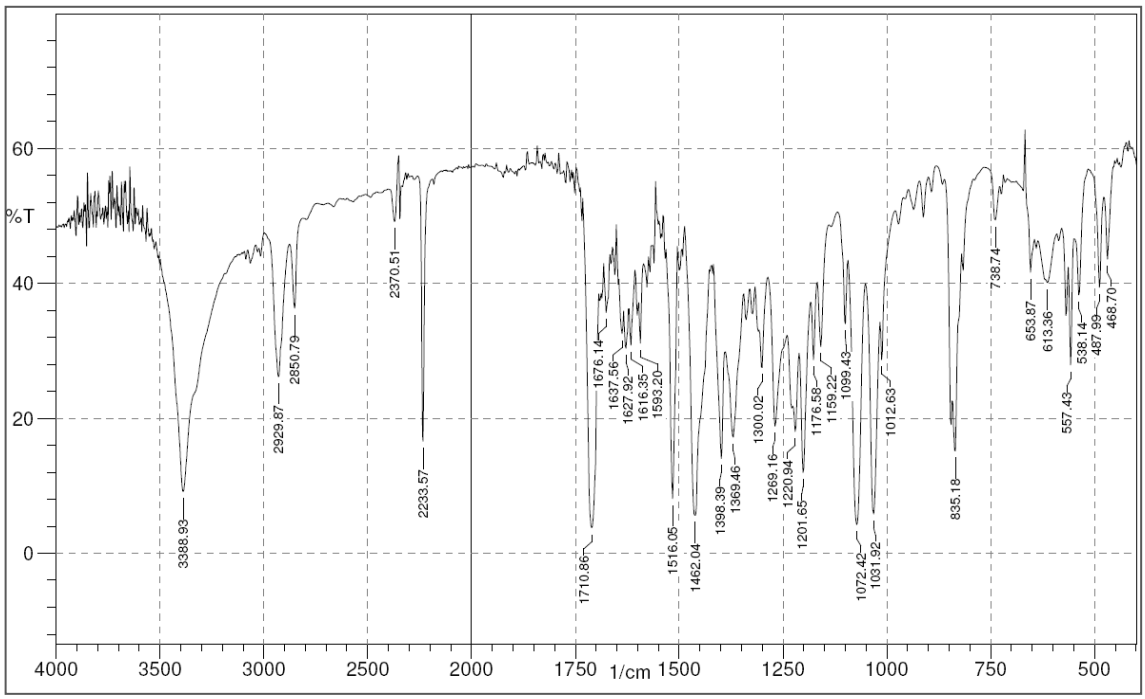
%T
60
40
20
0
4000
3500
3000
2500
2000
1750
1/cm
1500
1250
1000
750
500
3388.93
2929.87
2850.79
2370.51
2233.57
1710.86
1676.14
1637.56
1627.92
1616.35
1593.20
1516.05
1462.04
1398.39
1369.46
1300.02
1269.16
1220.94
1201.65
1176.58
1159.22
1099.43
1072.42
1031.92
1012.63
835.18
738.74
653.87
613.36
557.43
538.14
487.99
468.70

- UV

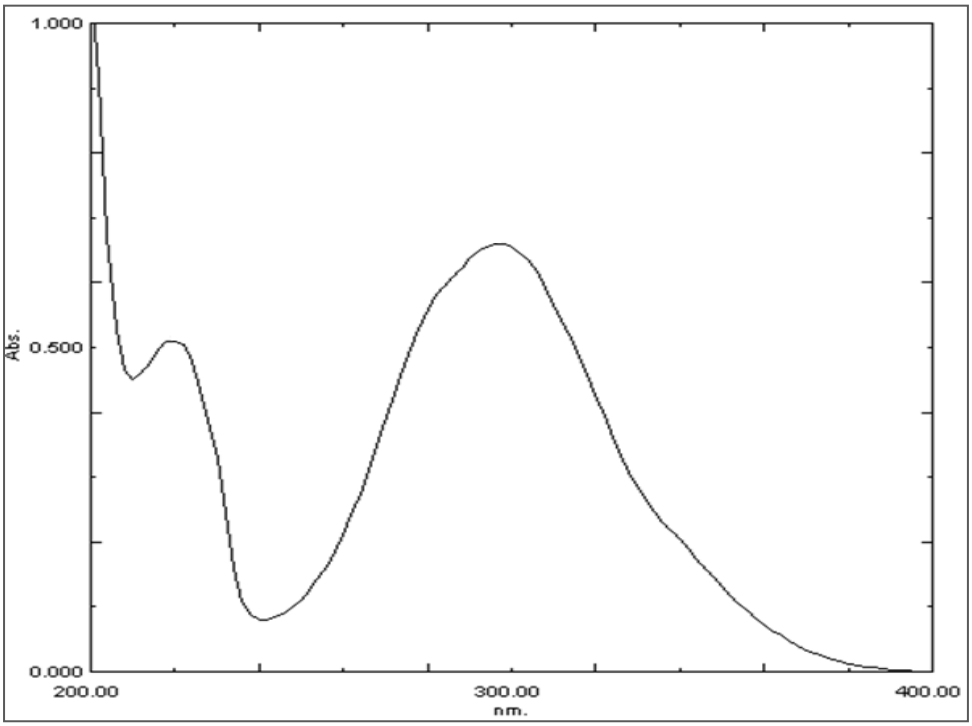
1.000
0.500
0.000
Abs.
200.00
300.00
400.00
nm.

- MASS (ESI-)

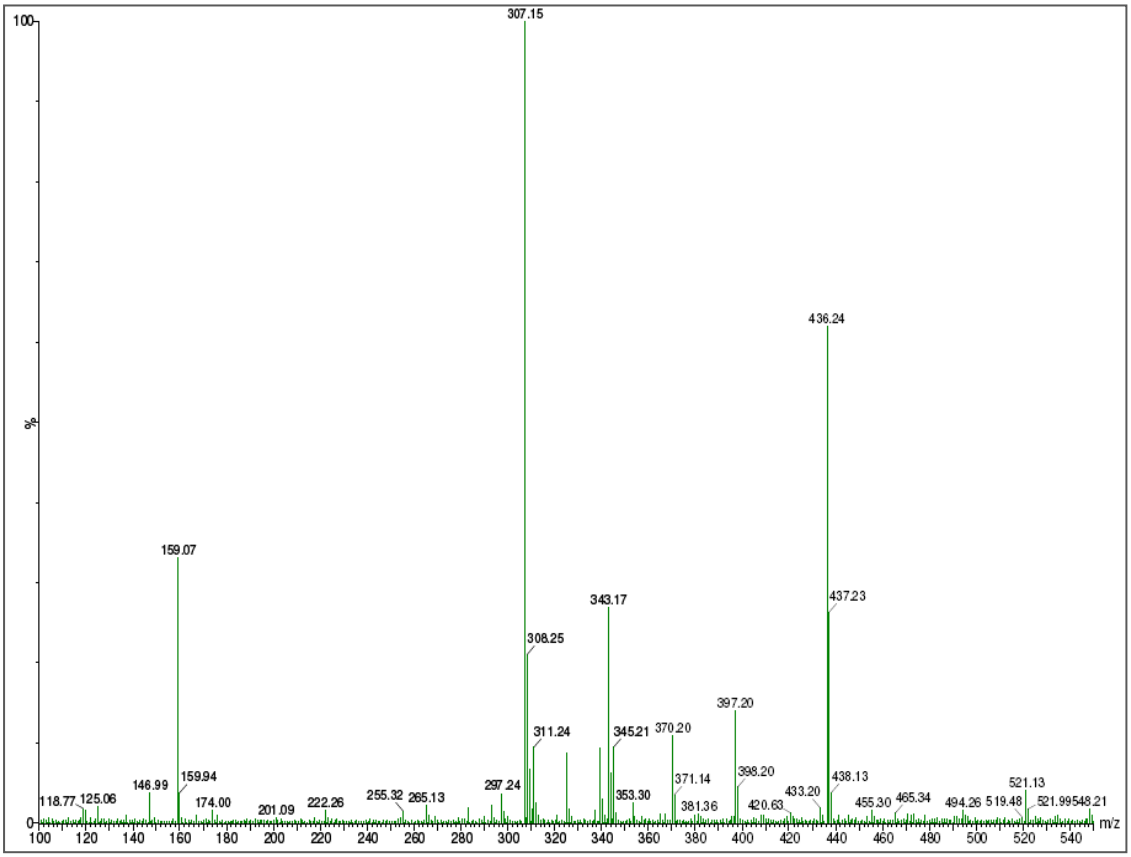
100
%
0
307.15
436.24
159.07
437.23
343.17
308.25
397.20
311.24
345.21
370.20
398.20
371.14
438.13
433.20
521.13
118.77
125.06
146.99
159.94
174.00
201.09
222.26
255.32
265.13
297.24
353.30
381.36
420.63
455.30
465.34
494.26
519.48
521.99548.21
m/z
100 120 140 160 180 200 220 240 260 280 300 320 340 360 380 400 420 440 460 480 500 520 540

Appendix 5 – Triazene prodrug 21e

- ^{1}H NMR

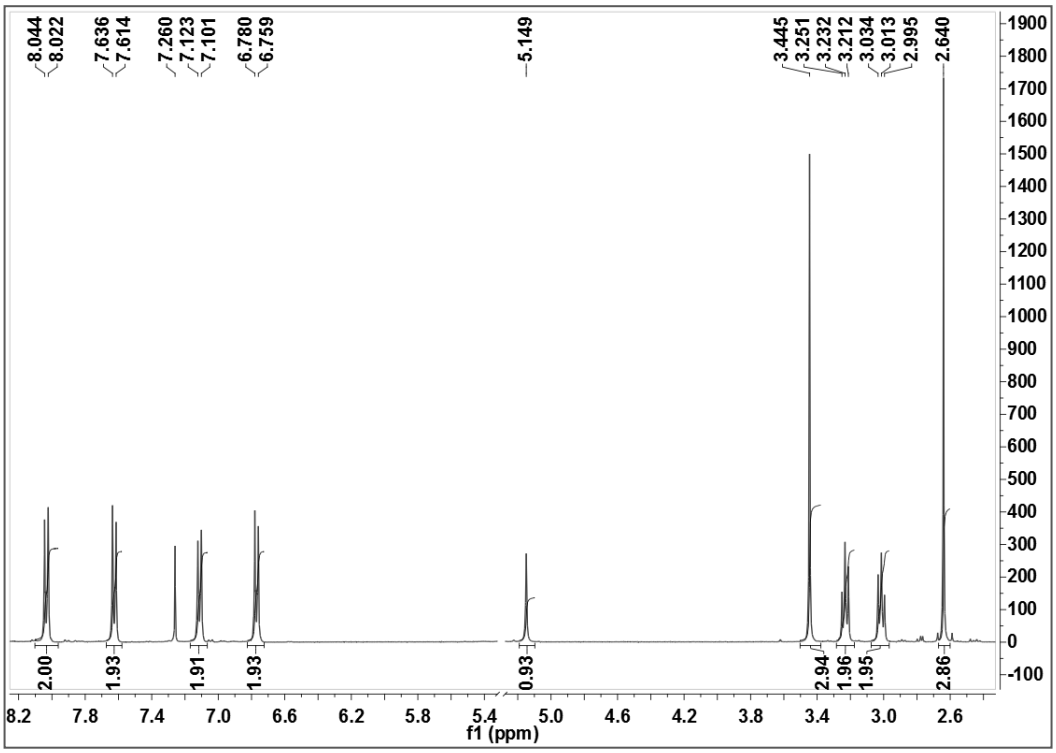

- ^{13}C NMR

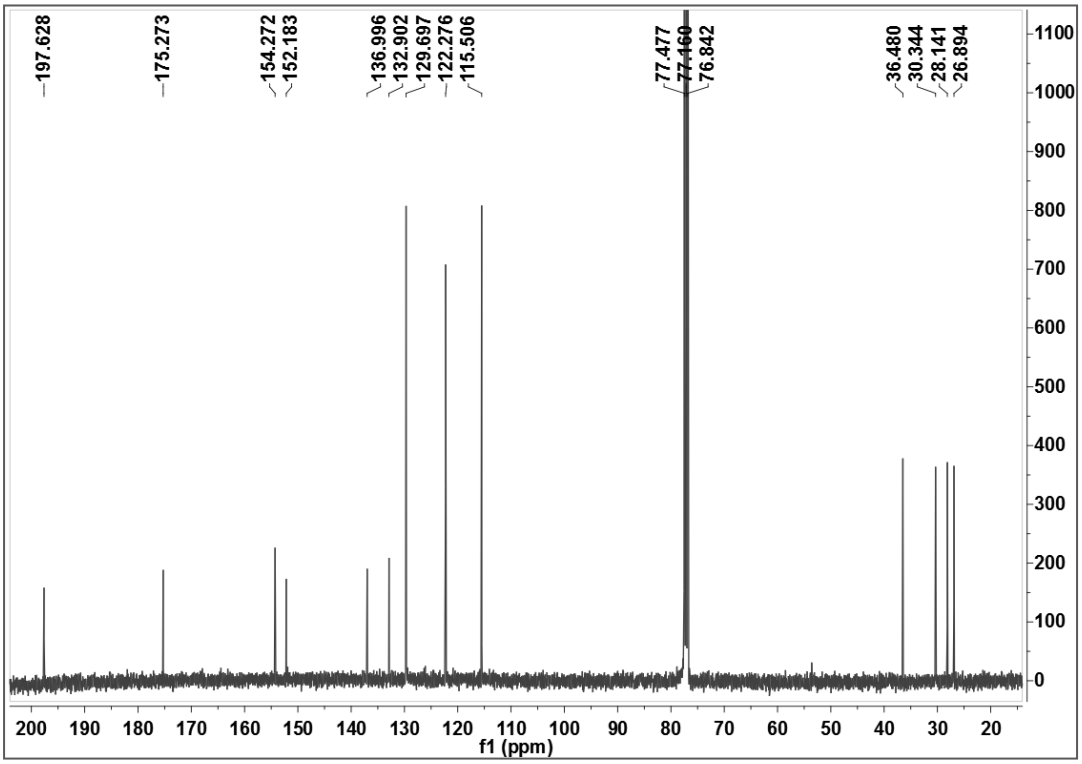

- HMQC

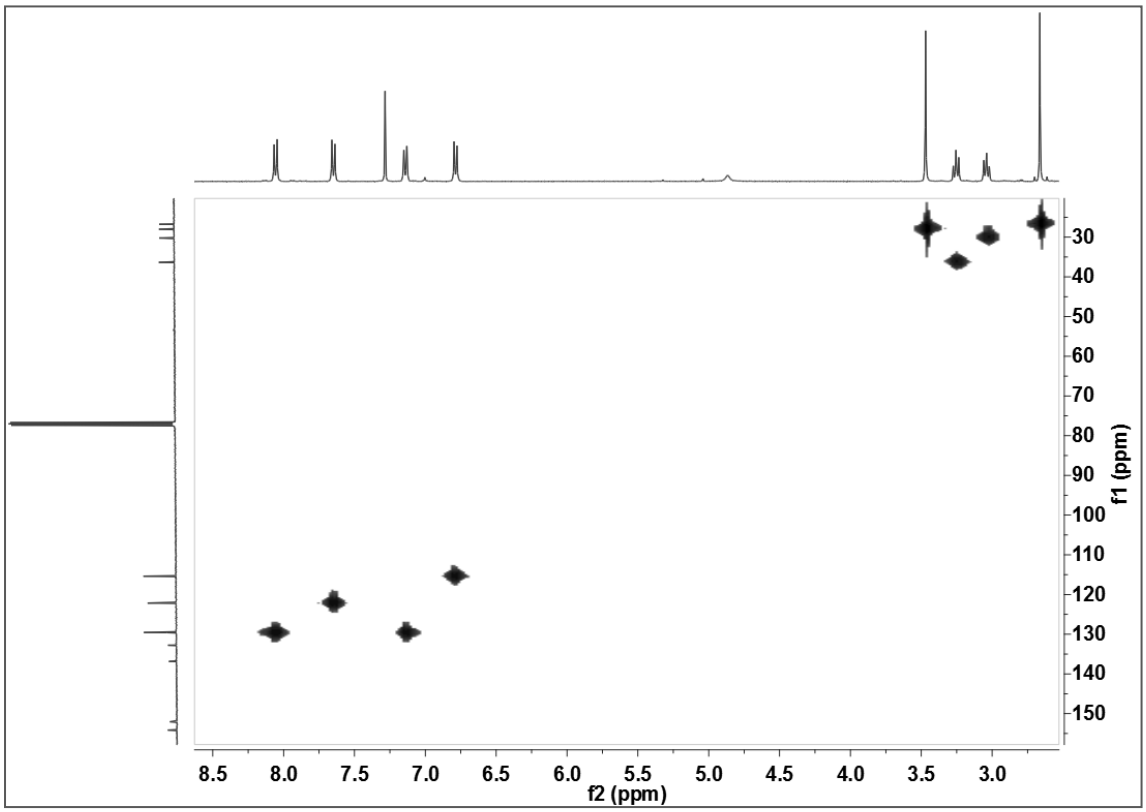
f1 (ppm)
f2 (ppm)
8.5
8.0
7.5
7.0
6.5
6.0
5.5
5.0
4.5
4.0
3.5
3.0
30
40
50
60
70
80
90
100
110
120
130
140
150

- IR

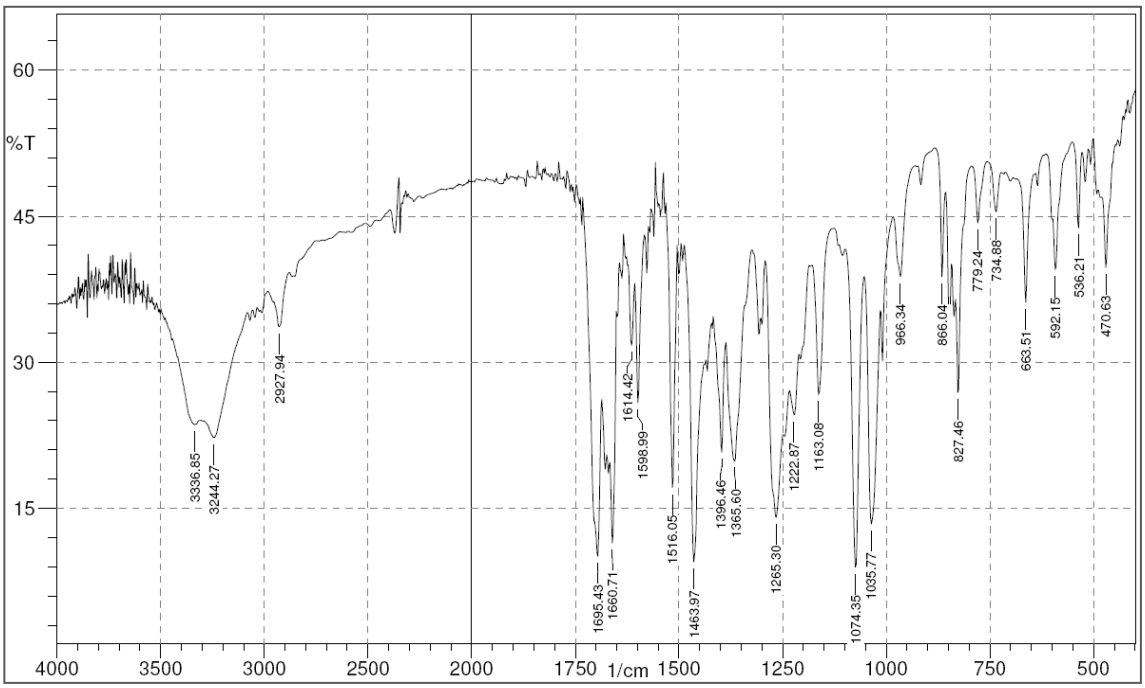
%T
60
45
30
15
3336.85
3244.27
2927.94
1695.43
1660.71
1614.42
1598.99
1516.05
1463.97
1396.46
1365.60
1265.30
1222.87
1163.08
1074.35
1035.77
966.34
866.04
827.46
779.24
734.88
663.51
592.15
536.21
470.63
4000
3500
3000
2500
2000
1750
1/cm
1500
1250
1000
750
500

- UV

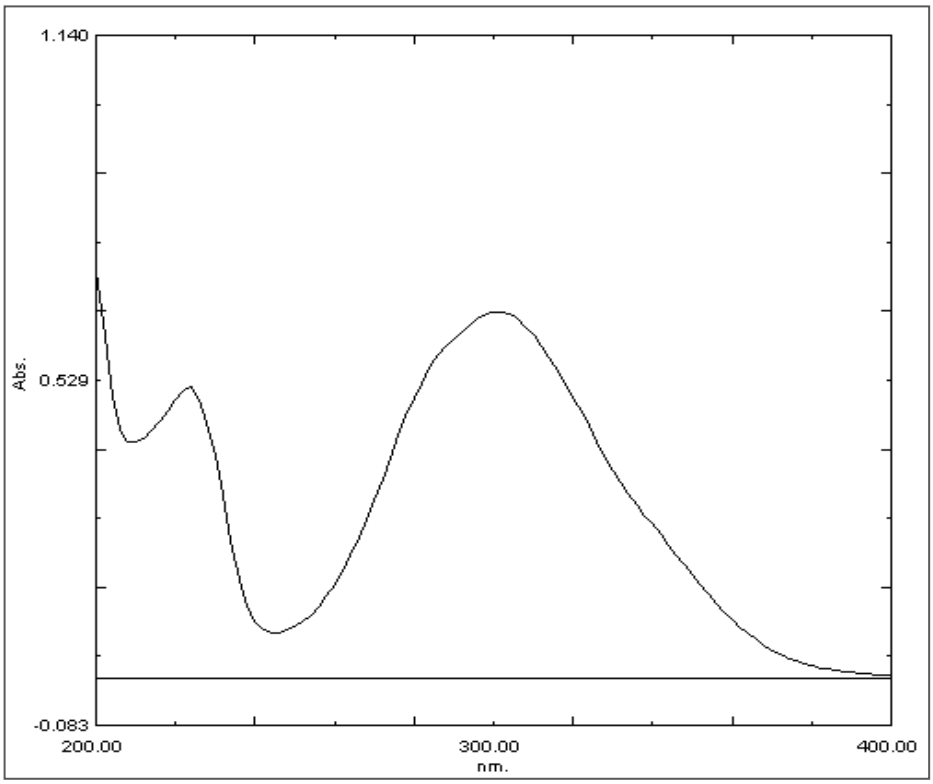
1.140
0.529
-0.083
Abs.
200.00
300.00
400.00
nm.

- MASS (ESI^-)

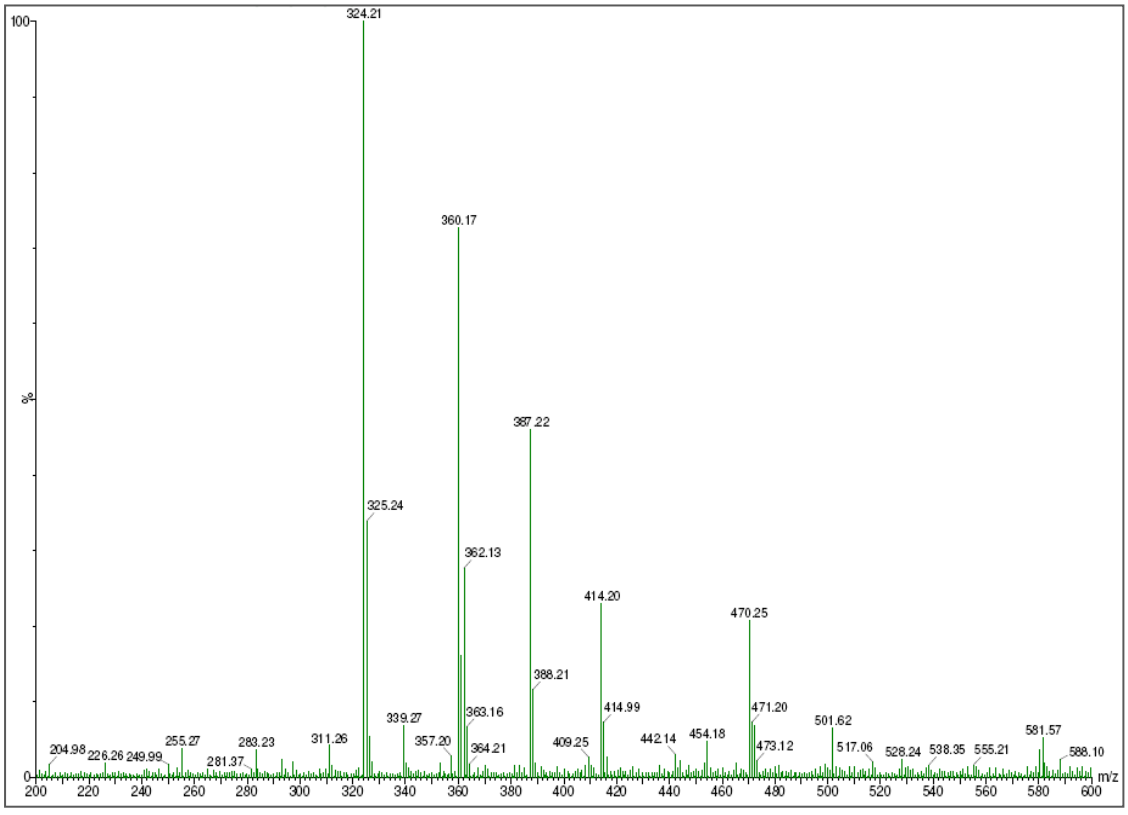
100
%
0
324.21
360.17
387.22
325.24
362.13
414.20
470.25
388.21
414.99
471.20
339.27
363.16
501.62
204.98
226.26
249.99
255.27
281.37
283.23
311.26
357.20
364.21
409.25
442.14
454.18
473.12
517.06
528.24
538.35
555.21
581.57
588.10
200
220
240
260
280
300
320
340
360
380
400
420
440
460
480
500
520
540
560
580
600
m/z

Appendix 6 – Triazene prodrug 21f

- ^{1}H NMR

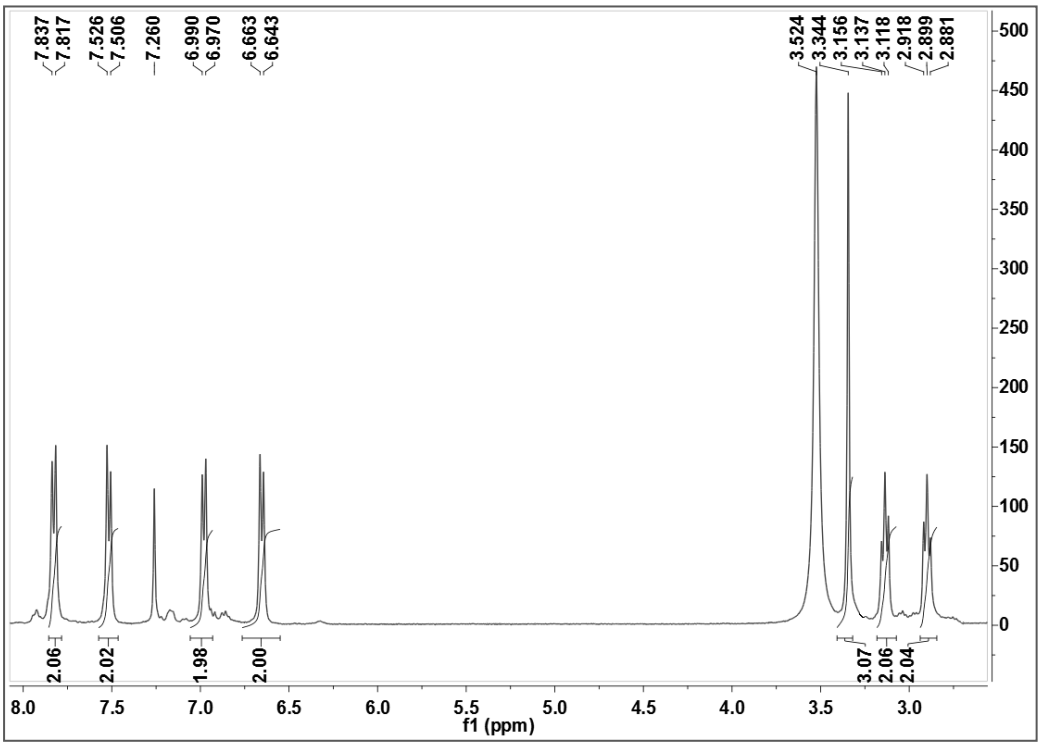

- ^{13}C NMR

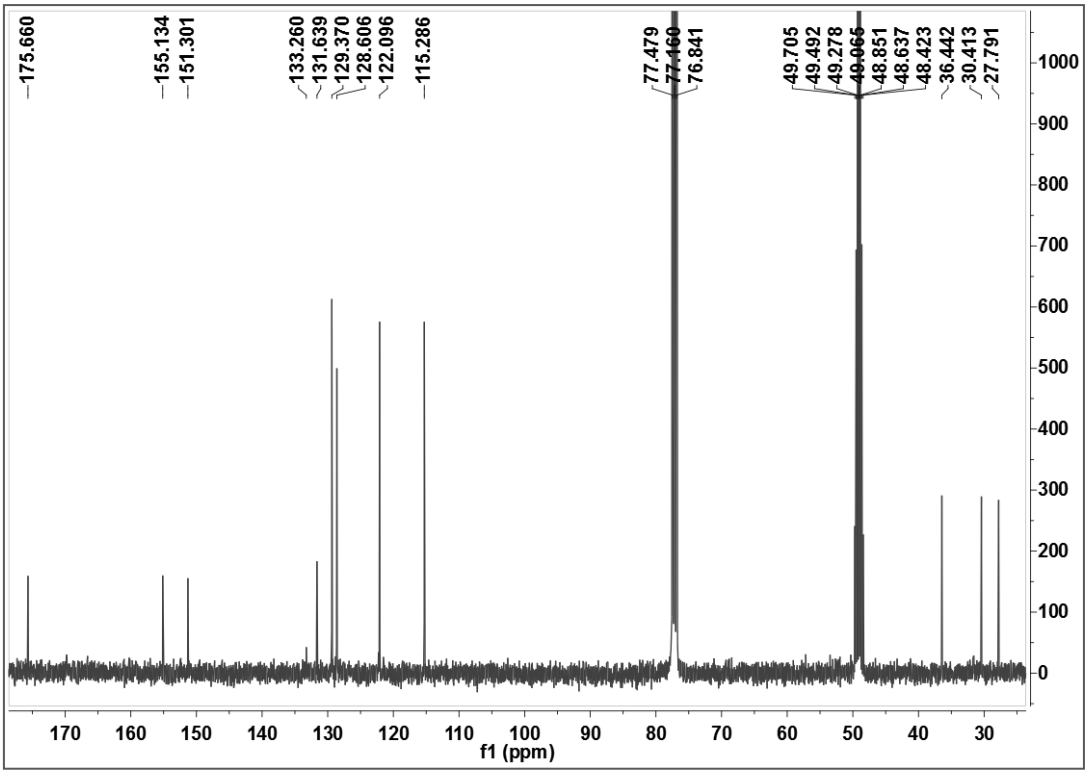

- HMQC

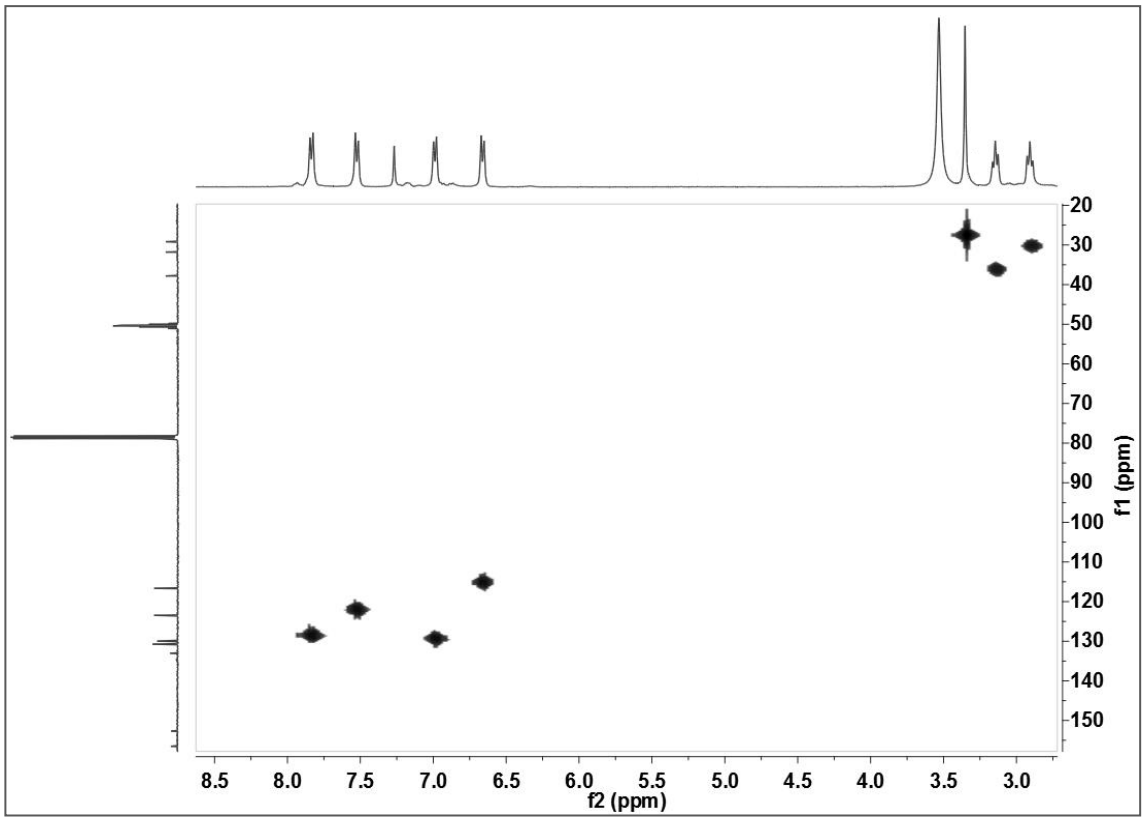
f1 (ppm)
f2 (ppm)

- IR

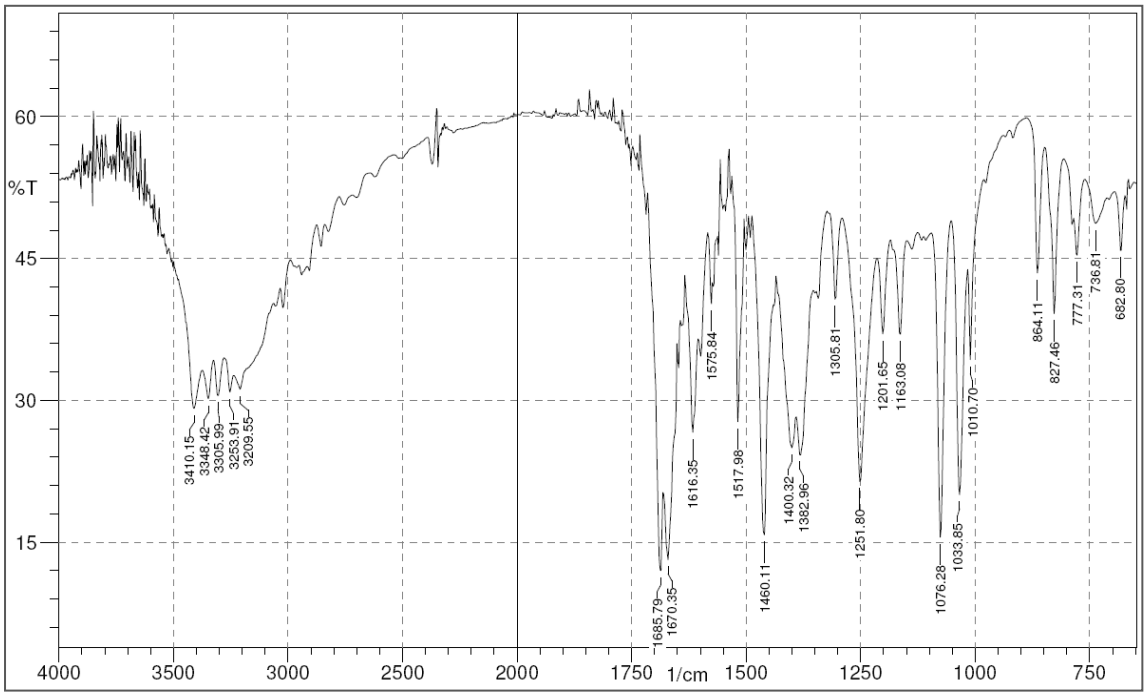
%T
1/cm
3410.15
3348.42
3305.99
3253.91
3209.55
1685.79
1670.35
1616.35
1575.84
1517.98
1460.11
1400.32
1382.96
1305.81
1251.80
1201.65
1163.08
1076.28
1033.85
1010.70
864.11
827.46
777.31
736.81
682.80

- UV

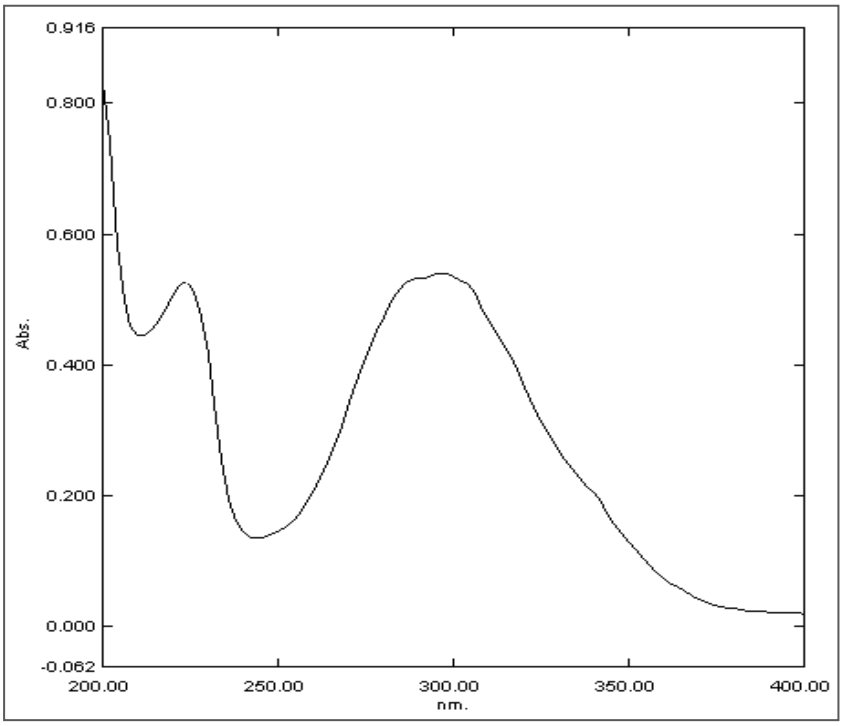
0.916
0.800
0.600
0.400
0.200
0.000
-0.062
Abs.
200.00
250.00
300.00
350.00
400.00
nm.

- MASS (ESI^+)

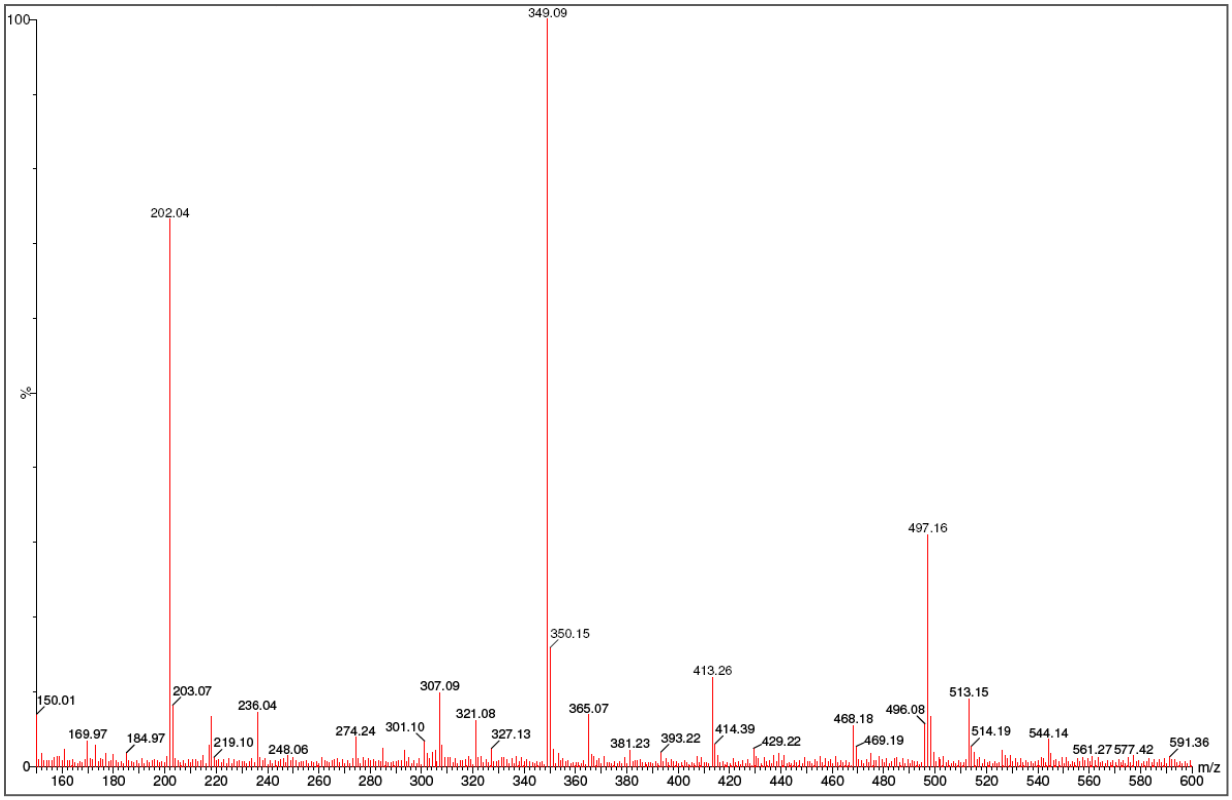
100
%
0
349.09
202.04
497.16
350.15
413.26
307.09
203.07
236.04
321.08
365.07
513.15
150.01
169.97
184.97
219.10
248.06
274.24
301.10
327.13
381.23
393.22
414.39
429.22
468.18
469.19
496.08
514.19
544.14
561.27
577.42
591.36
160
180
200
220
240
260
280
300
320
340
360
380
400
420
440
460
480
500
520
540
560
580
600
m/z

Appendix 7 – Compound 25a

- ^{1}H NMR

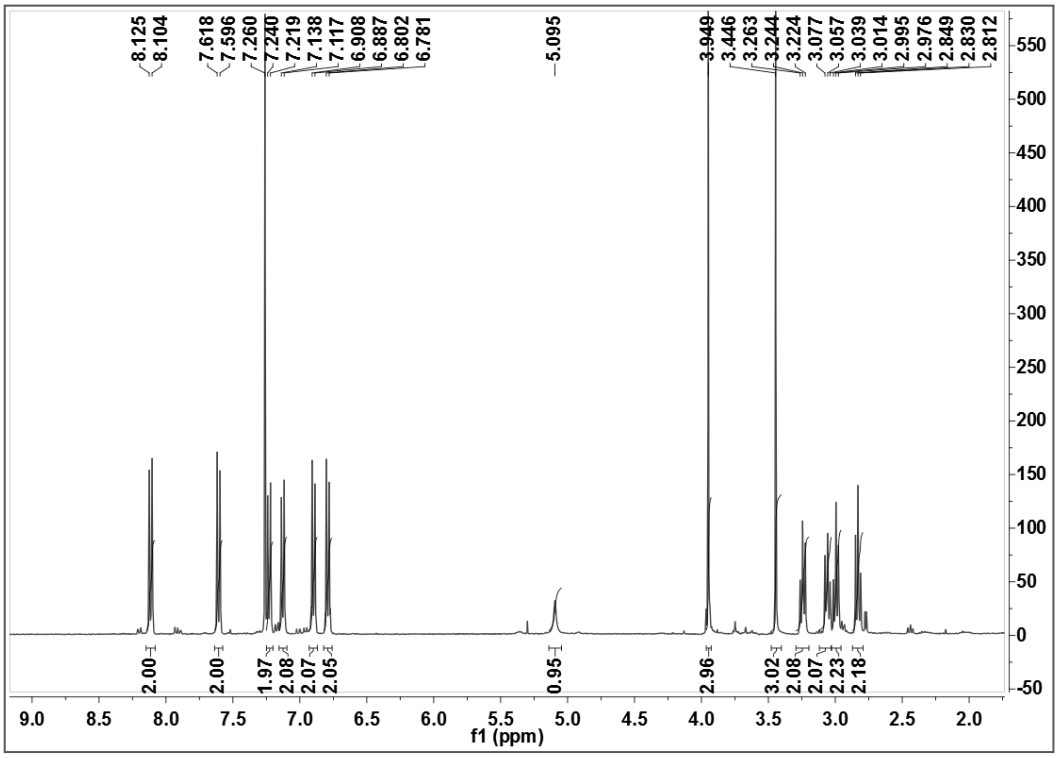

- IR

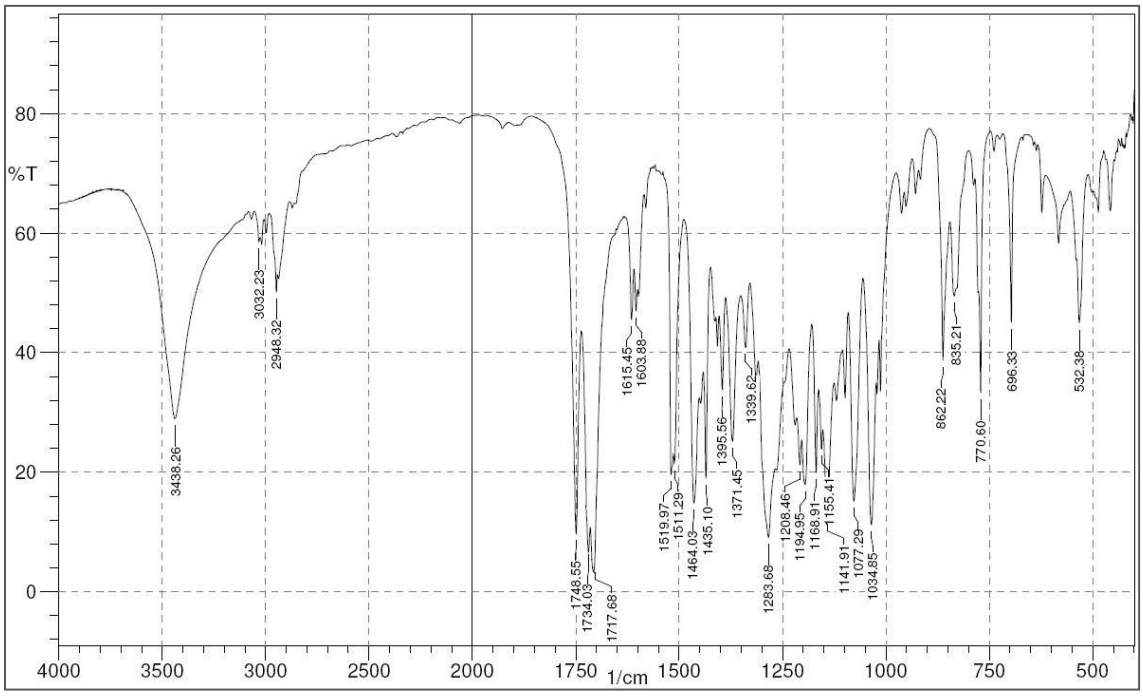

Appendix 8 – Compound 25b

- ^{1}H NMR

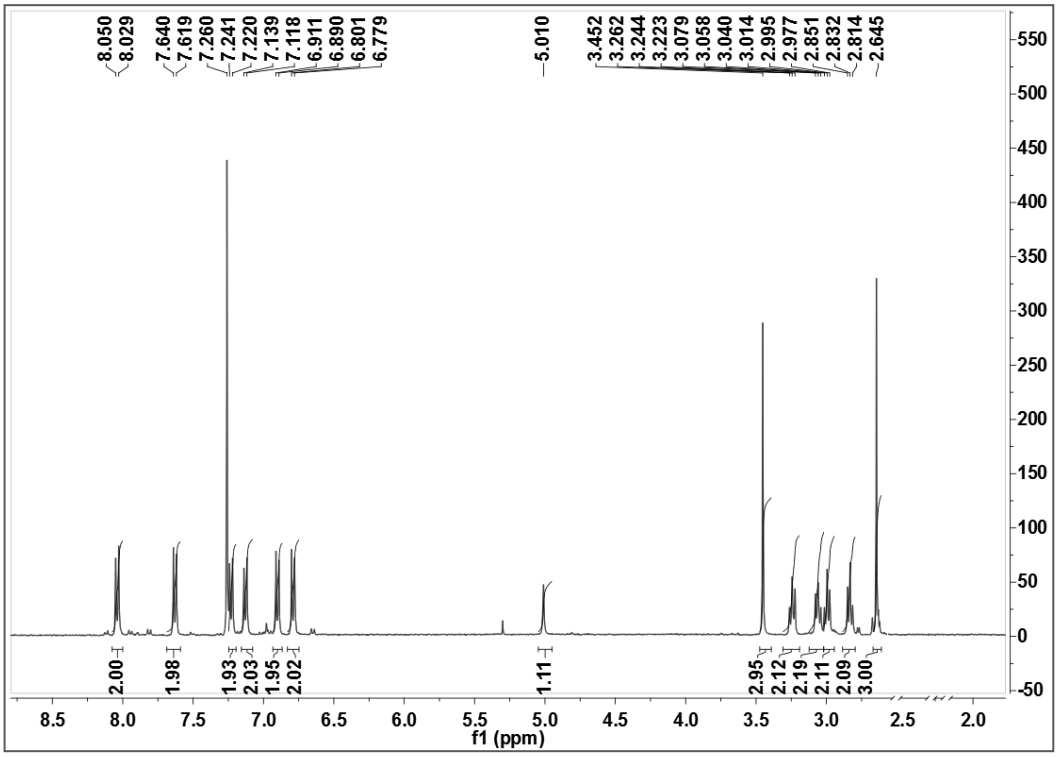

- IR

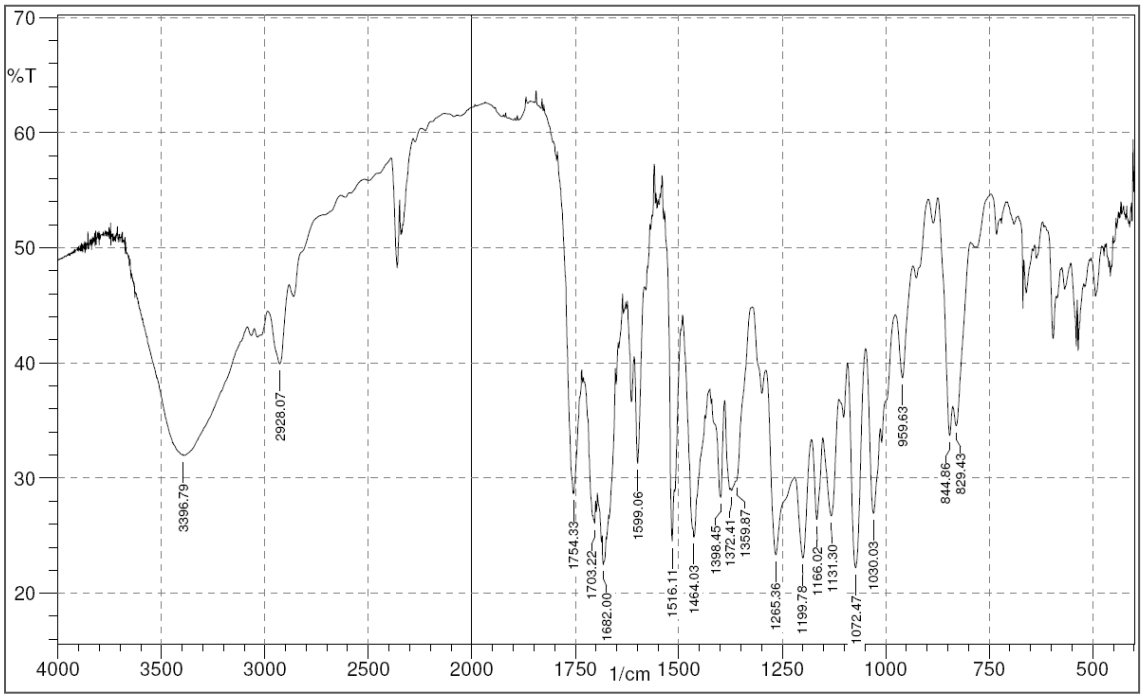

Appendix 9 – Triazene prodrug 21g

- ^{1}H NMR impure

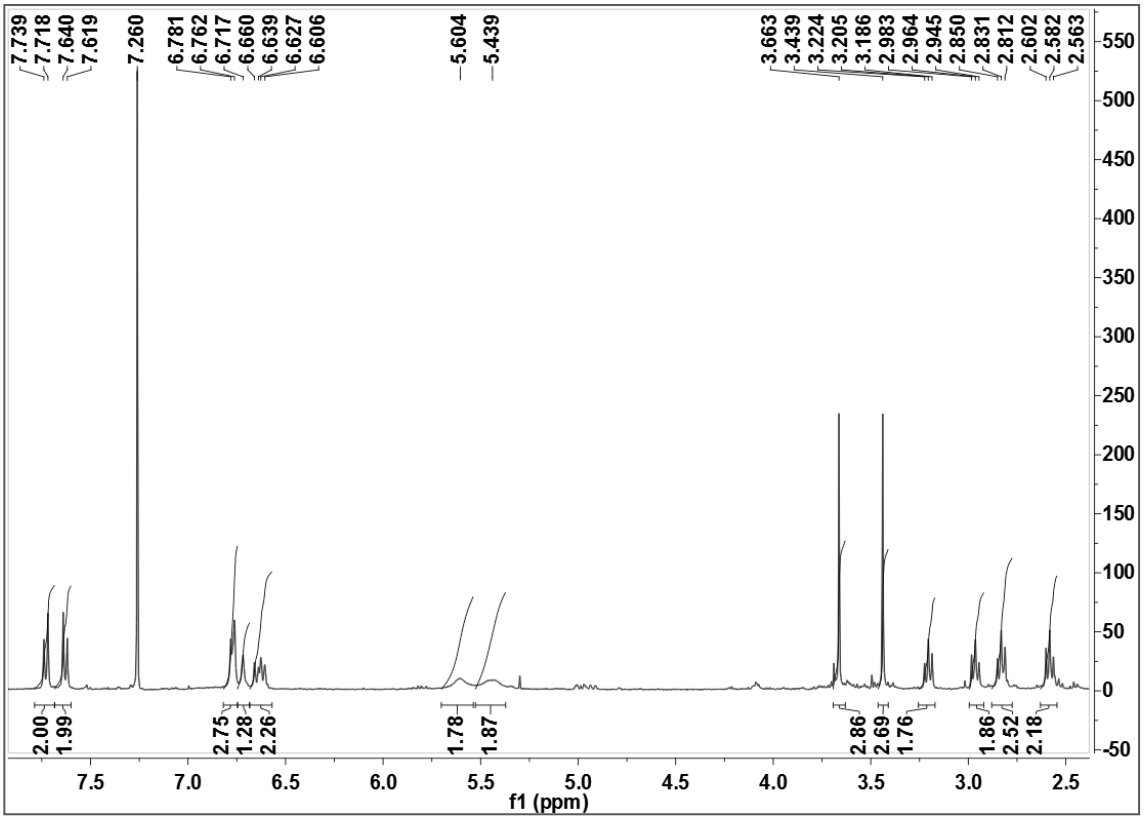

Appendix 10 – Poster - Synthesis and evaluation of novel triazene prodrugs as candidates for melanocyte-directed enzyme prodrug therapy

SYNTHESIS AND EVALUATION OF NOVEL TRIAZENE PRODRUGS AS CANDIDATES FOR MELANOCYTE-DIRECTED ENZYME PRODRUG THERAPY

Fábio M. F. Santos[a], M. Jesus Perry[a], Eduarda Mendes[a] , Ana Paula Francisco[a]

[a] *Research Institute for Medicines and Pharmaceutical Sciences (iMed.UL), Faculty of Pharmacy, University of Lisbon, Av. Prof. Gama Pinto 1649-019 Lisbon, Portugal*

Introduction

Metastatic malignant melanoma is the most aggressive form of skin cancer for which no reliable methods for treatment exist. The Institute of Cancer Research warns that the climate change will raise the incidence of melanoma, which is expected to increase three times over the next 30 years. Malignant melanocytes are up regulated in tyrosinase content. This enzyme has been considered as a target to selectively seek out chemotherapeutic strategies for the treatment of malignant melanoma[1]. One of these strategies is Melanocyte-Directed Enzyme Prodrug Therapy (MDEPT). MDEPT offers a highly selective triggering mechanism for drug delivery, as the release of the cytotoxic drug from prodrug only occurs effectively inside malignant melanocytes.[2] The first triazene compound introduced into medical practice as an effective drug in the treatment of malignant melanoma – Dacarbazine - still remains the single FDA-approved chemotherapeutic agent for metastatic melanoma[3]. In our group we are developing a novel set of triazene prodrugs **1** to apply in MDEPT strategy. In the design of these novel prodrugs the cytotoxic triazene is linked by an amide bond to a very good tyrosinase substrate.

Results and Discussion

❑ Synthesis of triazene prodrugs

Triazene prodrugs were synthesised according to scheme 1.

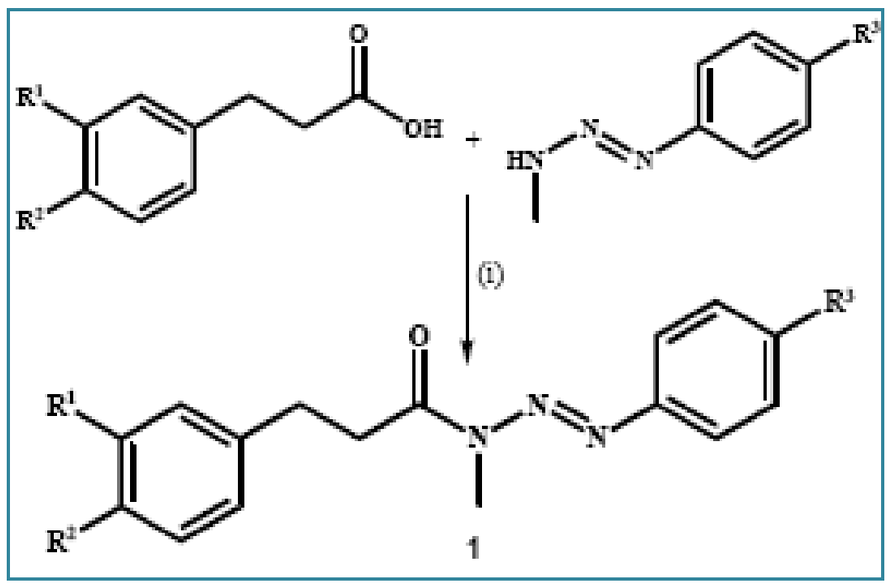

Scheme 1. Reagents and Conditions: (i) TBTU, Et_3N, DMF, MW (30 min; 55ºC; 100 W)

The use of microwave-assisted synthesis was efficient in the amide coupling, reducing the reaction time from 48h to 30 minutes, with comparable yields. The compounds were completely characterized by spectroscopic techniques.

❑ Stability Studies

These studies were performed at 37 ºC in three different conditions:

- Isotonic phosphate buffer pH 7.4 (PBS)
- Human Plasma 80%
- Mushroom Tyrosinase.

The assays were monitored by HPLC, following substrates 1 hydrolysis and the formation of reaction products - MMT and the corresponding amine (Figure 2). Half-lives for the hydrolysis of the prodrugs 1 under the conditions mentioned above are presented in Table 1.

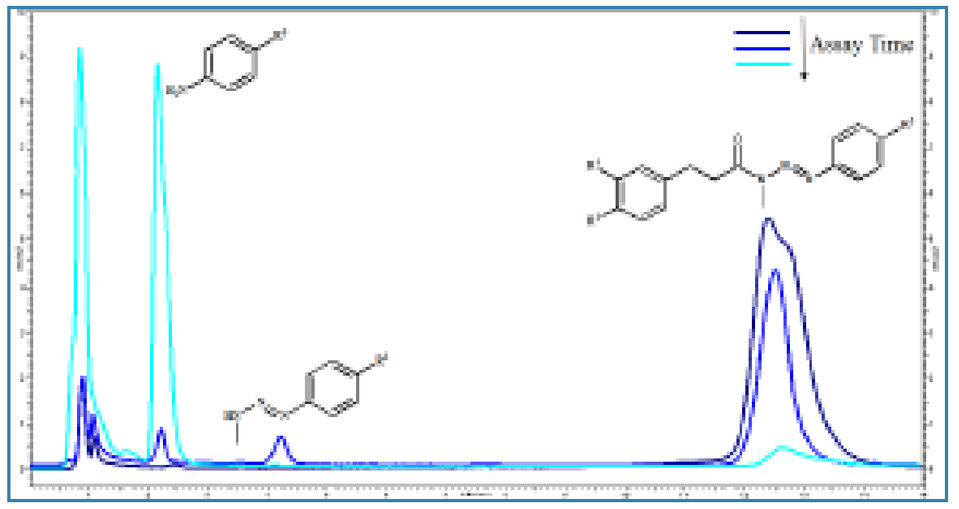

Figure 2. Tyrosinase assay example for prodrug 1a. In this assay is possible to observe the triazene prodrug decomposition in MMT and the hydrolysis of MMT in the corresponding amine over the time.

Table 1. Half-lives for compounds 1a-e.

Compound	R^1	R^2	R^3	$t_{1/2}$ (h)		
				PBS	Human Plasma	Tyrosinase
1a	OH	H	COOMe	94.75 ± 10.44	7.77 ± 0.11	21.22 ± 2.02 *
1b	OH	H	CN	60.14 ± 3.52	2.70 ± 0.07	19.54 ± 1.61 *
1c	H	OH	COOMe	101.53 ± 9.50	7.26 ± 0.24	0.041 ± 0.004 **
1d	H	OH	CN	75.98 ± 8.91	5.80 ± 0.25	0.025 ± 0.002 **
1e	H	OH	COMe	122.69 ± 1.85	14.59 ± 0.37	0.061 ± 0.006 **

* - 300 U/ml of tyrosinase; ** - 100 U/ml of tyrosinase

Results from Table 1 show that:

- **Prodrugs 1 display excellent stability in PBS, at physiological pH, with half-lives ranging from 60 h to 122 hours**
- **Triazene derivatives 1 hydrolyze in human plasma with half-lives ranging from 3h to 15 hours, implying that the majority of them exhibit the appropriate stability required for MEDPT strategy**
- **All the prodrugs synthesized act as tyrosinase substrates. Prodrugs with the OH group in the *para* position in the phenol moiety are much better substrates with half-lives 600 times smaller than the half-lives of prodrugs with the OH in *meta* position.**

Acknowledgements

The authors acknowledge Fundação para a Ciência e Tecnologia (Portugal) for financial support.

Conclusions

Current study demonstrates that triazene prodrugs with the OH in *para* positon provide an efficient prodrug system for MEDPT strategy since they combine chemical and human plasma stability with a very efficient enzymatic activation by tyrosinase. Studies will pursue in melanoma cell lines to assess the cytotoxicity of the prodrugs which have demonstrate better results in the stability studies performed.

References: [1]Samalia Jawaid, Tariq H. Khan, Helen M.I. Osborn and Nana Aba O. Williams. "Tyrosinase Activated Melanoma Prodrugs" in Anti-Cancer Agents in Medicinal Chemistry, 2009, Vol. 9, No. 7, 717-727. [2]M. Jesus Perry, Eduarda Mendes, Ana Luisa Simplício, Ana Coelho, Ricardo V. Soares, Jim Iley, Rui Moreira, Ana Paula Francisco. "Dopamine- and tyramine-based derivatives of triazenes: Activation by tyrosinase and implications for prodrug design" in European Journal of Medicinal Chemistry, 2009, Vol. 44, 3228–3234. [3]A. P. Francisco, M. J. Perry, R. Moreira and E. Mendes, "Alkylating Agents" in Anticancer Therapeutic, 2008, chapter 9, 133-157.